

# Improving soil carbon estimates by linking conceptual pools against measurable carbon fractions in the DAYCENT Model Version 4.5

Shree R.S. Dangal<sup>1</sup>, Christopher Schwalm<sup>2</sup>, Michel A Cavigelli<sup>3</sup>, Hero T. Gollany<sup>3</sup>, Virginia Lee Jin<sup>4</sup>, and Jonathan Sanderman<sup>2</sup>

<sup>1</sup>Woods Hole Research Center

<sup>2</sup>Woodwell Climate Research Center

<sup>3</sup>USDA-ARS

<sup>4</sup>USDA-Agricultural Research Service

November 22, 2022

## Abstract

Terrestrial soil organic carbon (SOC) dynamics play an important but uncertain role in the global carbon (C) cycle. Current modeling efforts to quantify SOC dynamics in response to global environmental changes do not accurately represent the size, distribution and flux of C from the soil. Here, we modified the Daily Century (DAYCENT) biogeochemical model by parameterizing conceptual SOC pools with C fraction data, followed by historical and future simulations of SOC dynamics. Results showed that simulations using modified DAYCENT (DCmod) led to better initialization of SOC stocks and distribution compared to default DAYCENT (DCdef) at long-term research sites. Regional simulation using DCmod demonstrated higher SOC stocks for both croplands (34.86 vs 26.17 MgC ha<sup>-1</sup>) and grasslands (54.05 vs 40.82 MgC ha<sup>-1</sup>) compared to DCdef for the contemporary period (2001-2005 average), which better matched observationally constrained data-driven maps of current SOC distributions. Projection of SOC dynamics to land cover change (IPCC AR4 A2 scenario) under IPCC AR5 RCP8.5 climate scenario showed absolute SOC loss of 8.44 and 10.43 MgC ha<sup>-1</sup> for grasslands and croplands, respectively, using DCmod whereas, SOC losses were 6.55 and 7.85 MgC ha<sup>-1</sup> for grasslands and croplands, respectively, using DCdef. The projected SOC loss using DCmod was 33% and 29% higher for croplands and grasslands compared to DCdef. Our modeling study demonstrates that initializing SOC pools with C fraction data led to more accurate representation of SOC stocks and individual carbon pool, resulting in larger absolute and relative SOC losses due to agricultural intensification in the warming climate.

**Improving soil carbon estimates by linking conceptual pools against measurable carbon fractions in the DAYCENT Model Version 4.5**

Shree R.S. Dangal<sup>1,\*</sup>, Christopher Schwalm<sup>1</sup>, Michel A. Cavigelli<sup>2</sup>, Hero T. Gollany<sup>3</sup>, Virginia L. Jin<sup>4</sup> & Jonathan Sanderman<sup>1</sup>

<sup>1</sup>Woodwell Climate Research Center, 149 Woods Hole Road, Falmouth, MA 02540, USA

<sup>2</sup>US Department of Agriculture - Agricultural Research Service, Sustainable Agricultural Systems Laboratory, Beltsville Agricultural Research Center, Beltsville, MD 20705, USA

<sup>3</sup>US Department of Agriculture - Agriculture Research Service, Columbia Plateau Conservation Research Center, Pendleton, OR 97810, USA

<sup>4</sup>US Department of Agriculture - Agricultural Research Service, Agroecosystem Management Research Unit, University of Nebraska-Lincoln, NE 68583, USA

*Correspondence to:* Shree R.S. Dangal (shree.dangal@unl.edu)

*\*Current Address:* School of Natural Resources, University of Nebraska-Lincoln, NE 68583

**Key points:**

1. The modified model overestimated measured SOC values at long term research sites but better approximated derived SOC values from other data products when calibrated to carbon (C) fraction compared to the default model.
2. Model modifications led to larger absolute and relative losses of SOC compared to the default model during 1895-2005.
3. Under the RCP8.5 scenario, projected SOC losses with the modified model were 33% and 29% larger for croplands and grasslands, respectively, compared to the default model.

## Abstract

Terrestrial soil organic carbon (SOC) dynamics play an important but uncertain role in the global carbon (C) cycle. Current modeling efforts to quantify SOC dynamics in response to global environmental changes do not accurately represent the size, distribution and flux of C from the soil. Here, we modified the Daily Century (DAYCENT) biogeochemical model by parameterizing conceptual SOC pools with C fraction data, followed by historical and future simulations of SOC dynamics. Results showed that simulations using modified DAYCENT ( $DC_{mod}$ ) led to better initialization of SOC stocks and distribution compared to default DAYCENT ( $DC_{def}$ ) at long-term research sites. Regional simulation using  $DC_{mod}$  demonstrated higher SOC stocks for both croplands (34.86 vs 26.17  $MgC\ ha^{-1}$ ) and grasslands (54.05 vs 40.82  $MgC\ ha^{-1}$ ) compared to  $DC_{def}$  for the contemporary period (2001-2005 average), which better matched observationally constrained data-driven maps of current SOC distributions. Projection of SOC dynamics to land cover change (IPCC AR4 A2 scenario) under IPCC AR5 RCP8.5 climate scenario showed absolute SOC loss of 8.44 and 10.43  $MgC\ ha^{-1}$  for grasslands and croplands, respectively, using  $DC_{mod}$  whereas, SOC losses were 6.55 and 7.85  $MgC\ ha^{-1}$  for grasslands and croplands, respectively, using  $DC_{def}$ . The projected SOC loss using  $DC_{mod}$  was 33% and 29% higher for croplands and grasslands compared to  $DC_{def}$ . Our modeling study demonstrates that initializing SOC pools with C fraction data led to more accurate representation of SOC stocks and individual carbon pool, resulting in larger absolute and relative SOC losses due to agricultural intensification in the warming climate.

## 1. Introduction

Soil is the largest terrestrial reservoir of organic carbon (C), storing about 1500 Pg C in the top 100 cm (Batjes, 2016; Nachtergaele et al., 2012). Any small changes in the magnitude, distribution and forms of terrestrial soil organic carbon (SOC) may lead to large release of C to the atmosphere (Sulman et al., 2018), with significant impact on food security and the global climate system (Lal, 2004). Given that changes in SOC represent one of the largest uncertainties in the global C budget (Ciais et al., 2014), accurate quantification of the distribution and forms of SOC can help to constrain the global C budget and provide key insights on the underlying processes related to SOC protection and cycling (Stockmann et al., 2013).

Changes in SOC stocks at any given time depend on the balance between organic matter inputs via plant production, additions of manure and compost, and outputs via decomposition, erosion and hydrologic leaching of various C compounds (Davidson and Janssens, 2006; Jobbágy and Jackson, 2000). Although higher organic matter inputs to the soil generally correlate with high SOC (Sanderman et al., 2017a), the biological stability of SOC is ultimately determined by the interactions among the soil physicochemical environment (soil moisture, temperature, pH and aeration), soil mineralogy, and the accessibility of the organic matter to microbes and enzymes (Schmidt et al., 2011). Current understanding of the SOC dynamics indicates that the soil physicochemical environment plays an important role in determining the C efflux from soil and that the efflux rates are modified by substrate availability and the affinities of enzymes for the substrates (Six et al., 2002). However, the extent to which different physicochemical characteristics of soil control the stabilization and cycling of SOC is still debated (Carvalhais et al., 2014; Doetterl et al., 2015; Rasmussen et al., 2018). Additionally, the complex molecular structure of C substrates and their sensitivity to climatic and environmental constraints add further



complexity in understanding SOC dynamics at different spatial and temporal scales (Davidson and Janssens, 2006).

Previous studies have shown that the factors affecting the stabilization/destabilization of SOC are numerous and that the changes in SOC over space and time are the result of complex interactions among climatic, biotic and edaphic factors (Rasmussen et al., 2018; Stockmann et al., 2013; Torn et al., 1997; Wiesmeier et al., 2019). For example, Carvalhais et al. (2014) have shown that climate, particularly temperature, strongly controls SOC turnover. Doetterl et al. (2015) found that geochemical characteristics such as base saturation, soil texture, silica content and pH also play a dominant role by altering the adsorption and aggregation of SOC. In addition, other studies indicate that soil nitrogen (N) availability affects SOC change due to constraints on microbial activity and plant productivity (Grandy et al., 2008; Janssens et al., 2010; Sinsabaugh et al., 2005). These findings have led to the view that the accumulation and decomposition of organic matter in soil is ultimately determined by the interactions among climate, vegetation type, topography and lithology.

Biogeochemical models commonly rely on capturing SOC heterogeneity associated with the complex interactions among climatic, biotic and edaphic factors by defining a number of distinct SOC pools with different potential turnover rates (Tian et al., 2015; Todd-Brown et al., 2014). The potential turnover rates of distinct soil pools are modified by climatic factors such as soil moisture and temperature, soil chemical factors such as pH and oxygen availability and the mechanism that facilitates C protection via organo-mineral interactions and aggregation, often loosely represented by clay content (Trumbore, 1997). Each of these pools is conceptual in nature, implying that the turnover times of these pools cannot be determined by chemical and physical fractionation (Paul

et al., 2001). As a result, there is increasing need and effort to link the conceptual pools with some measurable data to determine the turnover rates of SOC pools in the biogeochemical models.

In current biogeochemical models, there is a general agreement that the soil organic matter (SOM) contains at least three C pools: an active pool dominated by root exudates and the rapidly decomposable components of fresh plant litter, with mean residence time (MRT) ranging from days to years (Hsieh, 1993); a slow pool dominated by decomposed organic material, often of microbial origin, with MRT ranging from years to centuries (Torn et al., 2013); and a passive pool dominated by stabilized organic matter with MRT of several hundred to thousands of years (Czimczik and Masiello, 2007). Changes in the size and relative abundance of these pools are strongly influenced by climate, soil type and land use (Sanderman et al., 2021). Therefore, accounting for accurate distribution of SOC into different pools is paramount to quantify the current SOC stocks and examine the vulnerability of SOC to future environmental changes.

Relating these conceptual pools with SOC partitioned into laboratory defined fractions, such as particulate-, mineral associated- and pyrogenic-forms of C (POC, MOAC and PyC, respectively), can help to constrain the turnover rate of different pools in biogeochemical models. For example, Skjemstad et al. (2004) related POC, MOAC and PyC approximated using a combination of physical size fractionation and solid-state  $^{13}\text{C}$ -NMR spectroscopy with resistant plant material (RPM), humic (HUM) and inert organic material (IOM) pools in the Rothamsted carbon (RothC) model to predict changes in SOC in response to changes in soil type, climate and management. However, RothC does not explicitly simulate plant growth and plant response to dynamic changes in climate and other environmental factors (Zimmermann et al., 2007). In addition, the plant material is loosely partitioned into decomposable and resistant forms with large uncertainties in their respective sizes (Cagnarini et al., 2019). Unlike RothC, ecosystem models such as

Century, DeNitrification-DeComposition (DNDC) and Agricultural Production Systems sIMulator (APSIM) integrate the effects of climate, land use change and land management practices by simulating plant physiology and soil biogeochemistry, and explicitly consider the effects of climate, land use and land management on three conceptual soil C pools with different turnover rates (Hartman et al., 2011; Ogle et al., 2010).

In this study, we modified, calibrated and evaluated the version 4.5 of the Daily Century model (hereafter, DAYCENT) to improve the representation of SOC dynamics by linking conceptual pools of active, slow and passive SOC against estimates of the measurable POC, MOAC and PyC fractions, respectively. We then simulated the response of SOC to climate and land use change during the historical and future period using the default (hereafter, DC<sub>def</sub>) and modified (hereafter, DC<sub>mod</sub>) DAYCENT model in the US Great Plains ecoregion. The objectives of this study were to

- 1) modify the DC<sub>def</sub> model to link active, slow and passive pools of organic C to soil C fractions;
- 2) calibrate and evaluate DC<sub>mod</sub> performance by comparing the distribution of C in active, slow and passive pools against C fractions predicted at seven long-term research sites; 3) evaluate the differences between the DC<sub>mod</sub> and DC<sub>def</sub> in simulating contemporary SOC stocks and their distribution by comparing against other existing data products in the US Great Plains region; and
- 4) project the SOC change in response to climate and land cover change through 2100. We hypothesize that (i) calibrating the conceptual pools to C fraction data in the DAYCENT model leads to more accurate initialization of equilibrium pool structure (Skjemstad et al., 2004), thereby allowing a better comparison of measured and simulated SOC in response to climate, land use and management (Basso et al., 2011); (ii) conversion of native vegetation to any agricultural use significantly alters the distribution of SOC among the various soil pools (Guo and Gifford, 2002), but the rate and extent of SOC change depend on the intensity of agricultural use (Lal, 2018; Page

et al., 2014), with larger losses from models that allocate more C to active and slow pools; and (iii) land use under a warming climate would result in larger absolute and relative losses of SOC from the model that derive more SOC from the active pool due to rapid decomposition of fresh organic matter induced by warming (Crowther et al., 2016).

## **2. Materials and methods**

### **2.1 The DAYCENT Model**

The DAYCENT Version 4.5 is a daily time step version of the Century biogeochemical model that simulates the dynamics of C and N of both managed and natural ecosystems (Del Grosso et al., 2002; Parton et al., 1998). The exchange of C and N among the atmosphere, vegetation and soil is a function of climate, land use, land management and other environmental factors. The vegetation pool simulates potential plant growth at a weekly time step limited by water, light and nutrients. The DAYCENT model consists of multiple pools of SOM and simulates turnover as a function of the amount and quality of residue returned to the soil, the size of different soil pools and a series of environmental limitations. The type and timing of management events including tillage, fertilization, irrigation, harvest and grazing activities can affect plant production and SOM retention.

The DAYCENT model was originally developed from the monthly CENTURY model version 4.0. The CENTURY 4.0 is a general FORTRAN model of the plant-soil ecosystem that simulates carbon and nutrient dynamics of different types of terrestrial ecosystems (grasslands, forest, crops and savannas). CENTURY 4.0 primarily focused on simulation of soil organic matter dynamics of agro-ecosystems (Metherell et al., 1994). Earlier development of the CENTURY focused on simulation of soil organic matter dynamics of grasslands, forest and savanna ecosystems (Parton et al., 1988; Sanford Jr et al., 1991).

The first DAYCENT model was developed in FORTRAN 77 and C from CENTURY 4.0 to simulate the exchanges of C, water, nutrients, and gases ( $\text{CO}_2$ ,  $\text{CH}_4$ ,  $\text{N}_2\text{O}$ ,  $\text{NO}_x$ ,  $\text{N}_2$ ) among the atmosphere, soil and plants at a daily time step (Del Grosso et al., 2001; Kelly et al., 2000; Parton et al., 1988). The submodels used in DAYCENT are described in detail by Del Grosso et al. (2001), which includes submodels for plant productivity, soil organic matter decomposition, soil water and temperature dynamics, and trace gas fluxes. Other model developments while transitioning from CENTURY 4.0 to DAYCENT included dynamic carbon allocation and changes in growing degree days routine that triggers the start and end of growing season based on phenology (soil surface temperature, air temperature, and thermal units).

The first formal version DAYCENT 4.5 (Hartman et al., 2011) was developed from Del Grosso et al. (2002), with a focus on simulation of trace gas fluxes for major crop types in the US Great Plains region. Hartman et al. (2011) focused on calibrating and validating crop yield and trace gas fluxes for all the major crop types in 21 representative counties in the US Great Plains region.

The SOM sub-model consists of active, slow and passive pools with different turnover times. The active pool has a short (1-5 yr) turnover time and consists of live microbes and microbial products. The slow pool has an intermediate turn over time (20-50 yr) and contains physically protected organic matter and stabilized microbial products. The passive pool has a long turnover time (400-2000 yr) with physically and chemically stabilized SOC. In DAYCENT, the turnover of the active, slow and passive pools are simulated as a function of potential decomposition rates of respective pools modified by soil temperature, moisture, clay content, pH and cultivation effects. Changes in SOC are simulated for the top 20 cm of the soil.

In this study, we modified the DAYCENT and developed a methodology to calibrate the size of the conceptual soil pools by comparing it with carbon fraction data at long term research sites.

First, we developed measurable carbon fraction data using a combination of diffuse reflectance spectroscopy and a machine learning model (section 2.2). Second, we modified the DAYCENT model to link conceptual active, slow, and passive pools with the carbon fraction data (section 2.3 & 2.4). Third, we parameterized the DAYCENT by tuning the potential decomposition rates ( $k$ ) such that the size of the active, slow and passive soil pools match with the POC, MAOC and PyC, respectively at the long-term research sites (section 2.5). Fourth, we calibrated both the default and modified DAYCENT using input data developed in section 2.3 against observed total SOC at the long-term research sites (section 2.6), followed by model validation (section 2.7) and historical and future simulations (section 2.8).

## **2.2 Development of carbon fraction datasets to match with soil carbon pools**

To link the SOC pools in DAYCENT with measurable C fractions, we used seven long-term research sites located in the United States (Cavigelli et al., 2008; Gollany, 2016; Ingram et al., 2008; Liebig et al., 2010; Schmer et al., 2014; Sindelar et al., 2015; Syswerda et al., 2011), which span a range of climatic, land use and land management gradients (Table 1). Six of seven research sites are part of Long-Term Agroecosystem Research (LTAR) network focused on sustainable intensification of agricultural production. The remaining site is part of Columbia Plateau Conservation Research Center (CPCRC) Long-Term Experiment (LTE). At each site, we predicted the POC, MAOC and PyC fractions using a diffuse reflectance mid-infrared (MIR) spectroscopy-based model as detailed in Sanderman et al. (2021). The predictive models for the C fractions were developed from a database of fully fractionated soil samples using a combination of physical size separation and solid-state  $^{13}\text{C}$  NMR spectroscopy (Baldock et al., 2013b) of Australian (Baldock et al., 2013a) and US origin (Sanderman et al., 2021). All samples for model development were scanned using a Thermo Nicolet 6700 FTIR spectrometer with Pike AutoDiff reflectance

accessory located at the Commonwealth Scientific and Industrial Research Organization (CSIRO) in Australia. The soil samples from all the long-term research sites were scanned using a Bruker Vertex 70 FTIR equipped with a Pike AutoDiff reflectance accessory located at Woodwell Climate Research Center in the United States. For all samples, spectra were acquired on dried and finely milled soil samples. Since the SOC fraction model and the soil samples were scanned using different instruments, we developed a calibration transfer routine to account for the differences in spectral responses between the CSIRO (primary) and Woodwell (secondary) instruments by scanning a common set of 285 soil samples. The calibration transfer routine was developed using piecewise direct standardization (PDS) as described in Dangal & Sanderman (2020).

220  
221

**Table 1.** General attributes of the LTAR, LTER and CPCRC-LTE sites used for DAYCENT parameterization and calibration

Site Name	Sampling Location	Lon	Lat	T <sub>avg</sub> (°C)	Annual Precip. (mm)	Elev (m)	Land use	Data Avail.	Reference
Lower Chesa. Bay	Beltsville, MD	-76.9	39.1	12.8	1110	41	CS	1996-2016	Cavigelli et al. 2008
CPCRC-NTLTE	Pendleton, OR	-118.4	45.4	10.6	437	456	WW-FA	2005-2014	Gollany 2016
Cent. Plains Exp. Ran.	Cheyenne, WY	-104.9	41.2	8.6	425	1930	C3-C4 Gra.	2004-2013	Ingram et al. 2008
Northern Plains	Mandan, ND	-100.9	46.8	4	416	593	C3-C4 Gra.	1959-2014	Liebig et al 2010
Platte/High Plains Aq.	Lincoln, NE	-96.5	40.9	11	728	369	CC,CS	1998-2011	Sindelar et al 2015
Platte/High Plains Aq.	Mead, NE	-96.0	41.0	9.8	740	349	CC	2001-2015	Schmer et al. 2014
Kellogg Bio. Station	H. Corners, MI	-85.4	42.4	9.7	920	288	CSW-Gra.	1989-2017	Syswerda et al. 2011 <sup>‡</sup>

CS: Corn-Soya; WW: Winter Wheat; FA: Fallow; CC: Continuous Corn, SC: Soya-Corn, CSW: Corn-Soya-Wheat, Gra.: Grass  
#H. Corners, MI is a LTER & LTAR site; CPCRC-NTLTE: Columbia Plateau Conservation Research Center No-Till Long-Term Experiment.



For estimating C fractions of the prediction set (i.e., soil spectra of seven long-term research sites), we used a local memory based learning (MBL) approach that fits a unique target function corresponding to each sample in the prediction set (Dangal et al., 2019; Ramirez-Lopez et al., 2013). The MBL selects spectrally similar neighbors for each sample in the prediction sets to build a unique SOC fraction model for each target sample. The spectrally similar neighbors were optimized by developing a soil C fraction model using a range of spectrally similar neighbors and selecting the neighbors that produce the minimum root mean square error based on local cross validation. Before developing the soil C fraction model, the spectra of both the calibration and prediction sets were baseline transformed. Following baseline transformation, spectral outliers were detected using F-ratios (Hicks et al., 2015). The F-ratio estimates the probability distribution function of the spectra and picks samples that fall outside the calibration space as outliers (Dangal et al., 2019). Observation data used for building the soil C fraction model were square root transformed before model development and later back-transformed when estimating the goodness-of-fit. The performance of predictive models is shown in Table S1.

The predicted soil C fractions for the seven long-term research sites were then converted into C fraction stocks using the relationship between C fraction (%), bulk density (BD;  $\text{g/cm}^3$ ) and the depth (cm) of soil samples. Since the BD data were not available for all long-term research sites for different crop rotation and grazing intensities, we predicted BD using methods similar to those described above. The only difference was that the samples used to develop the BD model were based on a much larger database of soil spectra scanned at the Kellogg Soil Survey Laboratory (KSSL) in Lincoln, USA (Dangal et al., 2019). Before predicting BD, the calibration transfer, as documented in Dangal & Sanderman (2020), between the KSSL and Woodwell soil spectra were developed and the local modeling approach (i.e., MBL) was used to make final prediction for

samples with missing laboratory BD. Calibration transfer between the spectrometers at the  
 Woodwell (secondary instrument) and KSSL (primary instrument) laboratory was necessary to  
 improve prediction of BD ( $R^2 = 0.46-0.64$  and  $RMSE = 0.26-0.50$ ) (Dangal and Sanderman, 2020).  
 One of the technical challenges associated with the comparison of simulated pool sizes against  
 diffuse reflectance spectroscopy-based predictions of POC, MOAC and PyC at long-term research  
 sites was the absence of laboratory data on C fractions to validate the MIR based predictions. To  
 address this shortcoming, we first compared the sum of the MIR based predictions of POC, MOAC  
 and PyC against observation of total SOC available at these sites (Figure S1). When comparing  
 the total SOC against MIR based predictions, we did not limit the comparison to 20 cm, but  
 allowed it across the full soil depth profile based on the availability of SOC data at the seven long-  
 term research sites. Additionally, the laboratory data used for model comparison were available at  
 multiple depths of up to 60 cm often without a direct measurement for the 0-20 cm depth  
 necessitating an approximation of the 0-20 cm stock. For example, when soils were collected from  
 0-15 and 15-30 cm, we estimated the 20 cm SOC stock by adding 1/3 of the 15-30 cm SOC stock  
 to the entire 0-15 cm SOC stock.

### 2.3 Input datasets for driving the DAYCENT model

The US Great Plains region was delineated using the Level I ecoregions map (Omernik and  
 Griffith, 2014) available through the Environmental Protection Agency (<https://www.epa.gov/ecoresearch/ecoregions-north-america>). The datasets for driving the DAYCENT were divided into  
 two parts: 1) dynamic datasets that include time series of daily climate (precipitation, maximum  
 and minimum temperature), annual land cover land use change (LCLUC) and land management  
 practices (irrigation, fertilization and cropping system, tillage intensity) and 2) static datasets that  
 include information on soil properties (soil texture, pH and bulk density) (Sanderman et al., 2021),

and topography maps (Jarvis et al., 2008). For the historical period (1895-2005), we used a combination of VEMAP and PRISM (1895-1979) and Daymet (1980-2005) (Daly and Bryant, 2013; Kittel et al., 2004; Thornton et al., 2012). The VEMAP datasets are available at a daily time step and a coarser spatial resolution ( $0.5^\circ \times 0.5^\circ$ ), while the PRISM datasets are available at a monthly time step and a finer spatial resolution ( $10 \text{ km} \times 10 \text{ km}$ ). We interpolated the PRISM data at a daily time step by using the daily trend from the VEMAP datasets such that the monthly precipitation totals and monthly average temperature matches the monthly climate from the PRISM data. For the future (2006-2100), we used the Intergovernmental Panel on Climate Change (IPCC) 5<sup>th</sup> assessment report (AR5) RCP4.5 and RCP8.5 climate scenarios available at a spatial resolution of  $1/16^\circ \times 1/16^\circ$ .

**Table 2.** Default and modified decomposition ( $k$ ) parameters used in the DAYCENT to simulate the size of different carbon pools

Pools	Default	Modified $k$ ( $\text{yr}^{-1}$ )				
	$k$ ( $\text{yr}^{-1}$ )	grid search	N	Optimized	Absolute	Relative (%)
Active	7.30	(3,12)	301	3.50	-3.80	-52
Slow	0.20	(0.10,0.30)	201	0.14	-0.06	-30
Passive	0.0045	(0.001,0.0085)	351	0.0075	0.003	+67

For annual LCLUC, we used spatially explicit datasets available at a resolution of  $250\text{m} \times 250\text{m}$  for the historical (1938-2005) and future (2006-2100) periods under the IPCC 4<sup>th</sup> assessment report (AR4) A2 scenario (Sohl et al., 2012). We used only the A2 land cover scenario because there was not much difference in the trajectories of land cover change through 2100. For the period 1895-1937, we backcasted the proportional distribution of croplands and grasslands by integrating the Sohl et al. (2012) data with HYDE v3.2 data (Klein Goldewijk et al., 2017). We estimated the

fractional distribution of croplands and grasslands by calculating the total number of pixels dominated by each land cover type at 250m resolution within each  $1/16^\circ$  grid cell (Figure S2a). Irrigation and fertilization data are based on census of agriculture statistics (Falcone and LaMotte, 2016). All datasets were interpolated/aggregated to a common resolution of  $1/16^\circ \times 1/16^\circ$  (approximately 7km x 7km at the equator).

Cropping systems and crop rotation are based on county level data for the US Great Plains region available through Hartman et al. (2011), which were merged with tillage type and intensity data (Baker, 2011) to write 24 unique schedule files that describe grid-specific cropping system and crop management practices. The 24 unique schedule files include sequences of time blocks, with each block describing a unique set of crop types, crop rotation, tillage type, tillage intensity, fertilization, irrigation and residue removal (Hartman et al., 2011). Using these schedule files, we developed an unsupervised classification algorithm (K-means) to create 24 unique clusters as a function of long-term average climate (precipitation, minimum- and maximum-temperatures), land forms, land cover type and elevation. We then assigned all the grid cells to one of the 24 unique clusters to create a spatially explicit dataset on cropping system and crop rotation. While developing the unsupervised classification algorithm, the eastern part of the US Great Plains region dominated by corn (*Zea mays* L.) - soybean (*Glycine max* (L.) Merr.) rotation was underrepresented. To address this shortcoming, we used randomly selected grid points from the CropScape data (<https://nassgeodata.gmu.edu/CropScape/>) available through the USDA National Agricultural Statistics Service in the unsupervised classification algorithm. Additionally, cropping systems classified using the unsupervised algorithm was verified against current CropScape data allowing for realistic representation of cropping systems. The distribution of schedule files representing different crop rotation and crop types used to build the unsupervised classification is

shown in Figure S2b and the spatial distribution of crop rotations based on the unsupervised classification is shown in Figure S3.

#### **2.4 Linking DAYCENT conceptual pools with C fractions**

The SOC dynamics in the DAYCENT consists of the first-order kinetic exchanges among conceptual pools (active, slow, and passive) defined by empirical turnover rates (Parton et al., 1987). However, a major impetus for quantifying these pools comes from the fact that the size and distribution of SOC in the different pools cannot be directly linked with experimental data. Here, we developed a methodology to link the conceptual active, slow and passive pools to spectroscopy-based estimates of POC, MAOC and PyC fractions. The rate of decomposition across POC, MAOC and PyC are consistent with the potential turnover rates assigned to the active, slow, and passive pools in soil C models (Baldock et al., 2013b). As a result, we modified the potential turnover rates in the DAYCENT model such that the absolute difference between the simulated SOC and predicted C fractions was minimized (see section 2.5 below). When matching the soil pools with C fraction data, we compared the sum of belowground structural, metabolic and active pool SOC to POC, slow pool SOC to MAOC, and passive pool SOC to PyC. Details on matching the conceptual pools with C fraction data are provided in Figure S4.

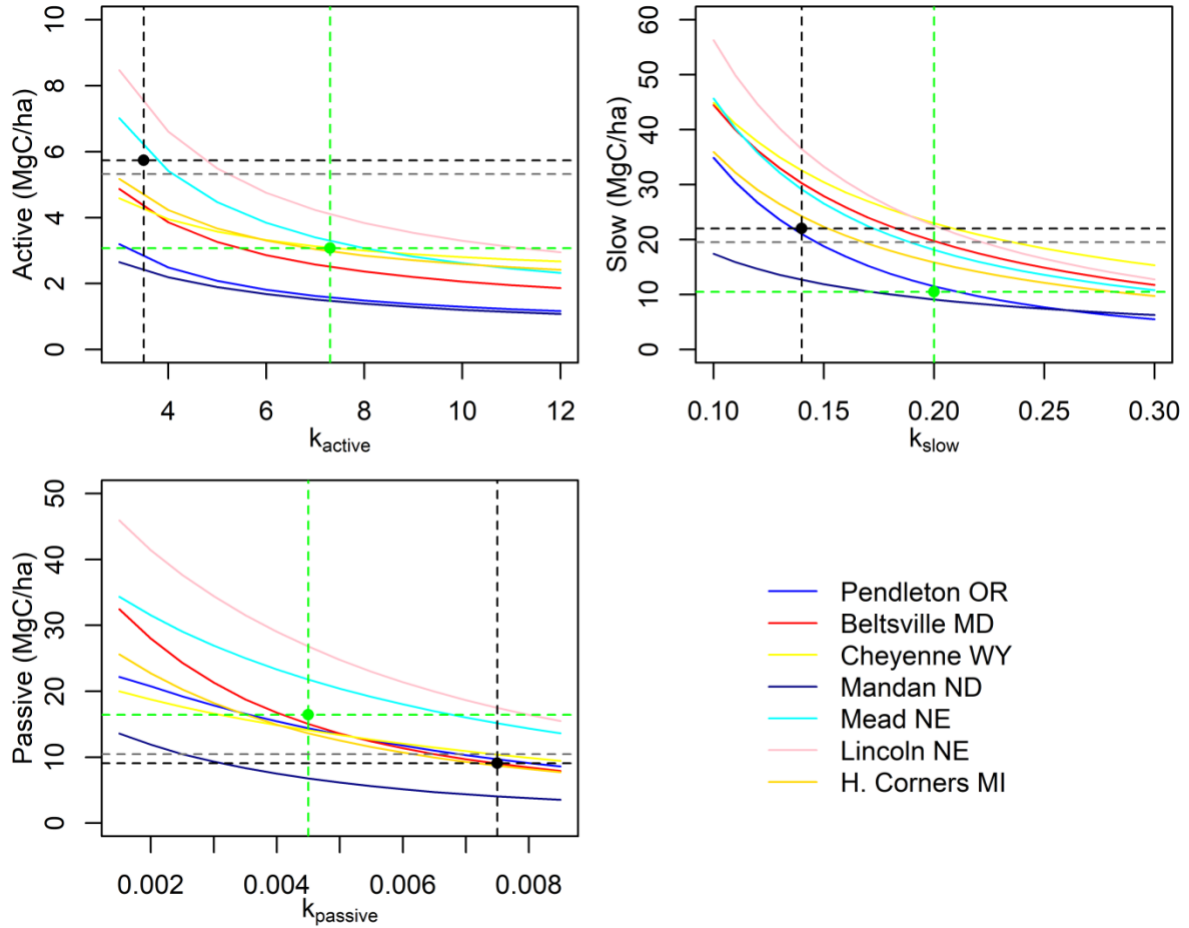


**Figure 1.** Parameterization of  $k_{active}$ ,  $k_{slow}$  and  $k_{passive}$  using carbon fractions predicted across long term research sites. The dashed black line represents the potential decomposition rates ( $k$ ) that is optimized when the absolute difference between the  $DC_{mod}$  simulated SOC in different pools and the predicted C fractions is minimum. The dashed green line represents the size of different soil SOC pools using the default  $k$  value based on  $DC_{def}$  model. The dashed grey line is the average POC (i.e. active), MAOC (i.e. slow) and PyC (i.e. passive) predicted using the combination of diffuse reflectance spectroscopy and machine learning at seven long term research sites {Citation}.

## 2.5 Model parameterization

In this study, we performed a grid search to parameterize the potential decomposition rates for respective soil pools by running the DAYCENT at seven long-term research sites (Figure 1; Table

2), and compare the simulated SOC in active, slow, and passive pools with the POC, MAOC and PyC fractions. In the current DAYCENT model, total SOC is defined as follows:

$$SOC_{total} = SOC_{strc} + SOC_{metab} + SOC_{active} + SOC_{slow} + SOC_{passive} \quad (1)$$

Where,

$SOC_{strc}$  = structural SOC pool

$SOC_{metab}$  = metabolic SOC pool

$SOC_{active}$  = active SOC pool

$SOC_{slow}$  = slow SOC pool

$SOC_{passive}$  = passive SOC pool

Each of the above SOC pool has a specific potential decomposition rates that determines the time (ranging from years to centuries) until decomposition. Plant material is transferred to the active, slow and passive pools from aboveground and belowground litter pools and three dead pools. Total C flow ( $CF_{act}$ ) out of the active pool is a function of potential decomposition rates modified by the effect of moisture, temperature, pH, and soil texture.

$$CF_{act} = k_{act} \times SOC_{act} \times bg_{dec} \times clt_{act} \times text_{ef} \times anerb_{dec} \times pH_{eff} \times dtm \quad (2)$$

Where,

$CF_{act}$  = the total amount of C flow out of the active pool (g C m<sup>-2</sup>)

$k_{act}$  = intrinsic decomposition rate of the active pool (yr<sup>-1</sup>)

$SOC_{act}$  = SOC in the active pool (g C m<sup>-2</sup>).

$bg_{dec}$  = the effect of moisture and temperature on the decomposition rate (0-1)

$clt_{act}$  = the effect of cultivation on the decomposition rate for crops (0-1) for the active pool

$text_{ef}$  = the effect of soil texture on the decomposition rate (0-1)

$anerb_{dec}$  = the effect of anaerobic conditions on the decomposition rate (0-1)

360  $pH_{eff}$  = the effect of pH on the decomposition rate (0-1)

361  $dtm$  = the time step (fraction of year)

362 The respiratory loss when the active pool decomposes is calculated as:

$$363 \quad CO_{2(act)} = CF_{act} \times p1CO_2 \quad (3)$$

364 Where,

365  $CO_{2(act)}$  = respiratory loss from the  $SOC_{act}$  pool (g C m<sup>-2</sup>)

366  $p1CO_2$  = scalar that control respiratory CO<sub>2</sub> loss computed as a function of intercept and slope

367 parameters modified by soil texture

368 The C flow from active to passive pool is then computed as:

$$369 \quad CF_{act2pas} = CF_{act} \times fps1s3 \times (1 + animpt \times (1 - anerb)) \quad (4)$$

370 Where,

371  $CF_{act2pas}$  = C flow from the active to the passive pool (g C m<sup>-2</sup>)

372  $fps1s3$  = impact of soil texture on the C flow (0-1)

373  $animpt$  = the slope term that controls the effect of soil anaerobic condition on C flows from active

374 to passive pool (0-1)

375  $anerb$  = effect of anaerobic condition on decomposition computed as a function of soil available

376 water and potential evapotranspiration rates

377 The C flow from active to the slow pool is then computed as the difference between total C flow

378 out of the active pool, respiratory CO<sub>2</sub> loss, C flow from active to passive pool and C lost due to

379 leaching. Mathematically,

$$380 \quad CF_{act2slo} = CF_{act} - CO_{2(act)} - CF_{act2pas} - C_{leach} \quad (5)$$

381 Where,

382  $C_{leach}$  = C lost due to leaching calculated as a function of leaching intensity (0-1) and soil texture



Likewise, total C flow ( $CF_{slo}$ ) out of the slow pool is a function of potential decomposition rates modified by the effect of moisture, temperature, pH, and soil texture.

$$CF_{slo} = k_{slo} \times SOC_{slo} \times bg_{dec} \times clt_{slo} \times anerb_{dec} \times pH_{eff} \times dtm \quad (6)$$

$k_{slo}$  = intrinsic decomposition rate of the slow pool ( $yr^{-1}$ )

$SOC_{slo}$  = SOC in the slow pool ( $g\ C\ m^{-2}$ ).

$clt_{slo}$  = the effect of cultivation on the decomposition rate for crops (0-1) for the slow pool

The respiratory loss when the slow pool decomposes is calculated as:

$$CO_{2(slo)} = CF_{slo} \times p2CO_2 \quad (7)$$

Where,

$CO_{2(slo)}$  = respiratory loss from the  $SOC_{slo}$  pool ( $g\ C\ m^{-2}$ )

$P2CO_2$  = parameter that controls decomposition rates of the slow pool (0-1)

The C flow from slow to passive pool is then computed as:

$$C_{slo2pas} = CF_{slo} \times fps2s3 \times (1 + animpt \times (1 - anerb)) \quad (8)$$

Where,

$fps2s3$  = impact of soil texture on decomposition (0-1)

The C flow from slow to active pool is then computed as a difference between total C flow out of the slow pool, respiratory CO<sub>2</sub> loss and total C flow from slow to passive pool. Mathematically,

$$CF_{slo2act} = CF_{act} - CO_{2(slo)} - C_{slo2pas} \quad (9)$$

Likewise, total C flow ( $CF_{pas}$ ) out of the passive pool is a function of potential decomposition rates modified by the effect of moisture, temperature and pH.

$$C_{pas} = k_{pas} \times SOC_{pas} \times bg_{dec} \times clt_{pas} \times pH_{eff} \times dtm \quad (10)$$

Where,

$k_{pas}$  = intrinsic decomposition rate of the passive pool ( $yr^{-1}$ )

406  $SOC_{pas}$  = SOC in the slow pool (g C m<sup>-2</sup>).

407  $clt_{pas}$  = the effect of cultivation on the decomposition rate for crops (0-1) for the passive pool

408 The  $CF_{pas}$  is either lost through respiratory processes or transferred to the active pool using the  
409 following equation:

$$410 \quad CO_{2(pas)} = CF_{pas} \times p3co2 \quad (11)$$

$$411 \quad CF_{pas2act} = CF_{pas} \times (1 - p3co2) \quad (12)$$

412 Where,

413  $CO_{2(pas)}$  = respiratory loss from the passive SOC pool (g C m<sup>-2</sup>)

414  $p3co2$  = parameter that control decomposition rates of passive pool (0-1)

415  $CF_{pas2act}$  = C flow from passive to active pool (g C m<sup>-2</sup>)

416 Since DAYCENT is a donor-controlled model and changes in organic matter are primarily driven  
417 by a top down approach, we first parameterize the active soil pool by comparing the simulated  
418 SOC in the active pool against POC predicted using diffuse reflectance spectroscopy. During the  
419 parameterization process, we varied the potential decomposition rates ( $k_{active}$ ) by running the model  
420 to equilibrium under native vegetation for 2000 years. We then used site history at seven long-  
421 term research sites to create schedule files and simulate the effects of historical cropping systems,  
422 land use change, land management and grazing practices on the active SOC. The potential  
423 decomposition rates for the active soil pool were optimized when the absolute difference between  
424 the average of SOC in the active pool and the POC for the top 20 cm across all sites was minimum.  
425 We repeated the above process for parameterizing the slow- and passive-carbon pools by  
426 comparing it with MOAC and PyC, respectively. Similar to the active pool, we performed a grid  
427 search using the existing parameters based on the default model that controls the potential  
428 decomposition rates ( $k_{slow}$  and  $k_{passive}$ ) of the slow- and passive-pools. We then optimized the

parameter by using the potential decomposition rates that provides the minimum difference in the absolute values across all sites.

## **2.6 Model calibration and simulation procedure**

The DAYCENT model has been well calibrated across a range of climatic, environmental, and land use gradients for different crop and grassland types. Details of the calibration procedure can be found in Hartman et al. (2011). Briefly, adjustment of key model parameters that control plant growth and SOM changes were made by changing the schedule files at each point in time. For example, transitioning to higher yielding corn varieties occurred in 1936, while the short and semi-dwarf wheat varieties were introduced in the 1960s. During the calibration process, model parameters that control the maximum photosynthetic rate and grain to stalk ratio were adjusted within realistic limits to account for improvement in crop varieties. Additionally, adjustments in the schedule files were made to account for residue removal in early years, while residues were retained in later years, thereby increasing nutrient input to the soils. These calibration strategies have allowed to better capture crop dynamics in the US Great Plains region (Hartman et al., 2011). Model simulation begins with the equilibrium run starting from year zero to year 1894 by repeating daily climate data from 1895-2005 and native vegetation without disturbance or land use change. Following the equilibrium run, we performed a historical simulation to quantify the effects of land use history, land management practices, and climate change on the evolution of SOC during 1895-2005. Finally, we performed future simulations using two climate scenarios (RCP4.5 and RCP8.5) and A2 LCLUC, with land management practices (i.e. irrigation, fertilization, tillage practices, and crop rotation) held at 2005 levels during 2006-2100.

## 2.7 Model validation at site and regional scales

The performance of the calibrated model was assessed by comparing simulated SOC in the active, slow, and passive pools against predictions of POC, MAOC and PyC, respectively, at the seven long-term research sites. In the validation procedure, we ran the model at these sites using plant growth and soil parameters determined from model calibration, but with changing climate, environmental, and land use data based on the land use history of the respective sites. For all the sites, we compared the distribution of SOC in different pools and evaluated model performance using linear regression and the goodness-of-fit statistics (bias,  $R^2$ , RMSE).

We also compared the distribution of SOC simulated using DAYCENT against the machine learning model-based predictions of POC, MAOC, and PyC for the US Great Plains ecoregion (Sanderman et al., 2021). Additionally, we compared simulated total SOC against two other SOC maps for the contemporary period (Hengl et al., 2017; Ramcharan et al., 2018).

## 2.8 Historical and future changes in SOC stocks

To quantify the effect of the new parameterization scheme linking measurable soil C pools with conceptual active, slow, and passive pools from the DAYCENT, we designed two scenarios. In the first scenario, we ran the model using the default ( $DC_{def}$ ) and the modified ( $DC_{mod}$ ) model that links conceptual pools with C fraction during the historical period (1895-2005) to quantify the differences in SOC across different pools associated with different parameterization. In the second scenario, we performed future simulations to understand if the different model structures ( $DC_{def}$  versus  $DC_{mod}$ ) result in different effects of climate and LCLUC on SOC stocks. We used the IPCC AR5 RCP8.5 and RCP4.5 climate scenarios and the IPCC AR4 A2 LCLUC scenarios to quantify the effects of future climate and LCLUC change on SOC stocks. The RCP8.5 corresponds to the pathway that tracks current global trajectories of cumulative  $CO_2$  emissions ( $CO_2$  levels reaching

960 ppm by 2100) with the assumption of high population growth and modest rates of technological change and energy intensity improvements (Riahi et al., 2011; Schwalm et al., 2020). The RCP4.5 is a modest emission scenario with CO<sub>2</sub> levels reaching 540 ppm by 2100 under the assumption of shift toward low emission technologies and the deployment of carbon capture and geologic storage technology (Thomson et al., 2011). The A2 land cover scenario emphasizes rapid population growth and economic development, and resembles closely to the RCP8.5 scenario. We used the AR4 for LCLUC because Sohl et al. (2012) data were available at high resolution and allowed for smoother transition between land cover types when moving from historical to future A2 LCLUC scenarios. The purpose of the second scenario is to better understand the response of SOC to future climate and LCLUC and examine the effect of the new model modification on the projected change in total SOC through 2100.

### 3. Results and Discussion

By quantifying the size and distribution of conceptual SOC pools of ecosystem models using a combination of diffuse reflectance spectroscopy and machine learning, we were able to modify DAYCENT by relating the conceptual active, slow and passive pools with measurable POC, MAOC and PyC fractions (section 3.1). Model modification led to more accurate representation of the magnitude and distribution of SOC (section 3.2) and was necessary to accurately quantify the legacy effect of previous land use under a changing climate and reproduce current SOC stocks compared to the default model (section 3.3). Projection of future SOC change show that the default model underestimates the SOC loss in response to climate and land cover change by 31% and 29% for croplands and grasslands, respectively (section 3.4). Overall, our results demonstrate that relating the pools sizes from the ecosystem model with C fraction data is

necessary to better initialize SOC pool and simulate SOC response to climate and land use into the future.

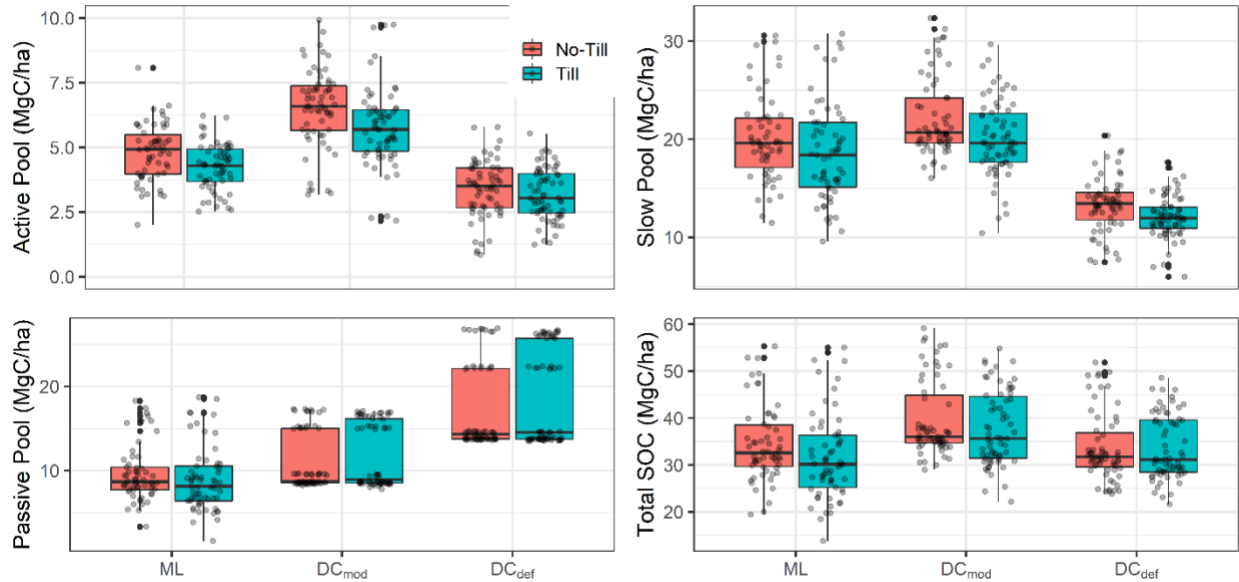


**Figure 2.** Comparison of the machine learning (ML) and DAYCENT simulated SOC using the modified ( $DC_{mod}$ ) and default ( $DC_{def}$ ) models at long-term research sites with a known cropping history. The black dots in the boxplot represent the SOC at the various sites plotted by adding a random value such that they do not overlap with each other.

### 3.1 Model evaluation of total SOC and the distribution of SOC at long-term research sites

The modified model ( $DC_{mod}$ ) linking conceptual soil pools to measurable C fractions showed better representation of the distribution of C stocks across different pools compared to the default model ( $DC_{def}$ ) (Figures 2 & 3). When the mean SOC at these sites were compared to  $DC_{mod}$  and  $DC_{def}$  simulated SOC,  $DC_{mod}$  had better fit ( $R^2 = 0.52$ ) and lower RMSE ( $8.49 \text{ Mg C ha}^{-1}$ ) compared to  $DC_{def}$  ( $R^2 = 0.40$ ; RMSE =  $8.93 \text{ Mg C ha}^{-1}$ ) (Figure S5). The mean SOC based on observation for these sites was  $38.96 \text{ Mg C ha}^{-1}$ , which is comparable to the sum of predicted C fractions ( $37.07 \text{ Mg C ha}^{-1}$ ) and simulated SOC using  $DC_{mod}$  ( $42.30 \text{ Mg C ha}^{-1}$ ) and  $DC_{def}$  ( $36.60 \text{ Mg C ha}^{-1}$ ) models. The  $DC_{mod}$  simulated SOC was higher than observation and machine learning based SOC

by 9 and 12%, respectively, while  $DC_{def}$  showed under-predicted SOC by 6% compared to observation. Although  $DC_{mod}$  showed a tendency toward over-prediction, assessment of the distribution of SOC demonstrated that  $DC_{mod}$  was able to better simulate the distribution of SOC in soil pools compared to  $DC_{def}$ . The  $DC_{mod}$  simulated the highest proportion of C in the slow (56%) pool followed by the passive (30%) and active (14%) pools, which is comparable to the machine learning model-based estimates of MAOC (57%), PyC (29%) and POC (14%), respectively. Unlike  $DC_{mod}$ ,  $DC_{def}$  model simulated the highest proportion of C in passive (53%), followed by slow (39%) and active (8%) pools (Table S2).

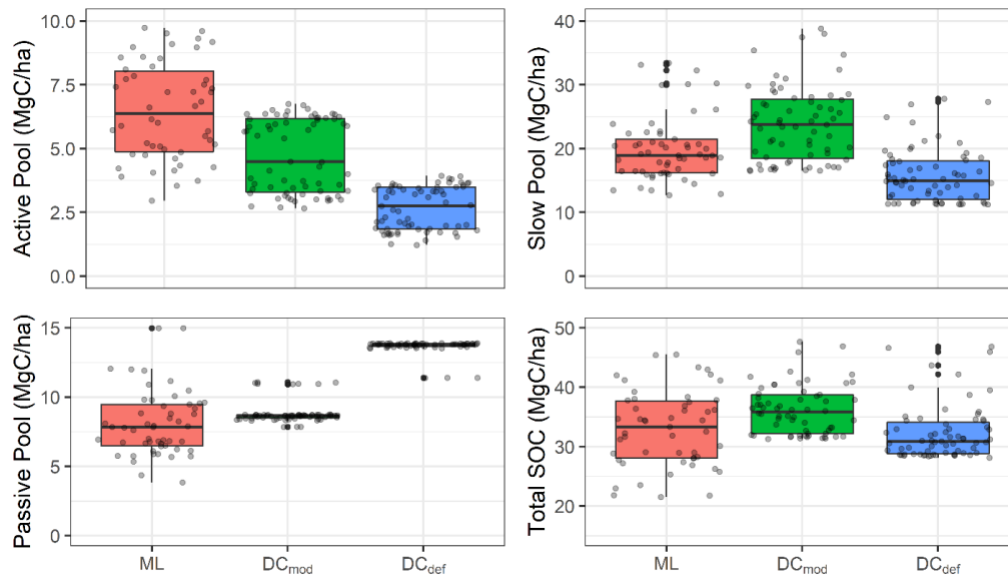


**Figure 3.** Comparison of the machine learning (ML) and DAYCENT simulated SOC using the modified ( $DC_{mod}$ ) and default ( $DC_{def}$ ) models across different pools at two long-term research sites dominated by grasslands with a known grazing history. The black dots in the boxplot represent the SOC across different sites plotted by adding a random value such that they do not overlap with each other.

Evaluation of the model performance ( $DC_{mod}$ ) for grasslands and croplands showed that the modified model ( $DC_{mod}$ ) outperformed the default model ( $DC_{def}$ ) with better model fit ( $R^2 = 0.60$ ),

lower bias ( $-1.94 \text{ Mg C ha}^{-1}$ ) and lower RMSE ( $6.7 \text{ Mg C ha}^{-1}$ ) for grasslands (Figure S6). The  $\text{DC}_{\text{mod}}$  also produced better model fit for croplands ( $R^2 = 0.48$ ), but higher bias ( $-5.84 \text{ Mg C ha}^{-1}$ ) and RMSE ( $8.86 \text{ Mg C ha}^{-1}$ ) compared to the default ( $\text{DC}_{\text{def}}$ ) model (bias =  $-0.82$  and RMSE =  $7.45 \text{ Mg C ha}^{-1}$ ). The  $\text{DC}_{\text{mod}}$  was able to better represent the distribution of C in the active, slow and passive pools for both grasslands and croplands, while  $\text{DC}_{\text{def}}$  showed large discrepancies when representing the distribution of SOC for croplands (Table S2).

The results of this exercise demonstrate that optimizing the model parameters to initialize the conceptual SOC pools by matching with C fraction data can reproduce the distribution of SOC (Figures 2 & 3), building confidence in the modeling of SOC stocks, and their pool distribution (Lee and Viscarra Rossel, 2020; Luo et al., 2016). A common approach to initializing soil C pools is based on the use of soil C steady-state conditions, which is primarily achieved by running the model over a long period of 100 to 10000 years under native vegetation. However, this approach has shown large uncertainty in the estimation of contemporary SOC partly due to differences in parameter values used to determine the initial SOC stocks, which vary many fold across models (Tian et al., 2015; Todd-Brown et al., 2014). Additionally, the size and distribution of the soil C pools are constrained by model structure and parameter values producing large differences in initial conditions, which ultimately propagates into uncertainties in historical and future projection of SOC change (Ogle et al., 2010; Shi et al., 2018). Relating these conceptual pools to measurable C fractions by optimizing parameters that control decomposition rates can help to constrain initial pool size and reduce uncertainties related to initial SOC stocks across different models (Christensen, 1996; Luo et al., 2016; Zimmermann et al., 2007). Results of this study show that tuning the potential decomposition rates within reasonable range (Figure 1) can effectively capture



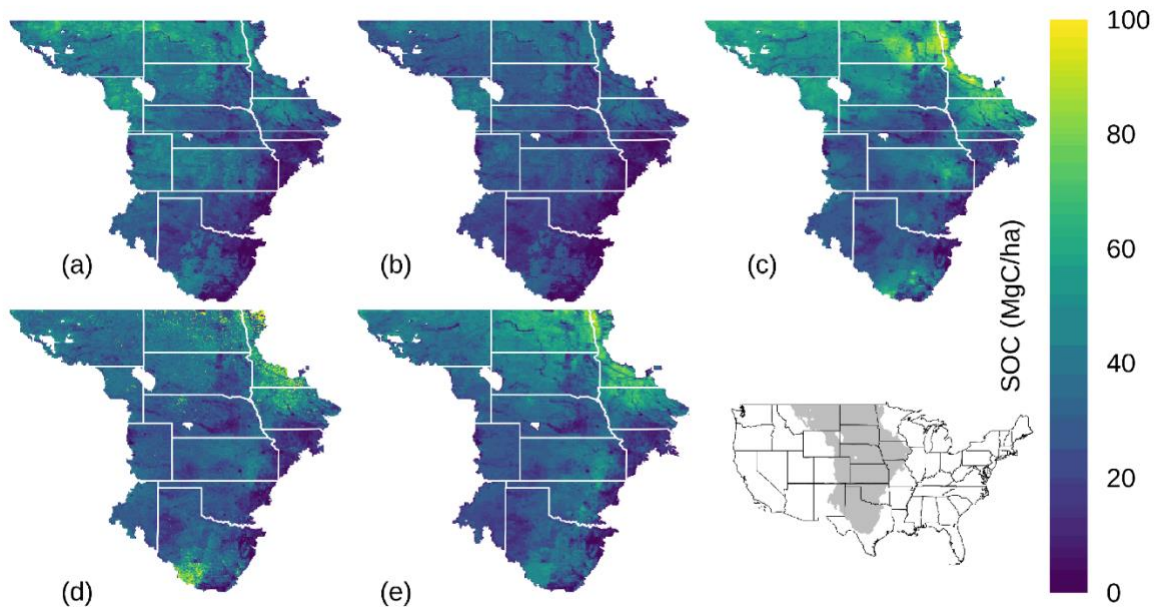
the distribution of SOC among different pools without significantly altering the magnitude of total SOC (Figures 2 & 3).

While tuning the parameters that control potential decomposition rates, active, and slow pools were adjusted by  $-3.8 \text{ yr}^{-1}$  (-52% compared to default rate) and  $-0.06 \text{ yr}^{-1}$  (-30%) respectively, and passive pool was increased by  $0.003 \text{ yr}^{-1}$  (67%) to match with C fractions data at the long-term research sites. These modifications were done such that the model was able to simulate total SOC and their distribution under current climatic, and land use conditions while also allowing to capture the legacy effect of previous land use, crop rotation, and tillage practices. It is important to note that other soil C models use C fraction data obtained under land use of varying intensities to run the model to steady state (Zimmermann et al., 2007), although soils under continuous use are in a transient state (Wieder et al., 2018). The rate and direction of SOC change can be modified by environmental factors, previous land use, and current management practices (e.g., intensity, cropping systems and fertilization/irrigation), which ultimately determine a new equilibrium or transient state (Chan et al., 2011; Van Groenigen et al., 2014). Here, we run the model to steady state conditions, and calibrated the SOC stocks to current land use and management practices by matching with C fractions data at all the sites.

### **3.2 Model evaluation of SOC stocks and their distribution at the regional scale**

Evaluation of the model performance at the regional level by comparing model simulations to three data-driven SOC maps showed that the default ( $\text{DC}_{\text{def}}$ ) model under-predicts SOC stocks for the contemporary period (2001-2005 average). The modified ( $\text{DC}_{\text{mod}}$ ) model was better able to reproduce the spatial pattern as observed in the data driven estimates of SOC (Figure 4). The  $\text{DC}_{\text{mod}}$  simulated contemporary SOC stocks of  $34.86 \text{ Mg C ha}^{-1}$  were closer to the estimates based on three data-driven models ( $32.38 - 39.19 \text{ Mg C ha}^{-1}$ ) (Figure S7). The  $\text{DC}_{\text{def}}$  simulated SOC stocks of  $26.17 \text{ Mg C ha}^{-1}$ , which is lower than the machine learning based predictions by 19-33%.

573 Interestingly, both  $DC_{def}$  and  $DC_{mod}$  were not able to reproduce the high C stocks in the  
 574 northeastern Great Plains although data driven modeling shows large SOC stocks.



575  
 576 **Figure 4.** Spatial pattern of SOC change during the contemporary period: modified ( $DC_{mod}$ ) (a),  
 577 default ( $DC_{def}$ ) (b), Sanderman et al. (2021) (c), Ramcharan et al. (2018) (d), and Hengl et al.  
 578 (2017) (e). Data-driven SOC maps were scaled by cropland and grassland distribution maps before  
 579 comparing against DAYCENT-simulated SOC.

580 Evaluation of the model performance using a scatterplot shows that calibration of active, slow, and  
 581 passive pools was necessary to produce unbiased estimates of SOC despite having slightly higher  
 582 RMSE values than the default model when compared to the different SOC data sets (Figure 5).  
 583 Among the three data driven models, Sanderman et al. (2021) also provided prediction of POC,  
 584 MAOC, and PyC in the US Great Plains region. Comparison of the distribution of SOC across  
 585 different pools indicate that the  $DC_{mod}$  was able to reproduce SOC in the slow/MAOC, and  
 586 passive/PyC pools but under-predicted the size of the active/POC pool (Figure S8).

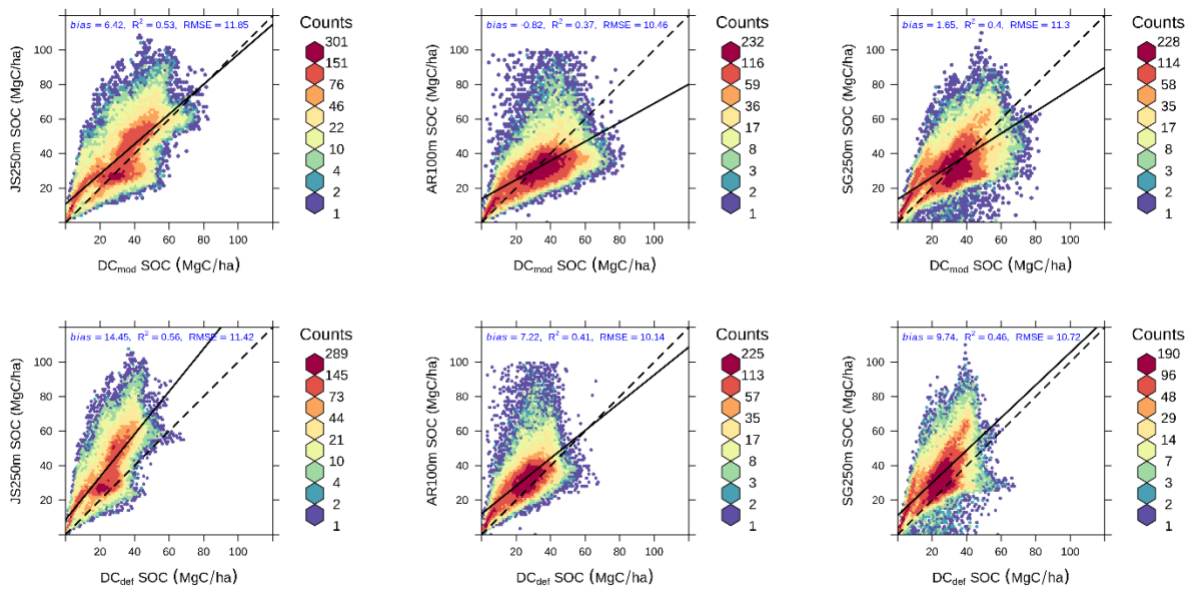


**Figure 5.** Scatter plots of the comparison of DAYCENT simulated SOC (DC<sub>mod</sub> & DC<sub>def</sub>) against Sanderman et al. (2021) – JS250m, Ramcharan et al. (2018) – AR100m, and Hengl et al. (2017) – SG250m.

While the modified (DC<sub>mod</sub>) model was able to better capture the magnitude and spatial pattern of SOC when compared against data based on machine learning models, the datasets themselves present a few challenges when comparing with the results from this study. First, these datasets were produced using the environmental covariates approach under current climatic and land use conditions, and thus represent SOC dynamics using aggregated climate, land use, and environmental conditions over a certain period. However, in the DAYCENT model, we used annual and daily time series data for climatic and land use conditions to simulate the processes that control SOM retention and stabilization, which could lead to inconsistencies when comparing results between this study and data driven products. Second, outputs based on machine learning models are sensitive to the number of samples used in the training sets. For example, machine learning-based SOC shows higher stocks in the northeastern Great Plains region compared to the DC<sub>mod</sub> or DC<sub>def</sub> models (Figure 4). This may be because the region contains thousands of shallow

seasonal wetlands with higher SOC stocks averaging between 78 to 109 Mg C ha<sup>-1</sup> to the depth of 20cm (Tangen and Bansal, 2020). Accounting for the large number of wetlands samples in the training set would likely produce higher SOC stocks in the region. We did not specifically model wetlands SOC and only considered grasslands and croplands, which cover >90% of the land area in the US Great Plains region and as such may have underrepresented these high SOC ecosystems.

### 3.3 Historical changes in SOC stocks and their distribution

When the baseline SOC (1895-1899 average) values were compared with the current (2001-2005 average) SOC stocks, the modified (DC<sub>mod</sub>) and default (DC<sub>def</sub>) models simulated a loss of 1063 Tg C (12%) and 634 Tg C (10%), respectively. On a per unit area basis, DC<sub>mod</sub> showed higher absolute (17.62 Mg C ha<sup>-1</sup>) and relative (33%) SOC losses compared to the loss of 10.60 Mg C ha<sup>-1</sup> (27%) using DC<sub>def</sub> for croplands. Grasslands showed similar patterns of higher absolute (2.51 Mg C ha<sup>-1</sup>) and relative (4%) SOC losses using DC<sub>mod</sub> compared to the loss of 1.06 Mg C ha<sup>-1</sup> (3%) using DC<sub>def</sub>. Overall, croplands showed a large and significant loss of C when compared against the baseline SOC using both models, while grasslands showed both losses and gains of SOC during 1895-2005 (Figure 6). The SOC loss from conversion of native vegetation to croplands were on average 14.70 Mg C ha<sup>-1</sup> and 9.29 Mg C ha<sup>-1</sup> using DC<sub>mod</sub> and DC<sub>def</sub>, respectively. This translates into a relative loss using DC<sub>mod</sub> that is higher than the loss using DC<sub>def</sub> by 58% during 1895-2005. For grid cells under native grasslands, DC<sub>mod</sub> simulated slightly higher average SOC loss (1.96 Mg C ha<sup>-1</sup>) compared to DC<sub>def</sub> (1.39 Mg C ha<sup>-1</sup>).

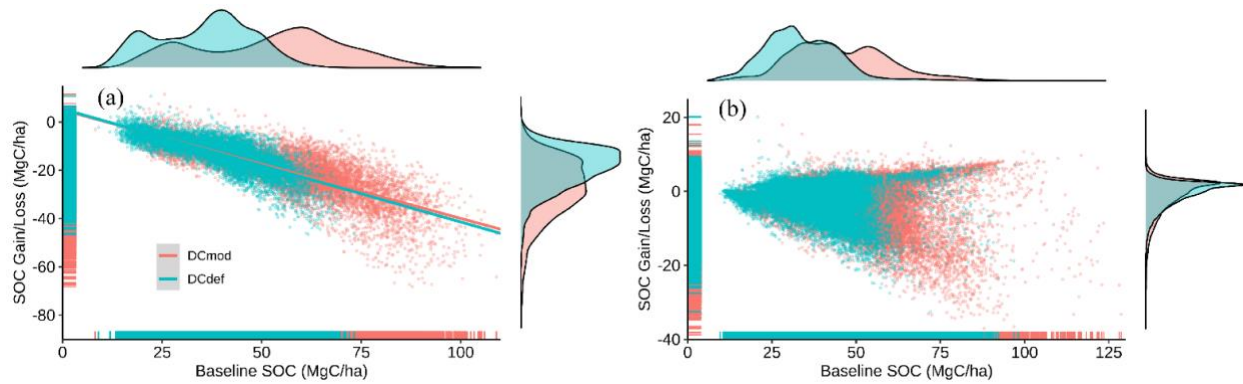
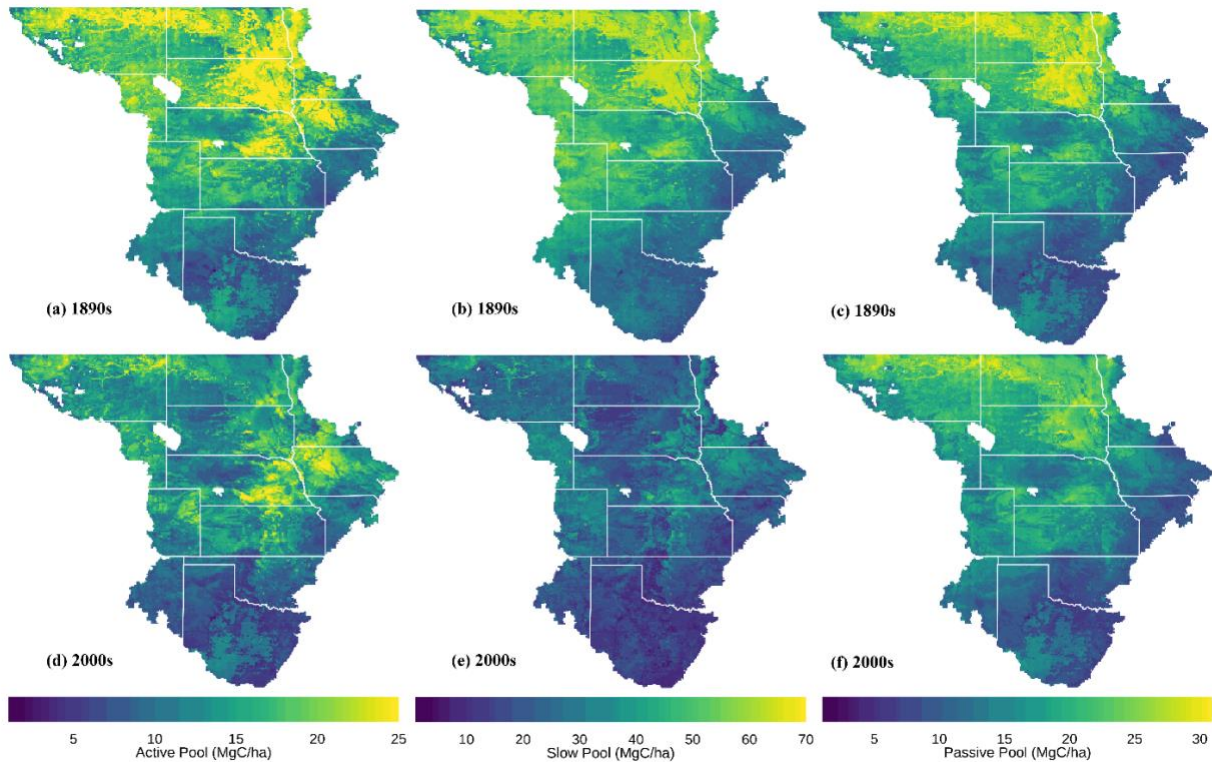


**Figure 6.** Changes in contemporary (2001-2005 average) SOC after conversion of native vegetation to croplands (a) and under native vegetation (b) as a function of baseline (1895-1899 average) SOC stocks. Negative values are losses while positive values are gains of SOC.

The simulation of total SOC stocks following historical land use under a changing climate is constrained by model parameters that determine the time until decomposition, modified by the interaction of land use intensity with changing climate (Arora and Boer, 2010; Eglin et al., 2010). Land use change can modify total SOC through its effect on individual soil pools, with the POC/active pool more vulnerable to loss compared to the MAOC/slow and PyC/passive pools (Poeplau and Don, 2013). The potential decomposition rates using the modified ( $DC_{mod}$ ) model were adjusted to match C fraction data such that higher SOC was allocated to rapid and slow cycling pools, which are more vulnerable to loss following land use change and management intensity at decadal to century time scales (Hobley et al., 2017; Sulman et al., 2018). We further compared the historical SOC loss following land use change against other studies to determine the robustness of the new parameterization using  $DC_{mod}$ . The SOC loss rate using  $DC_{mod}$  are closer to the mean 30 cm loss rate of  $17.7 \text{ Mg C ha}^{-1}$  (Sanderman et al., 2017b), and relative loss of 42-49% following conversion of forest/pasture to croplands (Guo and Gifford, 2002). However, it is important to note that these previous studies are not directly comparable with the results from this

640 study because of differences in sampling depth, the intensity of land use and the time since  
 641 disturbance.



642

643 **Figure 7.** The active, slow, and passive soil pools of SOC stocks (20 cm depth) based on the  
 644 modified ( $DC_{mod}$ ) model under native vegetation (1895-1899 average; top maps) and following  
 645 land cover land use change (2001-2005 average; bottom maps).

646 Comparison of the total SOC and its distribution in different pools between the two models  
 647 provided a more nuanced picture of the effect of new parameterization on SOC stocks and the  
 648 response of SOC to historical land use. The spatial pattern of the SOC stocks showed that the  
 649 baseline SOC in the active, slow and passive pools simulated by the modified ( $DC_{mod}$ ) model  
 650 (Figure 7) were higher than the default ( $DC_{def}$ ) model (Figure S9). As a result, there were higher  
 651 SOC losses from the active and slow pools using  $DC_{mod}$  compared to  $DC_{def}$  (Figure 7, S9). When  
 652 averaged over all pixels, the cropland SOC loss in the active, and slow, pools were 0.85, 10.09 and

gains in the passive pool was  $0.34 \text{ Mg C ha}^{-1}$ , respectively, using  $\text{DC}_{\text{def}}$ . The  $\text{DC}_{\text{mod}}$  simulated larger SOC loss for all pools with active, slow, and passive pools losing SOC by 1.48, 16.04 and  $0.09 \text{ Mg C ha}^{-1}$ , respectively. The magnitude of SOC loss from grasslands was lower compared to croplands for all three pools, with the largest SOC loss from the slow pool of 1.45 and  $0.49 \text{ Mg C ha}^{-1}$  using  $\text{DC}_{\text{mod}}$  and  $\text{DC}_{\text{def}}$  models, respectively. The distribution of SOC to different pools indicated that  $\text{DC}_{\text{def}}$  had 44%, 43% and 13% SOC in the passive, slow, and active pools for croplands, while  $\text{DC}_{\text{mod}}$  had 57% of the total SOC allocated to the slow pool, followed by the passive (23%) and active (20%) pools. For grasslands, both models were consistent in allocating the largest proportion of SOC (59% in default and 70% in modified) to slow pools, followed by passive and active pools.

The differences in the total SOC and their distribution between the models is constrained by the sensitivity of the SOC pools to environmental, climatic, and management factors (Davidson and Janssens, 2006; Dungait et al., 2012; Luo et al., 2016). The SOC stocks in the passive pool are not significantly different between the models at the regional level because the passive pool is less sensitive to environmental, climatic, and management factors, and it has a smaller contribution to total SOC (Collins et al., 2000), the SOC stocks in the passive pool were not significantly different between the models at the regional level. However, the active and slow pools respond strongly to environmental, climatic, and management constraints, which is largely driven by rapidly cycling fresh organic matter input in the active pool, and gradually decomposing detritus in the slow pool (Sherrod et al., 2005). In the  $\text{DC}_{\text{mod}}$ , the potential decomposition rates of the active and slow pools are adjusted, allowing the model to retain more SOC to match with C fraction data. This modification resulted in higher SOC stocks in these pools, which translated into higher total losses despite slower turnover rates relative to  $\text{DC}_{\text{def}}$ . Model modification was necessary not only to



match total SOC values but also to simulate the distribution of SOC into the active, slow and  
passive pools.

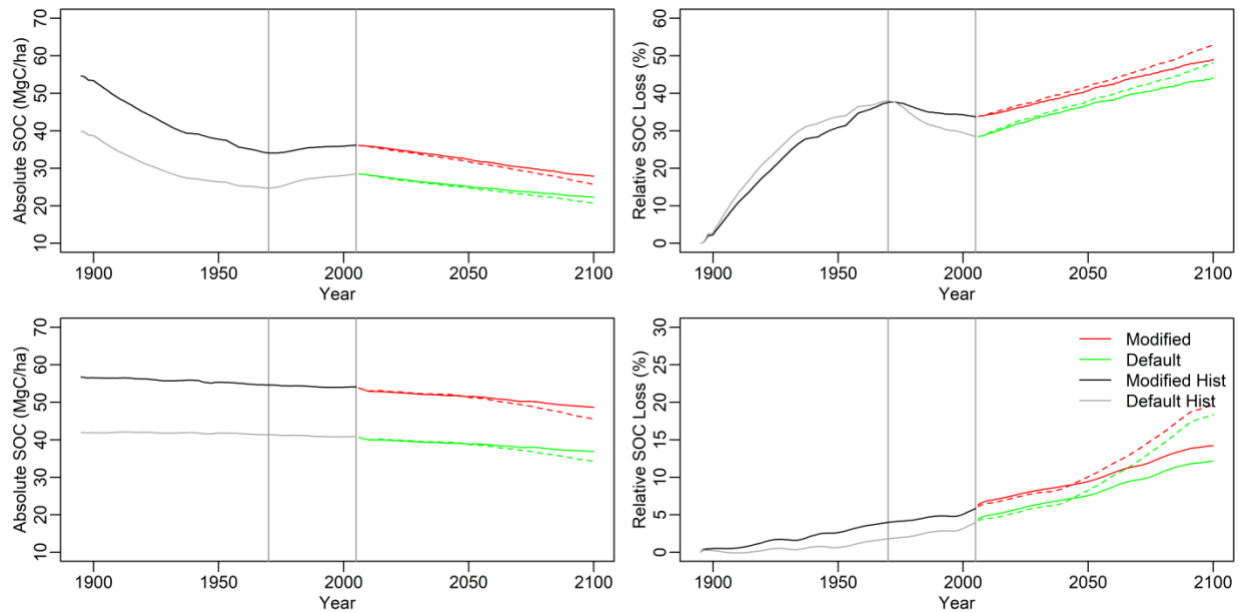


**Figure 8.** Temporal change in the absolute SOC stocks (20 cm depth) for croplands (a) and grasslands (c) and relative SOC loss compared to the 1895 SOC for croplands (b) and grasslands (d) in response to land use under a changing climate through 2100. The solid and dashed lines after 2006 represent RCP4.5 and RCP8.5 climate scenarios, respectively, both under the A2 land cover change scenario.

### 3.4 Future changes in SOC stocks and their distribution

Projection of the SOC dynamics in response to land cover change under a changing climate resulted in greater relative changes for both croplands and grasslands using the modified ( $DC_{mod}$ ) compared to the default ( $DC_{def}$ ) model (Figure 8). Despite greater rates of loss, by the end of the 21<sup>st</sup> century,  $DC_{mod}$  still simulated higher total SOC stocks compared to  $DC_{def}$  model (Table 3). By the end of 21<sup>st</sup> century, the  $DC_{mod}$  simulated total SOC stocks of 2818 and 2563 Tg C for croplands under the RCP4.5 and RCP8.5 scenarios, while the  $DC_{def}$  simulated total SOC stocks of



2266 and 2082 Tg C. Native grasslands had higher SOC stocks of 3310 and 3095 Tg C using the DC<sub>mod</sub> compared to the SOC stocks of 2505 and 2324 Tg C using the DC<sub>def</sub> under the RCP4.5 and RCP8.5 scenarios, respectively. On a per unit area basis, absolute loss (difference between the 2095s and 2000s) were slightly higher for croplands, with a mean loss rate 10.43 Mg C ha<sup>-1</sup> compared to 8.44 Mg C ha<sup>-1</sup> for grasslands using DC<sub>mod</sub> under the RCP8.5 scenario (Table 3). The DC<sub>def</sub> also simulated similar trend with slightly higher absolute losses for croplands (7.85 Mg C ha<sup>-1</sup>) compared to grasslands (6.55 Mg C ha<sup>-1</sup>) under the RCP8.5 scenario. Relative losses estimated as a percentage of contemporary SOC stocks were higher in croplands (29% for DC<sub>mod</sub> vs 28% for DC<sub>def</sub> model) compared to grasslands (16% for both DC<sub>mod</sub> and DC<sub>def</sub> model) under the RCP8.5 scenario. Using the DC<sub>mod</sub>, the SOC loss rate were 33% and 29% higher for croplands and grasslands, respectively, compared to the DC<sub>def</sub> by the end of the 21<sup>st</sup> century under the RCP8.5 scenario. While both models simulated total SOC loss over the 21<sup>st</sup> century, the difference in SOC between models sums to an additional loss of 1252 Tg SOC under the RCP8.5 scenario.

The turnover rates of SOM are primarily driven by temperature and environmental controls with significant impact on the dynamics of total SOC changes at decadal to century time scales (Knorr et al., 2005). The two model versions used the same climate and environmental data and only differ in the turnover rates of the active, slow, and passive pools. Because the sizes of active, and slow pools in the modified (DC<sub>mod</sub>) model were larger than the default (DC<sub>def</sub>) model, simulated absolute and relative losses were higher using the DC<sub>mod</sub> compared to the DC<sub>def</sub> for croplands. Larger losses using the DC<sub>mod</sub> are primarily associated with the legacy effects of management intensity and rising temperatures with larger rates of SOC loss from the active, and slow pools (Crow and Sierra, 2018) of DC<sub>mod</sub> compared to DC<sub>def</sub>. Additionally, the size of the passive pool in DC<sub>def</sub> is larger compared to DC<sub>mod</sub>, and this pool is less vulnerable to land use intensity and

warming climate compared to active and slow pools. Thus, there was a disproportionately larger SOC loss driven by the size of the slow pool and the interaction of climate and management intensity using the  $DC_{mod}$  compared to the  $DC_{def}$ , which translated into larger absolute and relative losses of SOC. For grasslands, we did not include any management driven changes. Both absolute and relative losses of SOC stocks in the grasslands are primarily driven by the warming climate (Jones and Donnelly, 2004), with active and slow pools losing more SOC stocks using  $DC_{mod}$  compared to  $DC_{def}$ . Future work should consider the interactive effects of grazing management with climate.

**Table 3.** DAYCENT (modified and default) simulated absolute changes in total and per unit area soil organic carbon (SOC) during the 2000s, 2045s and 2095s for croplands and grasslands in the US Great Plains region

Time	Total (TgC)						Per Unit Area (MgC/ha)			
	Default (DC <sub>def</sub> )			Modified (DC <sub>mod</sub> )			Default (DC <sub>def</sub> )		Modified (DC <sub>mod</sub> )	
	RCP4.5	RCP8.5		RCP4.5	RCP8.5		RCP4.5	RCP8.5	RCP4.5	RCP8.5
Croplands										
2000s		2113			2717		28.51		36.17	
2045s	1988	1938		2588	2513		25.20	24.80	32.41	31.87
2095s	2266	2082		2818	2563		22.31	20.66	27.91	25.87
Grasslands										
2000s		3891			5160		40.82		54.05	
2050s	3531	3523		4674	4659		38.90	38.80	51.51	51.34
2095s	2505	2324		3310	3095		36.88	34.27	48.65	45.61
Total		6004			7877		NA		NA	
(Croplands +	5519	5461		7262	7172		NA	NA	NA	NA
Grasslands)	4771	4406		6128	5658		NA	NA	NA	NA

Future land use, management intensity, nitrogen content, and climate interact in different ways to control C flow from soil pools with different mean residence times, which ultimately determine total SOC stocks (Deng et al., 2016; Luo et al., 2017; Sulman et al., 2018). Under a warming climate, SOC formed from fresh organic matter inputs controls the size of the active/POC pool, which is further constrained by the intensity of land use and is more vulnerable to loss (Crow and Sierra, 2018; Lavalley et al., 2020). The active/POC pool also acts as a donor to the slow/MAOC pool with C transfer and rates of SOC accumulation increasingly controlled by temperature (Crow and Sierra, 2018). In the DAYCENT, regardless of model version, the size of the active pool is relatively small as fresh organic matter is either decomposed rapidly or quickly enters the slow pool. Because the slow pool has longer residence times ranging from years to decades, the slow pool is less vulnerable to loss and can accrue C when transfer rates from the active pool exceed the rates of decomposition (Collins et al., 2000; Fontaine et al., 2007). In this study, the rates of decomposition due to rising temperatures had a stronger control on the size of the slow pool compared to the transfer of SOC from the active pool. As a result, the slow pool continued to lose SOC under projected climate changes in the future.

#### **4 Conclusions**

In this study, we developed an approach to link conceptual soil pools in biogeochemical models against C fraction data predicted using a combination of diffuse reflectance spectroscopy and machine learning. We then quantified the long-term evolution of SOC change and projected the SOC response to future climate and land cover scenarios using the modified ( $DC_{mod}$ ) model that has been calibrated to C fraction data. Our results demonstrate that matching the active, slow and passive pools against POC, MOAC and PyC data lead to better representation of total SOC stocks and the distribution of SOC into different pools. With the updated model, the long-term legacy

effect of past agricultural management results in larger absolute and relative losses of SOC compared to the default ( $DC_{def}$ ) model. Projecting the SOC response to climate and land cover change into the future (2005-2100) indicates that the new model modification ( $DC_{mod}$ ) increases SOC losses by 2100 by 32% and 28% for croplands and grasslands, respectively, under the RCP8.5 scenario compared to using the  $DC_{def}$  model.

There are several study limitations that need to be addressed in our future work. First, new modeling efforts should also consider quantifying how changes in aboveground biomass inputs quantity and quality affect SOC dynamics given mixed results in agricultural systems in response to litter inputs (Halvorson et al., 2002; Sanderman et al., 2017a). Second, current models rely on using clay content to modify rates of SOM stabilization and turnover, but recent research has shown that other soil physicochemical properties such as exchangeable calcium and extractable iron and aluminum are stronger predictors of SOM content (Rasmussen et al., 2018). Third, new modeling efforts should constrain model parameters affecting SOC dynamics by integrating them with data-driven modeling and long-term experimental data (Jandl et al., 2014). Finally, given the paucity of data related to C fractions, there is increasing need for measurement and modeling of C fractions across a wide range of environmental and management gradients (Luo et al., 2017). Despite these limitations, we have shown that models calibrated to pool sizes by matching with C fractions can improve long-term SOC predictions by more accurately representing soil C transformations in response to climate, land cover and land use change.

#### **Code and Data Availability:**

The DAYCENT model source code is available in Harvard dataverse repository (<https://dataverse.harvard.edu/dataverse/daycent45>). The new parameterization scheme and scripts for regional model simulation are available in github (<https://github.com/whrc/DAYCENT->

[soil-carbon-pools](#)). Input data for driving the models are freely available online from different sources and have been cited appropriately in the manuscript. Long term ecological data are part of United States Department of Agriculture – Agricultural Research Service and can be requested from the references listed in Table 1.

**Author Contributions:** S.D., C.S, and J.S designed the study and model development. S.D. performed model improvement, calibration, validation and regional historical and future simulation. All authors contributed to the manuscript.

**Competing Interest:** The authors declare that they have no conflict of interest.

#### **Acknowledgements**

Funding for this research was provided by USDA NIFA award #2017-67003-26481. We thank Melannie D Hartman at Colorado State University for providing access to the DAYCENT model and help with running the model. We also thank staff at the USDA National Soil Survey Center (NSSC) Kellogg Soil Survey Laboratory (KSSL) for providing access to the soil characterization database. This research also used data from the Long-Term Agroecosystem Research (LTAR) network and Columbia Plateau Conservation Research Center (CPCRC), which are both supported by the United States Department of Agriculture. The NSF Long-term Ecological Research Program (DEB 1832042) and Michigan State University AgBioResearch provided funding for the data and soil samples from the Kellogg Biological Station.

## References

- Arora, V.K., Boer, G.J., 2010. Uncertainties in the 20th century carbon budget associated with land use change. *Global Change Biology* 16, 3327–3348.
- Baker, N.T., 2011. Tillage Practices in the Conterminous United States, 1989–2004—datasets Aggregated by Watershed. US Department of the Interior, US Geological Survey Reston, Virginia.
- Baldock, J.A., Hawke, B., Sanderman, J., Macdonald, L.M., 2013a. Predicting contents of carbon and its component fractions in Australian soils from diffuse reflectance mid-infrared spectra. *Soil Research* 51, 577–595.
- Baldock, J.A., Sanderman, J., Macdonald, L.M., Puccini, A., Hawke, B., Szarvas, S., McGowan, J., 2013b. Quantifying the allocation of soil organic carbon to biologically significant fractions. *Soil Research* 51, 561–576.
- Basso, B., Gargiulo, O., Paustian, K., Robertson, G.P., Porter, C., Grace, P.R., Jones, J.W., 2011. Procedures for initializing soil organic carbon pools in the DSSAT-CENTURY model for agricultural systems. *Soil Science Society of America Journal* 75, 69–78.
- Batjes, N.H., 2016. Harmonized soil property values for broad-scale modelling (WISE30sec) with estimates of global soil carbon stocks. *Geoderma* 269, 61–68.
- Cagnarini, C., Renella, G., Mayer, J., Hirte, J., Schulin, R., Costerousse, B., Della Marta, A., Orlandini, S., Menichetti, L., 2019. Multi-objective calibration of RothC using measured carbon stocks and auxiliary data of a long-term experiment in Switzerland. *European Journal of Soil Science* 70, 819–832.
- Carvalho, N., Forkel, M., Khomik, M., Bellarby, J., Jung, M., Migliavacca, M., Saatchi, S., Santoro, M., Thurner, M., Weber, U., 2014. Global covariation of carbon turnover times with climate in terrestrial ecosystems. *Nature* 514, 213–217.
- Cavigelli, M.A., Teasdale, J.R., Conklin, A.E., 2008. Long-term agronomic performance of organic and conventional field crops in the mid-Atlantic region. *Agronomy Journal* 100, 785–794.
- Chan, K.Y., Conyers, M.K., Li, G.D., Helyar, K.R., Poile, G., Oates, A., Barchia, I.M., 2011. Soil carbon dynamics under different cropping and pasture management in temperate Australia: Results of three long-term experiments. *Soil Research* 49, 320–328.
- Christensen, B.T., 1996. Matching measurable soil organic matter fractions with conceptual pools in simulation models of carbon turnover: revision of model structure. *Evaluation of soil organic matter models* 143–159.
- Ciais, P., Sabine, C., Bala, G., Bopp, L., Brovkin, V., Canadell, J., Chhabra, A., DeFries, R., Galloway, J., Heimann, M., 2014. Carbon and other biogeochemical cycles, in: *Climate Change 2013: The Physical Science Basis. Contribution of Working Group I to the Fifth Assessment Report of the Intergovernmental Panel on Climate Change*. Cambridge University Press, pp. 465–570.
- Collins, H.P., Elliott, E.T., Paustian, K., Bundy, L.G., Dick, W.A., Huggins, D.R., Smucker, A.J.M., Paul, E.A., 2000. Soil carbon pools and fluxes in long-term corn belt agroecosystems. *Soil Biology and Biochemistry* 32, 157–168.
- Crow, S.E., Sierra, C.A., 2018. Dynamic, intermediate soil carbon pools may drive future responsiveness to environmental change. *Journal of environmental quality* 47, 607–616.
- Crowther, T.W., Todd-Brown, K.E., Rowe, C.W., Wieder, W.R., Carey, J.C., Machmuller, M.B., Snoek, B.L., Fang, S., Zhou, G., Allison, S.D., 2016. Quantifying global soil carbon losses in response to warming. *Nature* 540, 104–108.
- Czimczik, C.I., Masiello, C.A., 2007. Controls on black carbon storage in soils. *Global Biogeochemical Cycles* 21.
- Daly, C., Bryant, K., 2013. The PRISM climate and weather system—an introduction. Corvallis, OR: PRISM climate group.

- Dangal, S.R., Sanderman, J., 2020. Is Standardization Necessary for Sharing of a Large Mid-Infrared Soil Spectral Library? *Sensors* 20, 6729.
- Dangal, S.R., Sanderman, J., Wills, S., Ramirez-Lopez, L., 2019. Accurate and precise prediction of soil properties from a large mid-infrared spectral library. *Soil Systems* 3, 11.
- Davidson, E.A., Janssens, I.A., 2006. Temperature sensitivity of soil carbon decomposition and feedbacks to climate change. *Nature* 440, 165–173.
- Del Grosso, S., Ojima, D., Parton, W., Mosier, A., Peterson, G., Schimel, D., 2002. Simulated effects of dryland cropping intensification on soil organic matter and greenhouse gas exchanges using the DAYCENT ecosystem model. *Environmental pollution* 116, S75–S83.
- Del Grosso, S.J., Parton, W.J., Mosier, A.R., Hartman, M.D., Brenner, J., Ojima, D.S., Schimel, D.S., 2001. Simulated interaction of carbon dynamics and nitrogen trace gas fluxes using the DAYCENT model. *Modeling carbon and nitrogen dynamics for soil management* 303–332.
- Deng, L., Zhu, G., Tang, Z., Shangguan, Z., 2016. Global patterns of the effects of land-use changes on soil carbon stocks. *Global Ecology and Conservation* 5, 127–138.
- Doetterl, S., Stevens, A., Six, J., Merckx, R., Van Oost, K., Pinto, M.C., Casanova-Katny, A., Muñoz, C., Boudin, M., Venegas, E.Z., 2015. Soil carbon storage controlled by interactions between geochemistry and climate. *Nature Geoscience* 8, 780–783.
- Dungait, J.A., Hopkins, D.W., Gregory, A.S., Whitmore, A.P., 2012. Soil organic matter turnover is governed by accessibility not recalcitrance. *Global Change Biology* 18, 1781–1796.
- Eglin, T., Ciais, P., Piao, S.L., Barré, P., Bellassen, V., Cadule, P., Chenu, C., Gasser, T., Koven, C., Reichstein, M., 2010. Historical and future perspectives of global soil carbon response to climate and land-use changes. *Tellus B: Chemical and Physical Meteorology* 62, 700–718.
- Falcone, J.A., LaMotte, A.E., 2016. National 1-kilometer rasters of selected census of agriculture statistics allocated to land use for the time period 1950 to 2012. US Geological Survey Data Release.
- Fontaine, S., Barot, S., Barré, P., Bdioui, N., Mary, B., Rumpel, C., 2007. Stability of organic carbon in deep soil layers controlled by fresh carbon supply. *Nature* 450, 277–280.
- Gollany, H., 2016. CQESTR simulation of dryland agroecosystem soil organic carbon changes under climate change scenarios. *Synthesis and Modeling of Greenhouse Gas Emissions and Carbon Storage in Agricultural and Forest Systems to Guide Mitigation and Adaptation* 6, 59–87.
- Grandy, A.S., Sinsabaugh, R.L., Neff, J.C., Stursova, M., Zak, D.R., 2008. Nitrogen deposition effects on soil organic matter chemistry are linked to variation in enzymes, ecosystems and size fractions. *Biogeochemistry* 91, 37–49.
- Guo, L.B., Gifford, R.M., 2002. Soil carbon stocks and land use change: a meta analysis. *Global change biology* 8, 345–360.
- Halvorson, A.D., Wienhold, B.J., Black, A.L., 2002. Tillage, nitrogen, and cropping system effects on soil carbon sequestration. *Soil science society of America journal* 66, 906–912.
- Hartman, M.D., Merchant, E.R., Parton, W.J., Gutmann, M.P., Lutz, S.M., Williams, S.A., 2011. Impact of historical land-use changes on greenhouse gas exchange in the US Great Plains, 1883–2003. *Ecological Applications* 21, 1105–1119.
- Hengl, T., Mendes de Jesus, J., Heuvelink, G.B., Ruiperez Gonzalez, M., Kilibarda, M., Blagotić, A., Shangguan, W., Wright, M.N., Geng, X., Bauer-Marschallinger, B., 2017. SoilGrids250m: Global gridded soil information based on machine learning. *PLoS one* 12, e0169748.
- Hicks, W., Rossel, R.V., Tuomi, S., 2015. Developing the Australian mid-infrared spectroscopic database using data from the Australian Soil Resource Information System. *Soil Research* 53, 922–931.
- Hobley, E., Baldock, J., Hua, Q., Wilson, B., 2017. Land-use contrasts reveal instability of subsoil organic carbon. *Global Change Biology* 23, 955–965.
- Hsieh, Y.-P., 1993. Radiocarbon signatures of turnover rates in active soil organic carbon pools. *Soil Science Society of America Journal* 57, 1020–1022.



- Ingram, L.J., Stahl, P.D., Schuman, G.E., Buyer, J.S., Vance, G.F., Ganjegunte, G.K., Welker, J.M., Derner, J.D., 2008. Grazing impacts on soil carbon and microbial communities in a mixed-grass ecosystem. *Soil Science Society of America Journal* 72, 939–948.
- Jandl, R., Rodeghiero, M., Martinez, C., Cotrufo, M.F., Bampa, F., van Wesemael, B., Harrison, R.B., Guerrini, I.A., Richter Jr, D. deB, Rustad, L., 2014. Current status, uncertainty and future needs in soil organic carbon monitoring. *Science of the total environment* 468, 376–383.
- Janssens, I.A., Dieleman, W., Luyssaert, S., Subke, J.-A., Reichstein, M., Ceulemans, R., Ciais, P., Dolman, A.J., Grace, J., Matteucci, G., 2010. Reduction of forest soil respiration in response to nitrogen deposition. *Nature geoscience* 3, 315–322.
- Jarvis, A., Reuter, H.I., Nelson, A., Guevara, E., 2008. Hole-filled SRTM for the globe Version 4, available from the CGIAR-CSI SRTM 90m Database.
- Jobbágy, E.G., Jackson, R.B., 2000. The vertical distribution of soil organic carbon and its relation to climate and vegetation. *Ecological applications* 10, 423–436.
- Jones, M.B., Donnelly, A., 2004. Carbon sequestration in temperate grassland ecosystems and the influence of management, climate and elevated CO<sub>2</sub>. *New Phytologist* 164, 423–439.
- Kelly, R.H., Parton, W.J., Hartman, M.D., Stretch, L.K., Ojima, D.S., Schimel, D.S., 2000. Intra-annual and interannual variability of ecosystem processes in shortgrass steppe. *Journal of Geophysical Research: Atmospheres* 105, 20093–20100.
- Kittel, T.G., Rosenbloom, N.A., Royle, J.A., Daly, C., Gibson, W.P., Fisher, H.H., Thornton, P., Yates, D.N., Aulenbach, S., Kaufman, C., 2004. VEMAP phase 2 bioclimatic database. I. Gridded historical (20th century) climate for modeling ecosystem dynamics across the conterminous USA. *Climate Research* 27, 151–170.
- Klein Goldewijk, K., Beusen, A., Doelman, J., Stehfest, E., 2017. Anthropogenic land use estimates for the Holocene–HYDE 3.2. *Earth System Science Data* 9, 927–953.
- Knorr, W., Prentice, I.C., House, J.I., Holland, E.A., 2005. Long-term sensitivity of soil carbon turnover to warming. *Nature* 433, 298–301.
- Lal, R., 2018. Digging deeper: A holistic perspective of factors affecting soil organic carbon sequestration in agroecosystems. *Global Change Biology* 24, 3285–3301.
- Lal, R., 2004. Carbon sequestration in dryland ecosystems. *Environmental management* 33, 528–544.
- Lavallee, J.M., Soong, J.L., Cotrufo, M.F., 2020. Conceptualizing soil organic matter into particulate and mineral-associated forms to address global change in the 21st century. *Global Change Biology* 26, 261–273.
- Lee, J., Viscarra Rossel, R.A., 2020. Soil carbon simulation confounded by different pool initialisation. *Nutrient Cycling in Agroecosystems* 116, 245–255.
- Liebig, M.A., Gross, J.R., Kronberg, S.L., Phillips, R.L., 2010. Grazing management contributions to net global warming potential: A long-term evaluation in the Northern Great Plains. *Journal of Environmental Quality* 39, 799–809.
- Luo, Y., Ahlström, A., Allison, S.D., Batjes, N.H., Brovkin, V., Carvalhais, N., Chappell, A., Ciais, P., Davidson, E.A., Finzi, A., 2016. Toward more realistic projections of soil carbon dynamics by Earth system models. *Global Biogeochemical Cycles* 30, 40–56.
- Luo, Z., Feng, W., Luo, Y., Baldock, J., Wang, E., 2017. Soil organic carbon dynamics jointly controlled by climate, carbon inputs, soil properties and soil carbon fractions. *Global Change Biology* 23, 4430–4439.
- Metherell, A., Harding, L., Cole, C., Parton, W., 1994. CENTURY soil organic matter model environment, technical documentation, agroecosystem version 4.0 GPSR Technical Report No. 4. Great Plains System Research Unit, USDA-ARS, Fort Collins, CO.
- Nachtergaele, F., van Velthuisen, H., Verelst, L., 2012. Harmonized World Soil Database Version 1.2. Food and Agriculture Organization of the United Nations (FAO). International Institute for

- Applied Systems Analysis (IIASA), ISRIC-World Soil Information, Institute of Soil Science–Chinese Academy of Sciences (ISSCAS), Joint Research Centre of the European Commission (JRC).
- Ogle, S.M., Breidt, F.J., Easter, M., Williams, S., Killian, K., Paustian, K., 2010. Scale and uncertainty in modeled soil organic carbon stock changes for US croplands using a process-based model. *Global Change Biology* 16, 810–822.
- Omernik, J.M., Griffith, G.E., 2014. Ecoregions of the conterminous United States: evolution of a hierarchical spatial framework. *Environmental management* 54, 1249–1266.
- Page, K.L., Dalal, R.C., Dang, Y.P., 2014. How useful are MIR predictions of total, particulate, humus, and resistant organic carbon for examining changes in soil carbon stocks in response to different crop management? A case study. *Soil Research* 51, 719–725.
- Parton, W.J., Hartman, M., Ojima, D., Schimel, D., 1998. DAYCENT and its land surface submodel: description and testing. *Global and planetary Change* 19, 35–48.
- Parton, W.J., Schimel, D.S., Cole, C.V., Ojima, D.S., 1987. Analysis of factors controlling soil organic matter levels in Great Plains grasslands. *Soil Science Society of America Journal* 51, 1173–1179.
- Parton, W.J., Stewart, J.W., Cole, C.V., 1988. Dynamics of C, N, P and S in grassland soils: a model. *Biogeochemistry* 5, 109–131.
- Paul, E.A., Morris, S.J., Bohm, S., 2001. The determination of soil C pool sizes and turnover rates: biophysical fractionation and tracers. *Assessment methods for soil carbon* 14, 193–206.
- Poeplau, C., Don, A., 2013. Sensitivity of soil organic carbon stocks and fractions to different land-use changes across Europe. *Geoderma* 192, 189–201.
- Ramcharan, A., Hengl, T., Nauman, T., Brungard, C., Waltman, S., Wills, S., Thompson, J., 2018. Soil property and class maps of the conterminous United States at 100-meter spatial resolution. *Soil Science Society of America Journal* 82, 186–201.
- Ramirez-Lopez, L., Behrens, T., Schmidt, K., Stevens, A., Demattê, J.A.M., Scholten, T., 2013. The spectrum-based learner: A new local approach for modeling soil vis–NIR spectra of complex datasets. *Geoderma* 195, 268–279.
- Rasmussen, C., Heckman, K., Wieder, W.R., Keiluweit, M., Lawrence, C.R., Berhe, A.A., Blankinship, J.C., Crow, S.E., Druhan, J.L., Pries, C.E.H., 2018. Beyond clay: towards an improved set of variables for predicting soil organic matter content. *Biogeochemistry* 137, 297–306.
- Riahi, K., Rao, S., Krey, V., Cho, C., Chirkov, V., Fischer, G., Kindermann, G., Nakicenovic, N., Rafaj, P., 2011. RCP 8.5—A scenario of comparatively high greenhouse gas emissions. *Climatic change* 109, 33–57.
- Sanderman, J., Baldock, J.A., Dangal, S.R., Ludwig, S., Potter, S., Rivard, C., Savage, K., 2021. Soil organic carbon fractions in the Great Plains of the United States: an application of mid-infrared spectroscopy. *Biogeochemistry* 1–18.
- Sanderman, J., Creamer, C., Baisden, W.T., Farrell, M., Fallon, S., 2017a. Greater soil carbon stocks and faster turnover rates with increasing agricultural productivity. *Soil* 3, 1–16.
- Sanderman, J., Hengl, T., Fiske, G.J., 2017b. Soil carbon debt of 12,000 years of human land use. *Proceedings of the National Academy of Sciences* 114, 9575–9580.
- Sanford Jr, R.L., Parton, W.J., Ojima, D.S., Lodge, D.J., 1991. Hurricane effects on soil organic matter dynamics and forest production in the Luquillo Experimental Forest, Puerto Rico: results of simulation modeling. *Biotropica* 364–372.
- Schmer, M.R., Jin, V.L., Wienhold, B.J., Varvel, G.E., Follett, R.F., 2014. Tillage and residue management effects on soil carbon and nitrogen under irrigated continuous corn. *Soil Science Society of America Journal* 78, 1987–1996.
- Schmidt, M.W., Torn, M.S., Abiven, S., Dittmar, T., Guggenberger, G., Janssens, I.A., Kleber, M., Kögel-Knabner, I., Lehmann, J., Manning, D.A., 2011. Persistence of soil organic matter as an ecosystem property. *Nature* 478, 49–56.

- Schwalm, C.R., Glendon, S., Duffy, P.B., 2020. RCP8. 5 tracks cumulative CO<sub>2</sub> emissions. *Proceedings of the National Academy of Sciences* 117, 19656–19657.
- Sherrod, L.A., Peterson, G.A., Westfall, D.G., Ahuja, L.R., 2005. Soil organic carbon pools after 12 years in no-till dryland agroecosystems. *Soil Science Society of America Journal* 69, 1600–1608.
- Shi, Z., Crowell, S., Luo, Y., Moore, B., 2018. Model structures amplify uncertainty in predicted soil carbon responses to climate change. *Nature communications* 9, 1–11.
- Sindelar, A.J., Schmer, M.R., Jin, V.L., Wienhold, B.J., Varvel, G.E., 2015. Long-term corn and soybean response to crop rotation and tillage. *Agronomy Journal* 107, 2241–2252.
- Sinsabaugh, R.L., Gallo, M.E., Lauber, C., Waldrop, M.P., Zak, D.R., 2005. Extracellular enzyme activities and soil organic matter dynamics for northern hardwood forests receiving simulated nitrogen deposition. *Biogeochemistry* 75, 201–215.
- Six, J., Conant, R.T., Paul, E.A., Paustian, K., 2002. Stabilization mechanisms of soil organic matter: implications for C-saturation of soils. *Plant and soil* 241, 155–176.
- Skjemstad, J.O., Spouncer, L.R., Cowie, B., Swift, R.S., 2004. Calibration of the Rothamsted organic carbon turnover model (RothC ver. 26.3), using measurable soil organic carbon pools. *Soil Research* 42, 79–88.
- Sohl, T.L., Sleeter, B.M., Sayler, K.L., Bouchard, M.A., Reker, R.R., Bennett, S.L., Sleeter, R.R., Kanengieter, R.L., Zhu, Z., 2012. Spatially explicit land-use and land-cover scenarios for the Great Plains of the United States. *Agriculture, Ecosystems & Environment* 153, 1–15.
- Stockmann, U., Adams, M.A., Crawford, J.W., Field, D.J., Henakaarchchi, N., Jenkins, M., Minasny, B., McBratney, A.B., De Courcelles, V. de R., Singh, K., 2013. The knowns, known unknowns and unknowns of sequestration of soil organic carbon. *Agriculture, Ecosystems & Environment* 164, 80–99.
- Sulman, B.N., Moore, J.A., Abramoff, R., Averill, C., Kivlin, S., Georgiou, K., Sridhar, B., Hartman, M.D., Wang, G., Wieder, W.R., 2018. Multiple models and experiments underscore large uncertainty in soil carbon dynamics. *Biogeochemistry* 141, 109–123.
- Syswerda, S.P., Corbin, A.T., Mokma, D.L., Kravchenko, A.N., Robertson, G.P., 2011. Agricultural management and soil carbon storage in surface vs. deep layers. *Soil Science Society of America Journal* 75, 92–101.
- Tangen, B.A., Bansal, S., 2020. Soil organic carbon stocks and sequestration rates of inland, freshwater wetlands: Sources of variability and uncertainty. *Science of The Total Environment* 749, 141444.
- Thomson, A.M., Calvin, K.V., Smith, S.J., Kyle, G.P., Volke, A., Patel, P., Delgado-Arias, S., Bond-Lamberty, B., Wise, M.A., Clarke, L.E., 2011. RCP4. 5: a pathway for stabilization of radiative forcing by 2100. *Climatic change* 109, 77–94.
- Thornton, P.E., Thornton, M.M., Mayer, B.W., Wilhelmi, N., Wei, Y., Devarakonda, R., Cook, R., 2012. Daymet: Daily surface weather on a 1 km grid for North America, 1980-2008. Oak Ridge National Laboratory (ORNL) Distributed Active Archive Center for Biogeochemical Dynamics (DAAC).
- Tian, H., Lu, C., Yang, J., Banger, K., Huntzinger, D.N., Schwalm, C.R., Michalak, A.M., Cook, R., Ciais, P., Hayes, D., 2015. Global patterns and controls of soil organic carbon dynamics as simulated by multiple terrestrial biosphere models: Current status and future directions. *Global Biogeochemical Cycles* 29, 775–792.
- Todd-Brown, K.E.O., Randerson, J.T., Hopkins, F., Arora, V., Hajima, T., Jones, C., Shevliakova, E., Tjiputra, J., Volodin, E., Wu, T., 2014. Changes in soil organic carbon storage predicted by Earth system models during the 21st century. *Biogeosciences* 11, 2341–2356.
- Torn, M.S., Kleber, M., Zavaleta, E.S., Zhu, B., Field, C.B., Trumbore, S.E., 2013. A dual isotope approach to isolate soil carbon pools of different turnover times. *Biogeosciences* 10, 8067–8081.
- Torn, M.S., Trumbore, S.E., Chadwick, O.A., Vitousek, P.M., Hendricks, D.M., 1997. Mineral control of soil organic carbon storage and turnover. *Nature* 389, 170–173.

1028 Trumbore, S.E., 1997. Potential responses of soil organic carbon to global environmental change.  
 1029 Proceedings of the National Academy of Sciences 94, 8284–8291.  
 1030 Van Groenigen, K.J., Qi, X., Osenberg, C.W., Luo, Y., Hungate, B.A., 2014. Faster decomposition under  
 1031 increased atmospheric CO<sub>2</sub> limits soil carbon storage. *Science* 344, 508–509.  
 1032 Wieder, W.R., Hartman, M.D., Sulman, B.N., Wang, Y.-P., Koven, C.D., Bonan, G.B., 2018. Carbon cycle  
 1033 confidence and uncertainty: Exploring variation among soil biogeochemical models. *Global*  
 1034 *change biology* 24, 1563–1579.  
 1035 Wiesmeier, M., Urbanski, L., Hobbey, E., Lang, B., von Lützow, M., Marin-Spiotta, E., van Wesemael, B.,  
 1036 Rabot, E., Ließ, M., Garcia-Franco, N., 2019. Soil organic carbon storage as a key function of soils-  
 1037 A review of drivers and indicators at various scales. *Geoderma* 333, 149–162.  
 1038 Zimmermann, M., Leifeld, J., Schmidt, M.W.I., Smith, P., Fuhrer, J., 2007. Measured soil organic matter  
 1039 fractions can be related to pools in the RothC model. *European Journal of Soil Science* 58, 658–  
 1040 667.  
 1041  
 1042



Journal of Advances in Modeling Earth Systems

Supporting Information for

**Improving soil carbon estimates by linking conceptual pools against measurable carbon fractions in the DAYCENT Model Version 4.5**

Shree R.S. Dangal<sup>1,\*</sup>, Christopher Schwalm<sup>1</sup>, Michel A. Cavigelli<sup>2</sup>, Hero T. Gollany<sup>3</sup>, Virginia L. Jin<sup>4</sup> & Jonathan Sanderman<sup>1</sup>

<sup>1</sup>Woodwell Climate Research Center, 149 Woods Hole Road, Falmouth, MA 02540, USA

<sup>2</sup>US Department of Agriculture - Agricultural Research Service, Sustainable Agricultural Systems Laboratory, Beltsville Agricultural Research Center, Beltsville, MD 20705, USA

<sup>3</sup>US Department of Agriculture - Agriculture Research Service, Columbia Plateau Conservation Research Center, Pendleton, OR 97810, USA

<sup>4</sup>US Department of Agriculture - Agricultural Research Service, Agroecosystem Management Research Unit, University of Nebraska-Lincoln, NE 68583, USA

*Correspondence to:* Shree R.S. Dangal (shree.dangal@unl.edu)

*\*Current Address:* School of Natural Resources, University of Nebraska-Lincoln, NE 68583

**Contents of the file:**

Figures S1-S9

Tables S1-S2

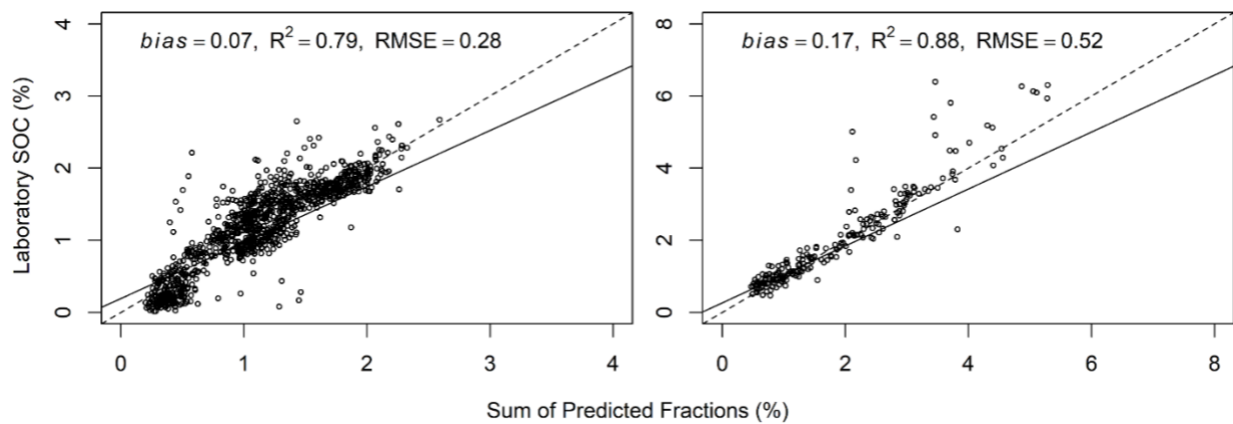


**Fig S1.** Comparison of machine learning based prediction of the sum of C fractions (POC, MAOC and PyC) against laboratory based total SOC for seven long term research sites in the continental US. The left panel figure represents croplands and the right panel figure represents grassland sites.

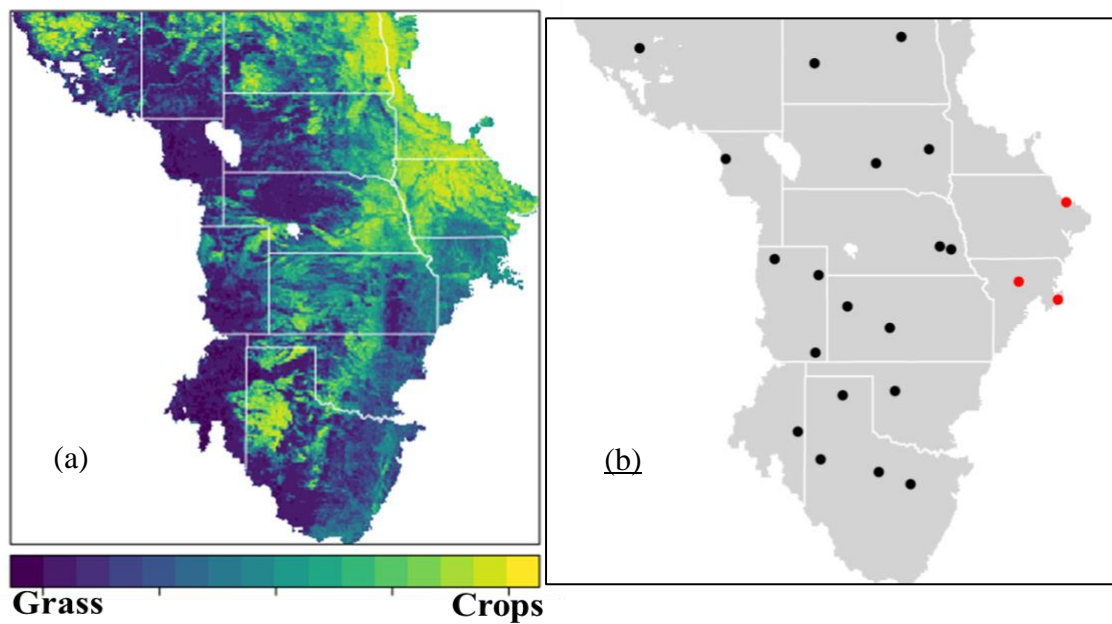


**Fig S2.** Cropland and grassland distribution (a) and distribution of the schedule files that represent different cropping systems (b) in the Great Plains region, US. The black dots in Fig. b represent 24 unique county level cropping systems and crop rotations, while the red dots represent new randomly selected grid points added to the clustering algorithm for building the unsupervised classification model.

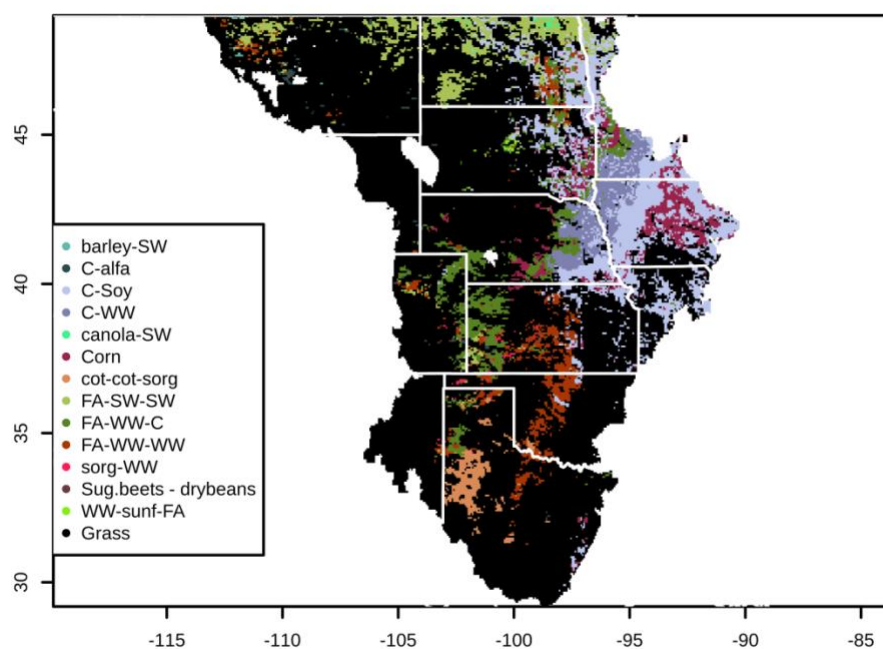


**Fig S3.** Crop rotation maps for the contemporary time period using the K-means unsupervised classification algorithm. The crop rotation map is used only when there is cropping in the given pixel. In the absence of cropping, the given pixel is assumed to be continuously grazed native grasslands.



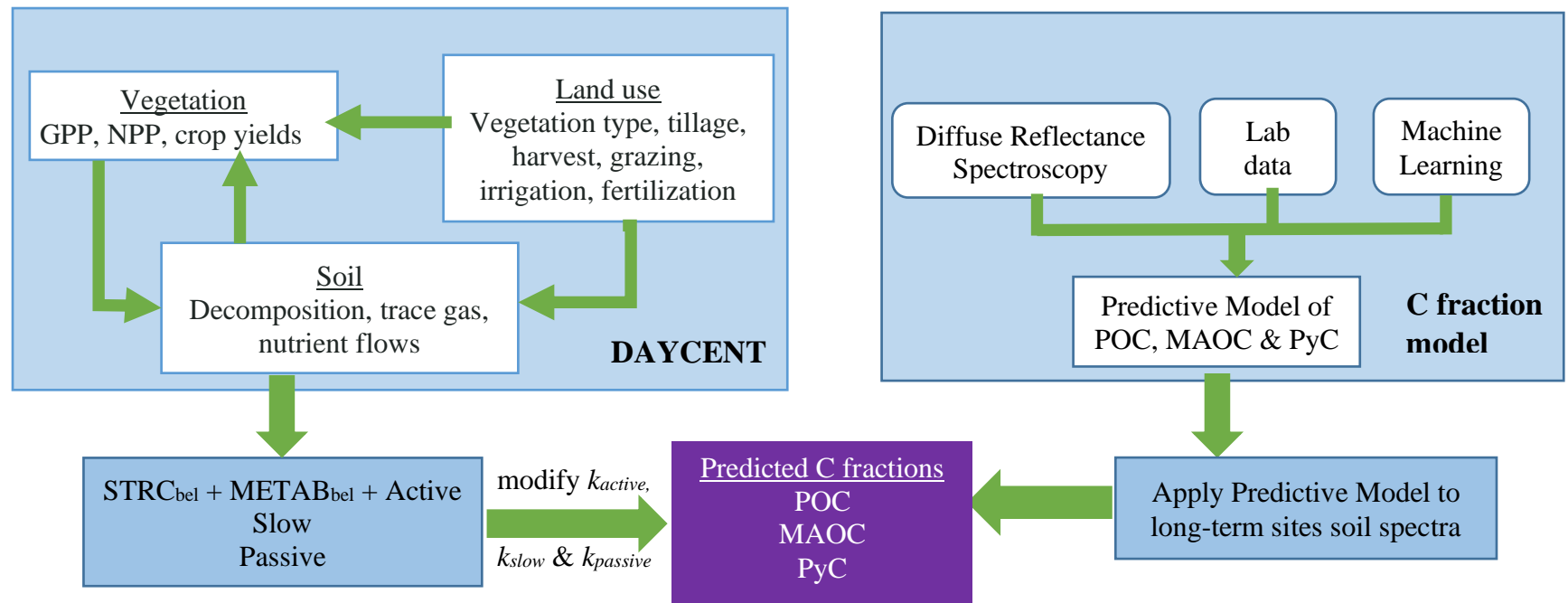


**Fig. S4.** Linking DAYCENT conceptual pools to C fraction data predicted using a combination of mid-infrared spectroscopy and a local memory-based learning approach, where STRC<sub>bel</sub> is structural, METAB<sub>bel</sub> is metabolic, Active, Slow and Passive are active, slow and passive soil C pools, and POC, MAOC and PyC are particulate, mineral associated and pyrogenic organic carbon.

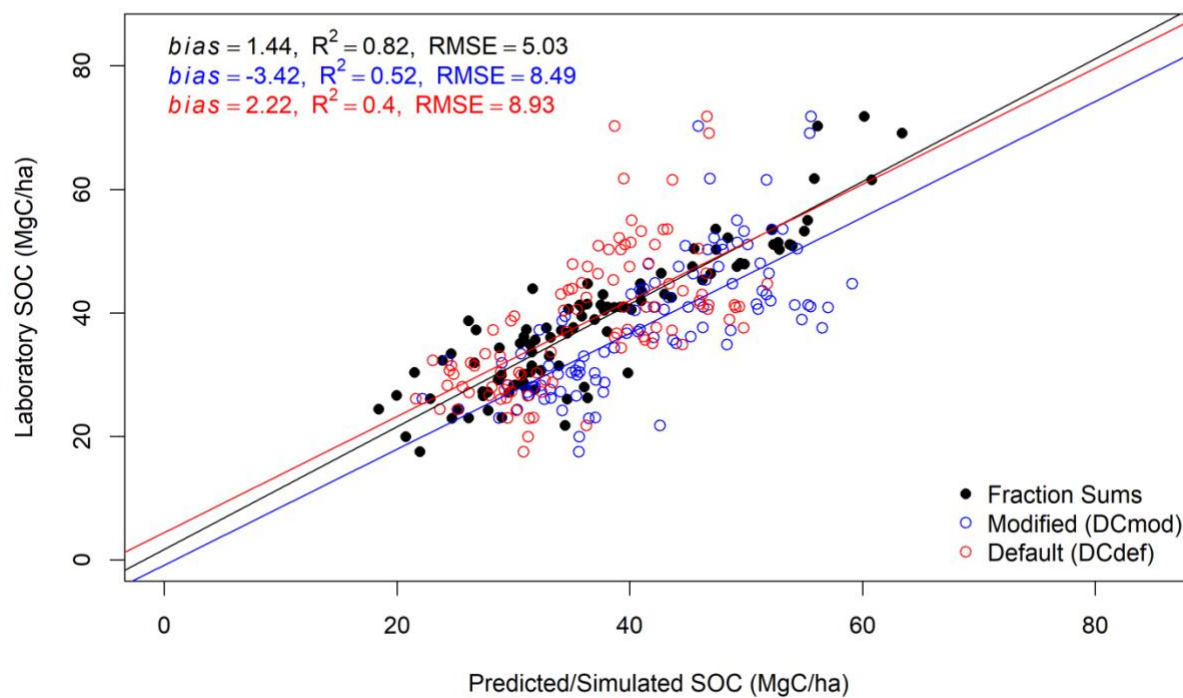


**Fig. S5.** Comparison of the sum of C fractions, DAYCENT simulated SOC using the default (DC<sub>def</sub>) and the modified (DC<sub>mod</sub>) models against laboratory based SOC estimates at the long-term research sites.

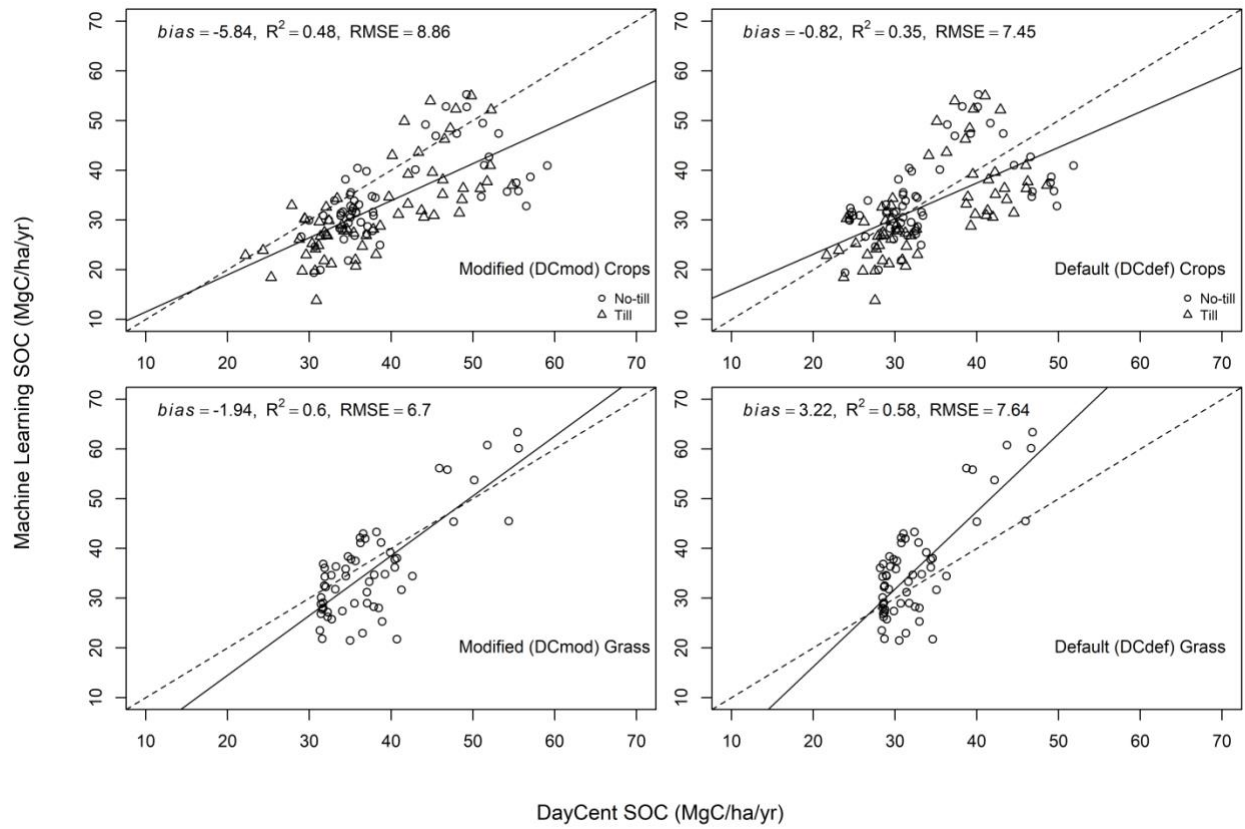


**Fig S6** Scatterplots of the comparison of modified (DC<sub>mod</sub>) and default (DC<sub>def</sub>) simulation against data-driven estimates of total SOC at the long-term research sites. The top and bottom panels show the comparison for croplands and grasslands, respectively.

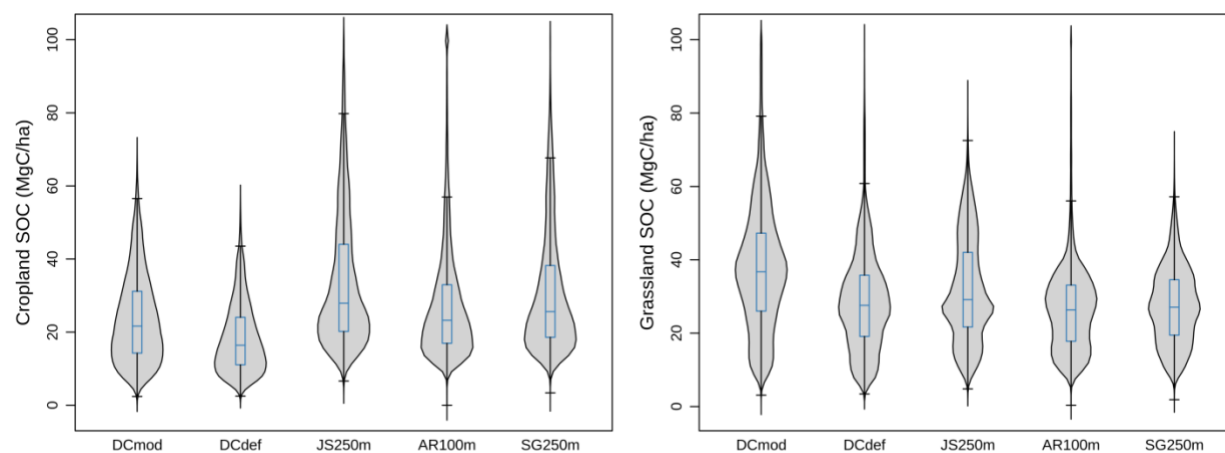


**Fig S7.** Comparison of total SOC (20 cm depth) between the DAYCENT and data driven modeling for the contemporary period. JS250, Sanderman et al. 2021; AR100m, Ramcharan et al. (2018); SG250m, Hengl et al. (2017).

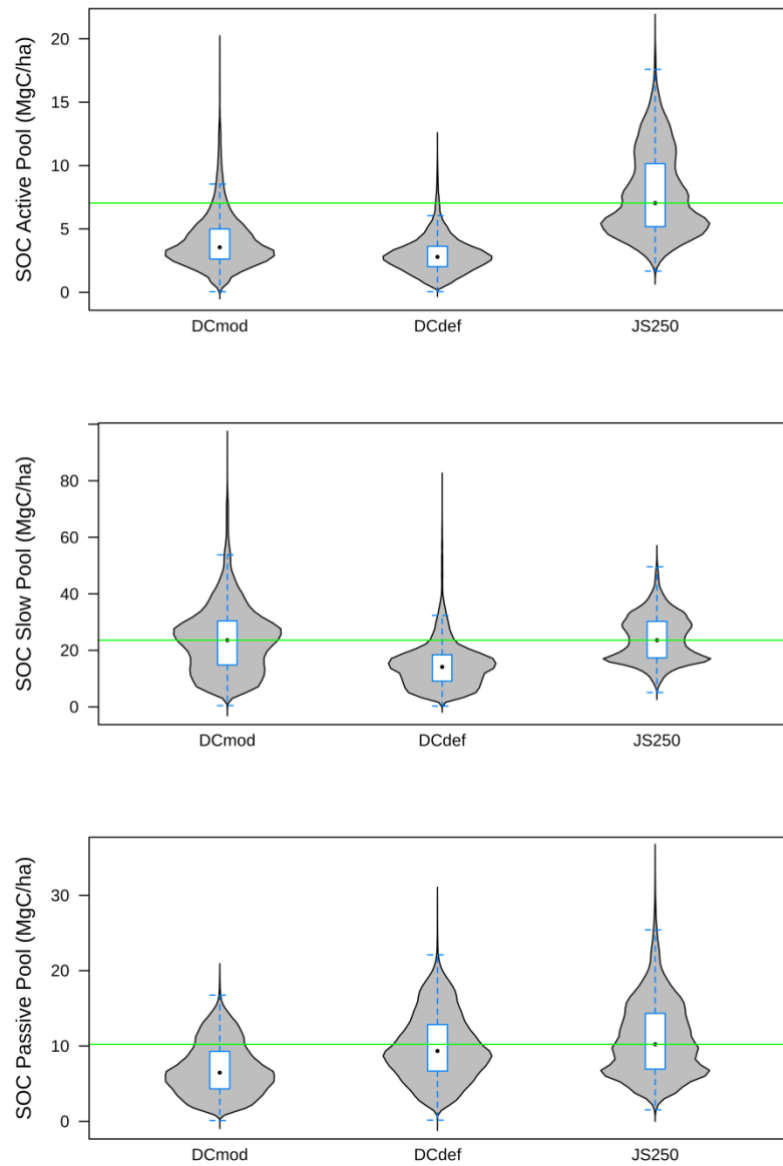


**Fig S8.** Comparison of the simulated active-, slow- and passive-SOC (20 cm depth) against Sanderman et al. (2020) for the US Great Plains Agricultural region during the contemporary period. The green line represents the median SOC values based on JS250 (Sanderman et al. 2021) C fraction predictions.

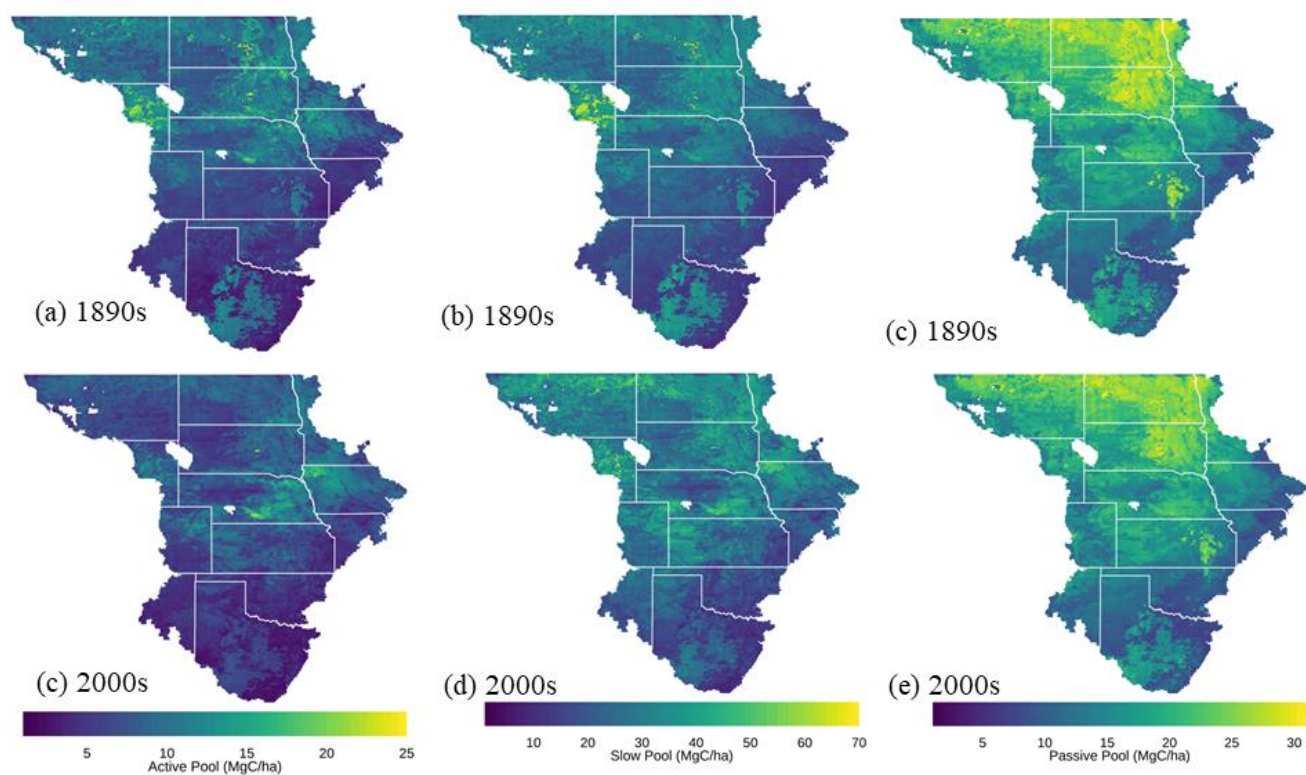


**Fig S9.** Active, slow and passive SOC pools at 20-cm depth based on the default ( $DC_{def}$ ) model under native vegetation (1895-1899 average; top maps) and following land cover land use change (2001-2005 average; bottom maps).

**Table S1.** Predictive performance of US Samples using spectra acquired on Woodwell instrument with and without calibration transfer

	No calibration transfer <sup>1</sup>			After calibration transfer <sup>1</sup>		
	Bias	R <sup>2</sup>	RMSE	Bias	R <sup>2</sup>	RMSE
POC (g/kg)	0.65	0.50	4.93	1.04	0.70	4.39
MAOC (g/kg)	0.86	0.81	3.30	0.62	0.88	2.84
PyC (g/kg)	0.38	0.49	2.83	0.29	0.68	2.29

<sup>1</sup>Leave-one-out cross validation on the 99 GP samples

**Table S2.** Distribution of SOC across different pools by plant functional types (PFTs) when compared to C fractions predictions at the long-term research sites.

	Grasslands			Croplands		
	C fractions	DC <sub>mod</sub>	DC <sub>def</sub>	C fractions	DC <sub>mod</sub>	DC <sub>def</sub>
Active	0.20	0.13	0.08	0.14	0.14	0.08
Slow	0.56	0.63	0.49	0.57	0.56	0.39
Passive	0.24	0.24	0.43	0.29	0.30	0.53



# Improving soil carbon estimates by linking conceptual pools against measurable carbon fractions in the DAYCENT Model Version 4.5

*By Shree Dangal*

1     **Improving soil carbon estimates by linking conceptual pools against measurable carbon**  
2     **fractions in the DAYCENT Model Version 4.5**

3  
4     Shree R.S. Dangal<sup>1,\*</sup>, Christopher Schwalm<sup>1</sup>, Michel A. Cavigelli<sup>2</sup>, Hero T. Gollany<sup>3</sup>, Virginia  
5     L. Jin<sup>4</sup> & Jonathan Sanderman<sup>1</sup>

6     <sup>1</sup>Woodwell Climate Research Center, 149 Woods Hole Road, Falmouth, MA 02540, USA

7     <sup>2</sup>US Department of Agriculture - Agricultural Research Service, Sustainable Agricultural  
8     Systems Laboratory, Beltsville Agricultural Research Center, Beltsville, MD 20705, USA

9     <sup>3</sup>US Department of Agriculture - Agriculture Research Service, Columbia Plateau Conservation  
10    Research Center, Pendleton, OR 97810, USA

11    <sup>4</sup>US Department of Agriculture - Agricultural Research Service, Agroecosystem Management  
12    Research Unit, University of Nebraska-Lincoln, NE 68583, USA

13  
14    *Correspondence to:* Shree R.S. Dangal (shree.dangal@unl.edu)

15    *\*Current Address:* School of Natural Resources, University of Nebraska-Lincoln, NE 68583  
16  
17  
18

19    **Key points:**

- 20    1. The modified model overestimated measured SOC values at long term research sites but  
21    better approximated derived SOC values from other data products when calibrated to  
22    carbon (C) fraction compared to the default model.  
23    2. Model modifications led to larger absolute and relative losses of SOC compared to the  
24    default model during 1895-2005.  
25    3. Under the RCP8.5 scenario, projected SOC losses with the modified model were 33%  
26    and 29% larger for croplands and grasslands, respectively, compared to the default  
27    model.

## Abstract<sup>61</sup>

Terrestrial soil organic carbon (SOC) dynamics play an important but uncertain role in the global carbon (C) cycle. Current modeling efforts to quantify SOC dynamics in response to global environmental changes do not accurately represent the size, distribution and flux of C from the soil. Here, we modified the Daily Century (DAYCENT) biogeochemical model by parameterizing conceptual SOC pools with C fraction data, followed by historical and future simulations of SOC dynamics. Results showed that simulations using modified DAYCENT (DC<sub>mod</sub>) led to better initialization of SOC stocks and distribution compared to default DAYCENT (DC<sub>def</sub>) at long-term research sites. Regional simulation using DC<sub>mod</sub> demonstrated higher SOC stocks for both croplands (34.86 vs 26.17 MgC ha<sup>-1</sup>) and grasslands (54.05 vs 40.82 MgC ha<sup>-1</sup>) compared to DC<sub>def</sub> for the contemporary period (2001-2005 average), which better matched observationally constrained data-driven maps of current SOC distributions. Projection of SOC dynamics to land cover change (IPCC AR4 A2 scenario) under IPCC AR5 RCP8.5 climate scenario showed absolute SOC loss of 8.44 and 10.43 MgC ha<sup>-1</sup> for grasslands and croplands, respectively, using DC<sub>mod</sub> whereas, SOC losses were 6.55 and 7.85 MgC ha<sup>-1</sup> for grasslands and croplands, respectively, using DC<sub>def</sub>. The projected SOC loss using DC<sub>mod</sub> was 33% and 29% higher for croplands and grasslands compared to DC<sub>def</sub>. Our modeling study demonstrates that initializing SOC pools with C fraction data led to more accurate representation of SOC stocks and individual carbon pool, resulting in larger absolute and relative SOC losses due to agricultural intensification in the warming climate.

62

## 1. Introduction

49  
50 Soil is the largest terrestrial reservoir of organic carbon (C), storing about 1500 Pg C in the top  
51 100 cm (Batjes, 2016; Nachtergaele et al., 2012). Any small changes in the magnitude,  
52 distribution and forms of terrestrial soil organic carbon (SOC) may lead to large release of C to  
53 the atmosphere (Sulman et al., 2018), with significant impact on food security and the global  
54 climate system (Lal, 2004). Given that changes in SOC represent one of the largest uncertainties  
55 in the global C budget (Ciais et al., 2014), accurate quantification of the distribution and forms of  
56 SOC can help to constrain the global C budget and provide key insights on the underlying  
57 processes related to SOC protection and cycling (Stockmann et al., 2013).  
58 Changes in SOC stocks at any given time depend on the balance between organic matter inputs  
59 via plant production, additions of manure and compost, and outputs via decomposition, erosion  
60 and hydrologic leaching of various C compounds (Davidson and Janssens, 2006; Jobbágy and  
61 Jackson, 2000). Although higher organic matter inputs to the soil generally correlate with high  
62 SOC (Sanderman et al., 2017a), the biological stability of SOC is ultimately determined by the  
63 interactions among the soil physicochemical environment (soil moisture, temperature, pH and  
64 aeration), soil mineralogy, and the accessibility of the organic matter to microbes and enzymes  
65 (Schmidt et al., 2011). Current understanding of the SOC dynamics indicates that the soil  
66 physicochemical environment plays an important role in determining the C efflux from soil and  
67 that the efflux rates are modified by substrate availability and the affinities of enzymes for the  
68 substrates (Six et al., 2002). However, the extent to which different physicochemical  
69 characteristics of soil control the stabilization and cycling of SOC is still debated (Carvalhais et  
70 al., 2014; Doetterl et al., 2015; Rasmussen et al., 2018). Additionally, the complex molecular  
71 structure of C substrates and their sensitivity to climatic and environmental constraints add

72 further complexity in understanding SOC dynamics at <sup>89</sup>different spatial and temporal scales  
 73 (Davidson and Janssens, 2006).

74 Previous studies have shown that the factors affecting the stabilization/destabilization of SOC are  
 75 numerous and that the changes in SOC over space and time are the result of complex interactions  
 76 among climatic, biotic and edaphic factors (Rasmussen <sup>10</sup>et al., 2018; Stockmann et al., 2013; Torn  
 77 et al., 1997; Wiesmeier et al., 2019). For example, Carvalhais et al. (2014) have shown that  
 78 climate, particularly temperature, strongly controls SOC turnover. Doetterl et al. (2015) found  
 79 that geochemical characteristics such as base saturation, soil texture, silica content and pH also  
 80 play a dominant role by altering the adsorption and aggregation of SOC. In addition, other  
 81 studies indicate that soil nitrogen (N) availability affects SOC change due to constraints on  
 82 microbial activity and plant productivity (Grandy <sup>78</sup>et al., 2008; Janssens et al., 2010; Sinsabaugh  
 83 et al., 2005). <sup>29</sup>These findings have led to the view that the accumulation and decomposition of  
 84 organic matter in soil is ultimately determined by the interactions among climate, vegetation  
 85 type, topography and lithology.

86 Biogeochemical models commonly rely on capturing SOC heterogeneity associated with the  
 87 complex interactions among climatic, biotic and edaphic factors by defining a number of distinct  
 88 <sup>85</sup>SOC pools with different potential turnover rates (Tian et al., 2015; Todd-Brown et al., 2014).  
 89 <sup>14</sup>The potential turnover rates of distinct soil pools are modified by climatic factors such as <sup>63</sup>soil  
 90 moisture and temperature, soil chemical factors such as pH and oxygen availability and the  
 91 <sup>88</sup>mechanism that facilitates C protection via organo-mineral interactions and aggregation, often  
 92 loosely represented by clay content (Trumbore, 1997). Each of these pools is conceptual in  
 93 nature, implying that the turnover times of these pools cannot be determined by chemical and  
 94 physical fractionation (Paul et al., 2001). As a result, there is increasing need and effort to link

95 the conceptual pools with some measurable data to determine the turnover rates of SOC pools in  
96 the biogeochemical models.

97 In current biogeochemical models, there is a general agreement that the soil organic matter  
98 (SOM) contains at least three C pools: an active pool dominated by root exudates and the rapidly  
99 decomposable components of fresh plant litter, with mean residence time (MRT) ranging from  
100 days to years (Hsieh, 1993); a slow pool dominated by decomposed organic material, often of  
101 microbial origin, with MRT ranging from years to centuries (Torn et al., 2013); and a passive  
102 pool dominated by stabilized organic matter with MRT of several hundred to thousands of years  
103 (Czimczik and Masiello, 2007). Changes in the size and relative abundance of these pools are  
104 strongly influenced by climate, soil type and land use (Sanderman et al., 2021). Therefore,  
105 accounting for accurate distribution of SOC into different pools is paramount to quantify the  
106 current SOC stocks and examine the vulnerability of SOC to future environmental changes.

107 Relating these conceptual pools with SOC partitioned into laboratory defined fractions, such as  
108 particulate-, mineral associated- and pyrogenic-forms of C (POC, MOAC and PyC,  
109 respectively), can help to constrain the turnover rate of different pools in biogeochemical  
110 models. For example, Skjemstad et al. (2004) related POC, MOAC and PyC approximated using  
111 a combination of physical size fractionation and solid-state  $^{13}\text{C}$ -NMR spectroscopy with resistant  
112 plant material (RPM), humic (HUM) and inert organic material (IOM) pools in the Rothamsted  
113 carbon (RothC) model to predict changes in SOC in response to changes in soil type, climate and  
114 management. However, RothC does not explicitly simulate plant growth and plant response to  
115 dynamic changes in climate and other environmental factors (Zimmermann et al., 2007). In  
116 addition, the plant material is loosely partitioned into decomposable and resistant forms with  
117 large uncertainties in their respective sizes (Cagnarini et al., 2019). Unlike RothC, ecosystem



<sup>121</sup> models such as Century, DeNitrification-DeComposition (DNDC) and <sup>68</sup> Agricultural Production  
118 Systems sIMulator (APSIM) integrate the effects of climate, land use change and land  
119 management practices by simulating plant physiology and soil biogeochemistry, and explicitly  
120 consider <sup>23</sup> the effects of climate, land use and land management on three conceptual soil C pools  
121 with different turnover rates (Hartman <sup>69</sup> et al., 2011; Ogle et al., 2010).  
122 In this study, we modified, calibrated and evaluated the version 4.5 of the <sup>114</sup> Daily Century model  
123 (hereafter, DAYCENT) to improve the representation of SOC dynamics by linking conceptual  
124 pools of active, slow and passive SOC against estimates of the measurable POC, MOAC and  
125 PyC fractions, respectively. We then simulated the response of SOC <sup>91</sup> to climate and land use  
126 change during the historical and future period using the default (hereafter, DC<sub>def</sub>) and modified  
127 (hereafter, DC<sub>mod</sub>) DAYCENT model <sup>67</sup> in the US Great Plains ecoregion. The objectives of this  
128 study were to 1) modify the DC<sub>def</sub> model to link active, slow and passive pools of organic C to  
129 soil C fractions; 2) calibrate and evaluate DC<sub>mod</sub> performance by comparing the distribution of C <sup>11</sup>  
130 in active, slow and passive pools against C fractions predicted at seven long-term research sites;  
131 3) evaluate the differences between the DC<sub>mod</sub> and DC<sub>def</sub> in simulating contemporary SOC stocks  
132 and their distribution by comparing against other existing data products in the US Great Plains  
133 region; and 4) project the SOC change <sup>46</sup> in response to climate and land cover change through  
134 2100. We hypothesize that (i) calibrating the conceptual pools to C fraction data in the  
135 DAYCENT model leads to more accurate initialization of equilibrium pool structure (Skjemstad  
136 et al., 2004), thereby allowing a better comparison of measured and simulated SOC in response  
137 to <sup>84</sup> climate, land use and management (Basso et al., 2011); (ii) conversion of native vegetation to  
138 any agricultural use significantly alters the distribution of SOC among the various soil pools  
139 (Guo and Gifford, 2002), but the rate and extent of SOC change depend on the intensity of  
140

141 agricultural use (Lal, 2018; Page et al., 2014), with larger losses from models that allocate more  
142 C to active and slow pools; and (iii) land use under a warming climate would result in larger  
143 absolute and relative losses of SOC from the model that derive more SOC from the active pool  
144 due to rapid decomposition of fresh organic matter induced by warming (Crowther et al., 2016).

## 145 2. Materials and methods

### 146 2.1 The DAYCENT Model

147 The DAYCENT Version 4.5 is a daily time step version of the Century biogeochemical model  
148 that simulates the dynamics of C and N of both managed and natural ecosystems (Del Grosso et  
149 al., 2002; Parton et al., 1998). The exchange of C and N among the atmosphere, vegetation and  
150 soil is a function of climate, land use, land management and other environmental factors. The  
151 vegetation pool simulates potential plant growth at a weekly time step limited by water, light and  
152 nutrients. The DAYCENT model consists of multiple pools of SOM and simulates turnover as a  
153 function of the amount and quality of residue returned to the soil, the size of different soil pools  
154 and a series of environmental limitations. The type and timing of management events including  
155 tillage, fertilization, irrigation, harvest and grazing activities can affect plant production and  
156 SOM retention.

157 The DAYCENT model was originally developed from the monthly CENTURY model version  
158 4.0. The CENTURY 4.0 is a general FORTRAN model of the plant-soil ecosystem that  
159 simulates carbon and nutrient dynamics of different types of terrestrial ecosystems (grasslands,  
160 forest, crops and savannas). CENTURY 4.0 primarily focused on simulation of soil organic  
161 matter dynamics of agro-ecosystems (Metherell et al., 1994). Earlier development of the  
162 CENTURY focused on simulation of soil organic matter dynamics of grasslands, forest and  
163 savanna ecosystems (Parton et al., 1988; Sanford Jr et al., 1991).



<sup>47</sup>  
164 The first DAYCENT model was developed in FORTRAN 77 and C from CENTURY 4.0 to  
165 simulate the exchanges of C, water, nutrients, and gases (CO<sub>2</sub>, CH<sub>4</sub>, N<sub>2</sub>O, NO<sub>x</sub>, N<sub>2</sub>) among the  
166 atmosphere, soil and plants at a daily time step (Del Grosso et al., 2001; Kelly et al., 2000;  
167 Parton et al., 1988). The submodels used in DAYCENT are described in detail by Del Grosso et  
168 al. (2001), which includes submodels for plant productivity, soil organic matter decomposition,  
169 soil water and temperature dynamics, and trace gas fluxes. Other model developments while  
170 transitioning from CENTURY 4.0 to DAYCENT included dynamic carbon allocation and  
171 changes in growing degree days routine that triggers the start and end of growing season based  
172 on phenology (soil surface temperature, air temperature, and thermal units).  
173 The first formal version DAYCENT 4.5 (Hartman et al., 2011) was developed from Del Grosso  
174 et al. (2002), with a focus on simulation of trace gas fluxes for major crop types in the US Great  
175 Plains region. Hartman et al. (2011) focused on calibrating and validating crop yield and trace  
176 gas fluxes for all the major crop types in 21 representative counties in the US Great Plains  
177 region.  
178 The SOM sub-model consists of active, slow and passive pools with different turnover times.  
179 The active pool has a short (1-5 yr) turnover time and consists of live microbes and microbial  
180 products. The slow pool has an intermediate turn over time (20-50 yr) and contains physically  
181 protected organic matter and stabilized microbial products. The passive pool has a long turnover  
182 time (400-2000 yr) with physically and chemically stabilized SOC. In DAYCENT, the turnover  
183 of the active, slow and passive pools are simulated as a function of potential decomposition rates  
184 of respective pools modified by soil temperature, moisture, clay content, pH and cultivation  
185 effects. Changes in SOC are simulated for the top 20 cm of the soil.

186 In this study, we modified the DAYCENT and developed a methodology to calibrate the size of  
187 the conceptual soil pools by comparing it with carbon fraction data at long term research sites.  
188 First, we developed measurable carbon fraction data using a combination of diffuse reflectance  
189 spectroscopy and a machine learning model (section 2.2). Second, we modified the DAYCENT  
190 model to link conceptual active, slow, and passive pools with the carbon fraction data (section  
191 2.3 & 2.4). Third, we parameterized the DAYCENT by tuning the potential decomposition rates  
192 ( $k$ ) such that the size of the active, slow and passive soil pools match with the POC, MAOC and  
193 PyC, respectively at the long-term research sites (section 2.5). Fourth, we calibrated both the  
194 default and modified DAYCENT using input data developed in section 2.3 against observed total  
195 SOC at the long-term research sites (section 2.6), followed by model validation (section 2.7) and  
196 historical and future simulations (section 2.8).

## 197 2.2 Development of carbon fraction datasets to match with soil carbon pools

198  
199 To link the SOC pools in DAYCENT with measurable C fractions, we used seven long-term  
200 research sites located in the United States (Cavigelli et al., 2008; Gollany, 2016; Ingram et al.,  
201 2008; Liebig et al., 2010; Schmer et al., 2014; Sindelar et al., 2015; Syswerda et al., 2011),  
202 which span a range of climatic, land use and land management gradients (Table 1). Six of seven  
203 research sites are part of Long-Term Agroecosystem Research (LTAR) network focused on  
204 sustainable intensification of agricultural production. The remaining site is part of Columbia  
205 Plateau Conservation Research Center (CPCRC) Long-Term Experiment (LTE). At each site, we  
206 predicted the POC, MAOC and PyC fractions using a diffuse reflectance mid-infrared (MIR)  
207 spectroscopy-based model as detailed in Sanderman et al. (2021). The predictive models for the  
208 C fractions were developed from a database of fully fractionated soil samples using a  
209 combination of physical size separation and solid-state  $^{13}\text{C}$  NMR spectroscopy (Baldock et al.,

210 <sup>2013b</sup> of Australian (Baldock et al., 2013a) and US origin (Sanderman et al., 2021). All samples  
211 for model development were scanned <sup>12</sup>using a Thermo Nicolet 6700 FTIR spectrometer with Pike  
212 AutoDiff reflectance accessory <sup>76</sup>located at the Commonwealth Scientific and Industrial Research  
213 Organization (CSIRO) in Australia. The soil samples <sup>from</sup> all the long-term research sites were  
214 scanned using <sup>3</sup>a Bruker Vertex 70 FTIR equipped with a Pike AutoDiff reflectance accessory  
215 located at Woodwell Climate Research Center in the United States. For all samples, <sup>3</sup>spectra were  
216 <sup>acquired on dried and finely milled soil samples</sup>. Since the SOC fraction model and the soil  
217 samples were scanned using different instruments, we developed a calibration transfer routine to  
218 account for the <sup>3</sup>differences in spectral responses between the CSIRO (primary) and Woodwell  
219 (secondary) instruments by scanning a common set of 285 soil samples. The calibration transfer  
220 routine was developed using piecewise direct standardization (PDS) as described in Dangal &  
221 Sanderman (2020).

222

**Table 1.** General attributes of the LTAR, LTER and CPCRC-LTE sites used for DAYCENT parameterization and calibration

Site Name	Sampling Location	Lon	Lat	T <sub>avg</sub> (°C)	Annual Precip. (mm)	Elev (m)	Land use	Data Avail.	Reference
Lower Chesa. Bay	Beltsville, MD	-76.9	39.1	12.8	1110	41	CS	1996-2016	Cavigelli et al. 2008
CPCRC-NTLTE	Pendleton, OR	-118.4	45.4	10.6	437	456	WW-FA	2005-2014	Gollany 2016
Cent. Plains Exp. Ran.	Cheyenne, WY	-104.9	41.2	8.6	425	1930	C3-C4 Gra.	2004-2013	Ingram et al. 2008
Northern Plains	Mandan, ND	-100.9	46.8	4	416	593	C3-C4 Gra.	1959-2014	Liebig et al 2010
Platte/High Plains Aq.	Lincoln, NE	-96.5	40.9	11	728	369	CC,CS	1998-2011	Sindelar et al 2015
Platte/High Plains Aq.	Mead, NE	-96.0	41.0	9.8	740	349	CC	2001-2015	Schmer et al. 2014
Kellogg Bio. Station	H. Corners, MI	-85.4	42.4	9.7	920	288	CSW-Gra.	1989-2017	Syswerda et al. 2011 <sup>‡</sup>

CS: Corn-Soya; WW: Winter Wheat; FA: Fallow; CC: Continuous Corn, SC: Soya-Corn, CSW: Corn-Soya-Wheat, Gra.: Grass  
<sup>‡</sup>H. Corners, MI is a LTER & LTAR site; CPCRC-NTLTE: Columbia Plateau Conservation Research Center No-Till Long-Term Experiment.

225 For estimating C fractions of the prediction set (i.e., soil spectra of seven long-term research  
226 sites), we used a local memory based learning (MBL) approach that fits a unique target function  
227 corresponding to each sample in the prediction set (Dangal et al., 2019; Ramirez-Lopez et al.,  
228 2013). The MBL selects spectrally similar neighbors for each sample in the prediction sets to  
229 build a unique SOC fraction model for each target sample. The spectrally similar neighbors were  
230 optimized by developing a soil C fraction model using a range of spectrally similar neighbors  
231 and selecting the neighbors that produce the minimum root mean square error based on local  
232 cross validation. Before developing the soil C fraction model, the spectra of both the calibration  
233 and prediction sets were baseline transformed. Following baseline transformation, spectral  
234 outliers were detected using F-ratios (Hicks et al., 2015). The F-ratio estimates the probability  
235 distribution function of the spectra and picks samples that fall outside the calibration space as  
236 outliers (Dangal et al., 2019). Observation data used for building the soil C fraction model were  
237 square root transformed before model development and later back-transformed when estimating  
238 the goodness-of-fit. The performance of predictive models is shown in Table S1.

239 The predicted soil C fractions for the seven long-term research sites were then converted into C  
240 fraction stocks using the relationship between C fraction (%), bulk density (BD;  $\text{g/cm}^3$ ) and the  
241 depth (cm) of soil samples. Since the BD data were not available for all long-term research sites  
242 for different crop rotation and grazing intensities, we predicted BD using methods similar to  
243 those described above. The only difference was that the samples used to develop the BD model  
244 were based on a much larger database of soil spectra scanned at the Kellogg Soil Survey  
245 Laboratory (KSSL) in Lincoln, USA (Dangal et al., 2019). Before predicting BD, the calibration  
246 transfer, as documented in Dangal & Sanderman (2020), between the KSSL and Woodwell soil  
247 spectra were developed and the local modeling approach (i.e., MBL) was used to make final

248 prediction for samples with missing laboratory BD. Calibration transfer between the  
249 spectrometers at the Woodwell (secondary instrument) and KSSL (primary instrument)  
250 laboratory was necessary to improve prediction of BD ( $R^2 = 0.46-0.64$  and RMSE = 0.26-0.50)  
251 (Dangal and Sanderman, 2020).

252 One of the technical challenges associated with the comparison of simulated pool sizes against  
253 diffuse reflectance spectroscopy-based predictions of POC, MOAC and PyC at long-term  
254 research sites was the absence of laboratory data on C fractions to validate the MIR based  
255 predictions. To address this shortcoming, we first compared the sum of the MIR based  
256 predictions of POC, MOAC and PyC against observation of total SOC available at these sites  
257 (Figure S1). When comparing the total SOC against MIR based predictions, we did not limit the  
258 comparison to 20 cm, but allowed it across the full soil depth profile <sup>110</sup>based on the availability of  
259 SOC data at the seven long-term research sites. Additionally, the laboratory data used for model  
260 comparison were available at multiple depths of up to 60 cm often without a direct measurement  
261 for the 0-20 cm depth necessitating an approximation of the 0-20 cm stock. For example, when  
262 <sup>8</sup>soils were collected from 0-15 and 15-30 cm, we estimated the 20 cm SOC stock by adding 1/3  
263 of the 15-30 cm SOC stock to the entire 0-15 cm SOC stock.

### 264 2.3 Input datasets for driving the DAYCENT model

265 The US Great Plains region was delineated using the Level I ecoregions map (Omernik and  
266 Griffith, 2014) available through the Environmental Protection Agency  
267 <sup>71</sup>(<https://www.epa.gov/eco-research/ecoregions-north-america>). The datasets for driving the  
268 DAYCENT were divided into two parts: 1) dynamic datasets that include <sup>34</sup>time series of daily  
269 climate (precipitation, maximum and minimum temperature), annual <sup>6</sup>land cover land use change  
270 (LCLUC) and land management practices (irrigation, fertilization and cropping system, tillage



271 intensity) and 2) static datasets that include 87 information on soil properties (soil texture, pH and  
272 bulk density) (Sanderman et al., 2021), and topography maps (Jarvis et al., 2008). For the  
273 historical period (1895-2005), we used a combination of VEMAP and PRISM (1895-1979) and  
274 Daymet (1980-2005) (Daly and Bryant, 2013; Kittel et al., 2004; Thornton et al., 2012). The  
275 VEMAP datasets are available 97 at a daily time step and a coarser spatial resolution (0.5° x 0.5°),  
276 while the PRISM datasets are available at a monthly time step and a finer spatial resolution (10  
277 km × 10 km). We interpolated the PRISM data 135 at a daily time step by using the daily trend from  
278 the VEMAP datasets such that the monthly precipitation totals and monthly average temperature  
279 matches the monthly climate from the PRISM data. For the future (2006-2100), we used the  
280 4 Intergovernmental Panel on Climate Change (IPCC) 5<sup>th</sup> assessment report (AR5) RCP4.5 and  
281 143 RCP8.5 climate scenarios available at a spatial resolution of 1/16° x 1/16°.

282 **Table 2.** Default and modified decomposition (k) parameters used in the DAYCENT to simulate  
283 the size of different carbon pools

Pools	Default		Modified $k$ (yr <sup>-1</sup> )			
	$k$ (yr <sup>-1</sup> )	grid search	N	Optimized	Absolute	Relative (%)
Active	7.30	(3,12)	301	3.50	-3.80	-52
Slow	0.20	(0.10,0.30)	201	0.14	-0.06	-30
Passive	0.0045	(0.001,0.0085)	351	0.0075	0.003	+67

284  
285 For annual LCLUC, we used spatially explicit datasets available at a resolution of 250m × 250m  
286 for the historical (1938-2005) and future (2006-2100) periods under the IPCC 4<sup>th</sup> assessment  
287 report (AR4) A2 scenario (Sohl et al., 2012). We used only the A2 land cover scenario because  
288 there was not much difference in the trajectories of land cover change through 2100. For the  
289 period 1895-1937, we backcasted the proportional distribution of croplands and grasslands by

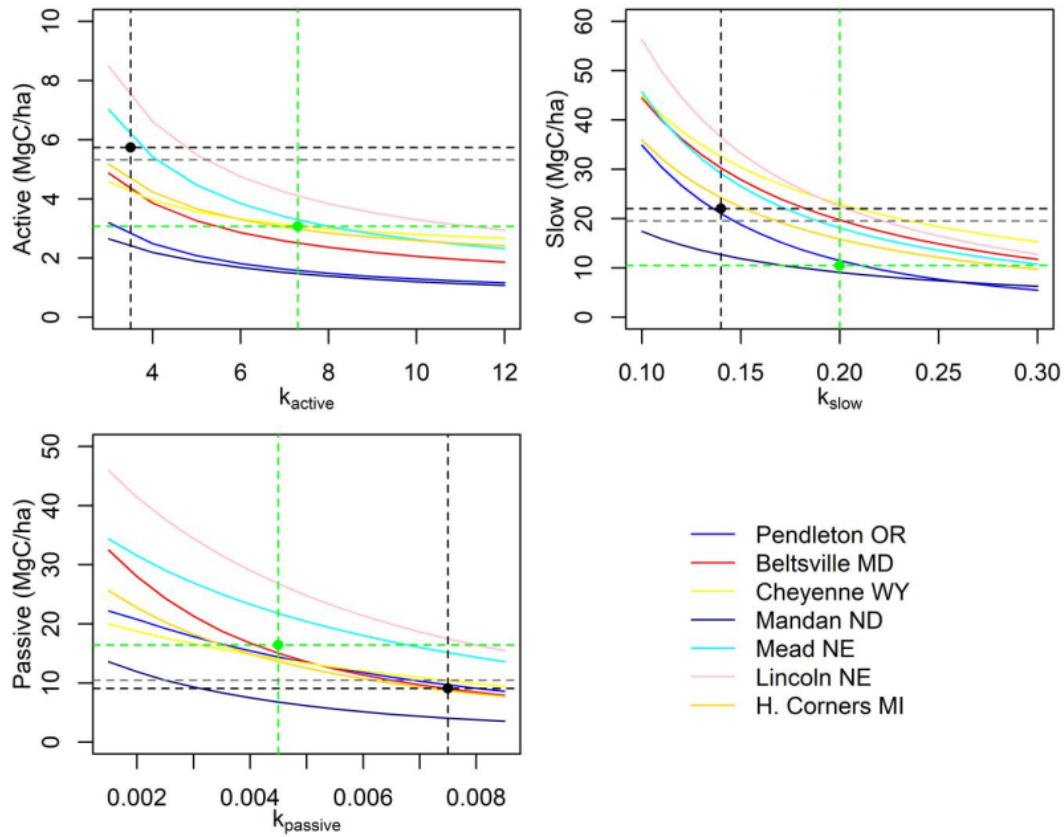
290 integrating the Sohl et al. (2012) data with <sup>99</sup>HYDE v3.2 data (Klein Goldewijk et al., 2017). We  
 291 estimated the fractional distribution of croplands and grasslands <sup>4</sup>by calculating the total number  
 292 of pixels dominated by each land cover type at 250m resolution within each 1/16 ° grid cell  
 293 (Figure S2a). Irrigation and fertilization data are based on census of agriculture statistics  
 294 (Falcone and LaMotte, 2016). All datasets were interpolated/aggregated to a common resolution  
 295 of 1/16° x 1/16° (approximately 7km x 7km at the equator).  
 296 Cropping systems and crop rotation are based on county level data <sup>139</sup>for the US Great Plains region  
 297 available through Hartman et al. (2011), which were merged with tillage type and intensity data  
 298 (Baker, 2011) to write 24 unique schedule files that describe grid-specific cropping system and  
 299 crop management practices. The 24 unique <sup>7</sup>schedule files include sequences of time blocks, with  
 300 each block describing a unique set of crop types, crop rotation, tillage type, tillage intensity,  
 301 fertilization, irrigation and residue removal (Hartman et al., 2011). Using these schedule files, we  
 302 developed an unsupervised classification algorithm (K-means) to create 24 unique clusters as a  
 303 function of long-term average climate (precipitation, minimum- and maximum-temperatures),  
 304 land forms, land cover type and elevation. We then assigned all the grid cells to one of the 24  
 305 unique clusters to create a spatially explicit dataset on cropping system and crop rotation. While  
 306 developing the unsupervised classification algorithm, the eastern part of the US <sup>4</sup>Great Plains  
 307 region dominated by corn (*Zea mays* L.) - soybean (*Glycine max* (L.) Merr.) rotation was  
 308 underrepresented. To address this shortcoming, we used randomly selected grid points from the  
 309 CropScape data (<https://nassgeodata.gmu.edu/CropScape/>) available through the USDA National  
 310 Agricultural Statistics Service in the unsupervised classification algorithm. Additionally,  
 311 cropping systems classified using the unsupervised algorithm was verified against current  
 312 CropScape data allowing for realistic representation of cropping systems. The distribution of



313 schedule files representing different crop rotation and crop types used to build the unsupervised  
314 classification is shown in Figure S2b and the spatial distribution of crop rotations based on the  
315 unsupervised classification is shown in Figure S3.

#### 316 **2.4 Linking DAYCENT conceptual pools with C fractions**

317 The SOC dynamics in the DAYCENT consists of the first-order kinetic exchanges among  
318 conceptual pools (65 active, slow, and passive) defined by empirical turnover rates (Parton et al.,  
319 1987). However, a major impetus for quantifying these pools comes from the fact that the size  
320 and distribution of SOC in the different pools cannot be directly linked with experimental data.  
321 Here, we developed a methodology to link the conceptual active, slow and passive pools to  
322 spectroscopy-based estimates of POC, MAOC and PyC fractions. The rate of decomposition  
323 across POC, MAOC and PyC are consistent with the potential 111 turnover rates assigned to the  
324 active, slow, and passive pools in soil C models (Baldock et al., 2013b). As a result, we modified  
325 the potential turnover rates in the DAYCENT model such that the absolute difference between  
326 the simulated SOC and predicted C fractions was minimized (see section 2.5 below). When  
327 matching the soil pools with C fraction data, we compared the sum of belowground structural,  
328 metabolic and active pool SOC to POC, slow pool SOC to MAOC, and passive pool SOC to  
329 PyC. Details on matching the conceptual pools with C fraction data are provided in Figure S4.



330

331 **Figure 1.** Parameterization of  $k_{active}$ ,  $k_{slow}$  and  $k_{passive}$  using carbon fractions predicted across long  
332 term research sites. The dashed black line represents the potential decomposition rates ( $k$ ) that is  
333 optimized when the absolute difference between the  $DC_{mod}$  simulated SOC in different pools and  
334 the predicted C fractions is minimum. The dashed green line represents the size of different soil  
335 SOC pools using the default  $k$  value based on  $DC_{def}$  model. The dashed grey line is the average  
336 POC (i.e. active), MAOC (i.e. slow) and PyC (i.e. passive) predicted using the combination of  
337 diffuse reflectance spectroscopy and machine learning at seven long term research sites  
338 {Citation}.

## 2.5 Model parameterization

In this study, we performed a grid search to parameterize the potential decomposition rates for respective soil pools by running the DAYCENT at seven long-term research sites (Figure 1; Table 2), and compare the simulated SOC in active, slow, and passive pools with the POC, MAOC and PyC fractions. In the current DAYCENT model, total SOC is defined as follows:

$$SOC_{total} = SOC_{strc} + SOC_{metab} + SOC_{active} + SOC_{slow} + SOC_{passive} \quad (1)$$

Where,

$SOC_{strc}$  = structural SOC pool

$SOC_{metab}$  = metabolic SOC pool

$SOC_{active}$  = active SOC pool

$SOC_{slow}$  = slow SOC pool

$SOC_{passive}$  = passive SOC pool

Each of the above SOC pool has a specific potential decomposition rates that determines the time (ranging from years to centuries) until decomposition. Plant material is transferred to the active, slow and passive pools from aboveground and belowground litter pools and three dead pools.

Total C flow ( $CF_{act}$ ) out of the active pool is a function of potential decomposition rates modified by the effect of moisture, temperature, pH, and soil texture.

$$CF_{act} = k_{act} \times SOC_{act} \times bg_{dec} \times clt_{act} \times text_{ef} \times anerb_{dec} \times pH_{eff} \times dtm \quad (2)$$

Where,

$CF_{act}$  = the total amount of C flow out of the active pool ( $g\ C\ m^{-2}$ )

$k_{act}$  = intrinsic decomposition rate of the active pool ( $yr^{-1}$ )

$SOC_{act}$  = SOC in the active pool ( $g\ C\ m^{-2}$ ).

$bg_{dec}$  = the effect of moisture and temperature on the decomposition rate (0-1)

362  $clt_{act}$  = the effect of cultivation on the decomposition rate for crops (0-1) for the active pool

363  $text_{ef}$  = the effect of soil texture on the decomposition rate (0-1)

364  $anerb_{dec}$  = the effect of anaerobic conditions on the decomposition rate (0-1)

365  $pH_{eff}$  = the effect of pH on the decomposition rate (0-1)

366  $dtm$  = the time step (fraction of year)

367 The respiratory loss when the active pool decomposes is calculated as:

$$368 \quad CO_{2(act)} = CF_{act} \times p1CO_2 \quad (3)$$

369 Where,

370  $CO_{2(act)}$  = respiratory loss from the  $SOC_{act}$  pool ( $g\ C\ m^{-2}$ )

371  $p1CO_2$  = scalar that control respiratory  $CO_2$  loss computed as a function of intercept and slope  
372 parameters modified by soil texture

373 The C flow from active to passive pool is then computed as:

$$374 \quad CF_{act2pas} = CF_{act} \times fps1s3 \times (1 + animpt \times (1 - anerb)) \quad (4)$$

375 Where,

376  $CF_{act2pas}$  = C flow from the active to the passive pool ( $g\ C\ m^{-2}$ )

377  $fps1s3$  = impact of soil texture on the C flow (0-1)

378  $animpt$  = the slope term that controls the effect of soil anaerobic condition on C flows from  
379 active to passive pool (0-1)

380  $anerb$  = effect of anaerobic condition on decomposition computed as a function of soil available  
381 water and potential evapotranspiration rates

382 The C flow from active to the slow pool is then computed as the difference between total C flow  
383 out of the active pool, respiratory  $CO_2$  loss, C flow from active to passive pool and C lost due to  
384 leaching. Mathematically,

$$CF_{act2slo} = CF_{act} - CO_{2(act)} - CF_{act2pas} - C_{leach} \quad (5)$$

Where,

$C_{leach}$  = C lost due to leaching calculated as a function of leaching intensity (0-1) and soil texture

Likewise, total C flow ( $CF_{slo}$ ) out of the slow pool is a function of potential decomposition rates

modified by the effect of moisture, temperature, pH, and soil texture.

$$CF_{slo} = k_{slo} \times SOC_{slo} \times bg_{dec} \times clt_{slo} \times anerb_{dec} \times pH_{eff} \times dtm \quad (6)$$

$k_{slo}$  = intrinsic decomposition rate of the slow pool ( $yr^{-1}$ )

$SOC_{slo}$  = SOC in the slow pool ( $g\ C\ m^{-2}$ ).

$clt_{slo}$  = the effect of cultivation on the decomposition rate for crops (0-1) for the slow pool

The respiratory loss when the slow pool decomposes is calculated as:

$$CO_{2(slo)} = CF_{slo} \times p2CO_2 \quad (7)$$

Where,

$CO_{2(slo)}$  = respiratory loss from the  $SOC_{slo}$  pool ( $g\ C\ m^{-2}$ )

$p2CO_2$  = parameter that controls decomposition rates of the slow pool (0-1)

The C flow from slow to passive pool is then computed as:

$$C_{slo2pas} = CF_{slo} \times fps2s3 \times (1 + animpt \times (1 - anerb)) \quad (8)$$

Where,

$fps2s3$  = impact of soil texture on decomposition (0-1)

The C flow from slow to active pool is then computed as a difference between total C flow out of

the slow pool, respiratory  $CO_2$  loss and total C flow from slow to passive pool. Mathematically,

$$CF_{slo2act} = CF_{act} - CO_{2(slo)} - CF_{slo2pas} \quad (9)$$

Likewise, total C flow ( $CF_{pas}$ ) out of the passive pool is a function of potential decomposition

rates modified by the effect of moisture, temperature and pH.

$$C_{pas} = k_{pas} \times SOC_{pas} \times bg_{dec} \times clt_{pas} \times pH_{eff} \times dtm \quad (10)$$

Where,

$k_{pas}$  = intrinsic decomposition rate of the passive pool ( $yr^{-1}$ )

$SOC_{pas}$  = SOC in the slow pool <sup>6</sup> ( $g\ C\ m^{-2}$ ).

$clt_{pas}$  = the effect of cultivation on the decomposition rate for crops (0-1) for the passive pool

The  $CF_{pas}$  is either lost through respiratory processes or transferred to the active pool using the following equation:

$$CO_{2(pas)} = CF_{pas} \times p3co2 \quad (11)$$

$$CF_{pas2act} = CF_{pas} \times (1 - p3co2) \quad (12)$$

Where,

$CO_{2(pas)}$  = respiratory loss from the passive SOC pool ( $g\ C\ m^{-2}$ )

$p3co2$  = parameter that control decomposition rates of passive pool (0-1)

$CF_{pas2act}$  = C flow from passive to active pool ( $g\ C\ m^{-2}$ )

Since DAYCENT is a donor-controlled model and changes in organic matter are primarily driven by a top down approach, we first parameterize the <sup>17</sup> active soil pool by comparing the simulated SOC in the active pool against POC predicted using diffuse reflectance spectroscopy.

During the parameterization process, we varied the potential decomposition rates ( $k_{active}$ ) <sup>107</sup> by

running the model to equilibrium under native vegetation for 2000 years. We then used site

history at seven long-term research sites to create schedule files and <sup>109</sup> simulate the effects of

historical cropping systems, land use change, land management and grazing practices on the

active SOC. The potential decomposition rates for the active soil pool were optimized when the

absolute difference between the average of SOC in the active pool and the POC for the top 20 cm

across all sites was minimum.



431 We repeated the above process for parameterizing the slow- and passive-carbon pools by  
432 comparing it with MOAC and PyC, respectively. Similar to the active pool, we performed a grid  
433 search using the existing parameters based on the default model that controls the potential  
434 decomposition rates ( $k_{slow}$  and  $k_{passive}$ ) of the slow- and passive-pools. We then optimized the  
435 parameter by using the potential decomposition rates that provides the minimum difference in  
436 the absolute values across all sites.

## 437 <sup>122</sup> 2.6 Model calibration and simulation procedure

438 The DAYCENT model has been well calibrated across a range of climatic, environmental, and  
439 land use gradients for different crop and grassland types. <sup>83</sup> Details of the calibration procedure can  
440 be found in Hartman et al. (2011). Briefly, adjustment of key model parameters that control plant  
441 growth and SOM changes were made by changing the <sup>23</sup> schedule files at each point in time. For  
442 <sup>7</sup> example, transitioning to higher yielding corn varieties occurred in 1936, while the short and  
443 semi-dwarf <sup>4</sup> wheat varieties were introduced in the 1960s. During the calibration process, model  
444 parameters that control the maximum photosynthetic rate and grain to stalk ratio were adjusted  
445 within realistic limits to account for improvement in crop varieties. Additionally, adjustments in  
446 the schedule files were made to account for residue removal in early years, while residues were  
447 retained in later years, thereby increasing nutrient input to the soils. These calibration strategies  
448 have allowed to better capture crop dynamics in the US Great Plains region (Hartman et al.,  
449 2011).

450 Model simulation begins with the equilibrium run starting from <sup>7</sup> year zero to year 1894 by  
451 repeating daily climate data from 1895-2005 and native vegetation without disturbance or land  
452 use change. Following the equilibrium run, we performed a historical simulation to quantify the  
453 <sup>70</sup> effects of land use history, land management practices, and climate change on the evolution of

<sup>98</sup>  
SOC during 1895-2005. Finally, we performed future simulations using two climate scenarios  
(RCP4.5 and RCP8.5) and A2 LCLUC, with land management practices (i.e. irrigation,  
fertilization, tillage practices, and crop rotation) held at 2005 levels during 2006-2100.

## 457 2.7 Model validation at site and regional scales

<sup>5</sup>  
The performance of the calibrated model was assessed by comparing simulated SOC in the  
active, slow, and passive pools against predictions of POC, MAOC and PyC, respectively, at the  
seven long-term research sites. In the validation procedure, we ran the model at these sites using  
plant growth and soil parameters determined from model calibration, but with <sup>136</sup>changing climate,  
environmental, and land use data based on the land use history of the respective sites. For all the  
<sup>123</sup>sites, we compared the distribution of SOC in different pools and evaluated model performance  
using linear regression and the goodness-of-fit statistics (bias,  $R^2$ , RMSE).

We also compared the distribution of SOC simulated using DAYCENT against the machine  
learning model-based predictions of POC, MAOC, and PyC for the US Great Plains ecoregion  
(Sanderman et al., 2021). Additionally, we compared simulated total SOC against two other SOC  
<sup>125</sup>maps for the contemporary period (Hengl et al., 2017; Ramcharan et al., 2018).

## 469 2.8 Historical and future <sup>38</sup>changes in SOC stocks

<sup>9</sup>  
To quantify the effect of the new parameterization scheme linking measurable soil C pools with  
conceptual active, slow, and passive pools from the DAYCENT, we designed two scenarios. In  
the first scenario, we ran the model using the default (DC<sub>def</sub>) and the modified (DC<sub>mod</sub>) model  
that links conceptual pools with C fraction during the historical period (1895-2005) to quantify  
the differences in SOC across different pools associated with different parameterization. In the  
second scenario, we performed future simulations to understand if the different model structures  
<sup>21</sup>(DC<sub>def</sub> versus DC<sub>mod</sub>) result in different effects of climate and LCLUC on SOC stocks. We used



477 the IPCC AR5 RCP8.5 and RCP4.5 climate scenarios and the IPCC AR4 A2 LCLUC scenarios  
478 to quantify the effects of future climate and LCLUC change on SOC stocks. The RCP8.5  
479 corresponds to the pathway that tracks current global trajectories of cumulative CO<sub>2</sub> emissions  
480 (CO<sub>2</sub> levels reaching 960 ppm by 2100) with the assumption of high population growth and  
481 modest rates of technological change and energy intensity improvements (Riahi et al., 2011;  
482 Schwalm et al., 2020). The RCP4.5 is a modest emission scenario with CO<sub>2</sub> levels reaching 540  
483 ppm by 2100 under the assumption of shift toward low emission technologies and the  
484 deployment of carbon capture and geologic storage technology (Thomson et al., 2011). The A2  
485 land cover scenario emphasizes rapid population growth and economic development, and  
486 resembles closely to the RCP8.5 scenario. We used the AR4 for LCLUC because Sohl et al.  
487 (2012) data were available at high resolution and allowed for smoother transition between land  
488 cover types when moving from historical to future A2 LCLUC scenarios. The purpose of the  
489 second scenario is to better understand the response of SOC to future climate and LCLUC and  
490 examine the effect of the new model modification on the projected change in total SOC through  
491 2100.

### 492 3. Results and Discussion

493 By quantifying the size and distribution of conceptual SOC pools of ecosystem models using a  
494 combination of diffuse reflectance spectroscopy and machine learning, we were able to modify  
495 DAYCENT by relating the conceptual active, slow and passive pools with measurable POC,  
496 MAOC and PyC fractions (section 3.1). Model modification led to more accurate representation  
497 of the magnitude and distribution of SOC (section 3.2) and was necessary to accurately quantify  
498 the legacy effect of previous land use under a changing climate and reproduce current SOC  
499 stocks compared to the default model (section 3.3). Projection of future SOC change show that

the default model underestimates the SOC loss in <sup>160</sup>response to climate and land cover change by 31% and 29% for croplands and grasslands, respectively (section 3.4). Overall, our results demonstrate that relating the pools sizes from the ecosystem model with C fraction data is necessary to better initialize SOC pool and simulate SOC response to <sup>21</sup>climate and land use into the future.

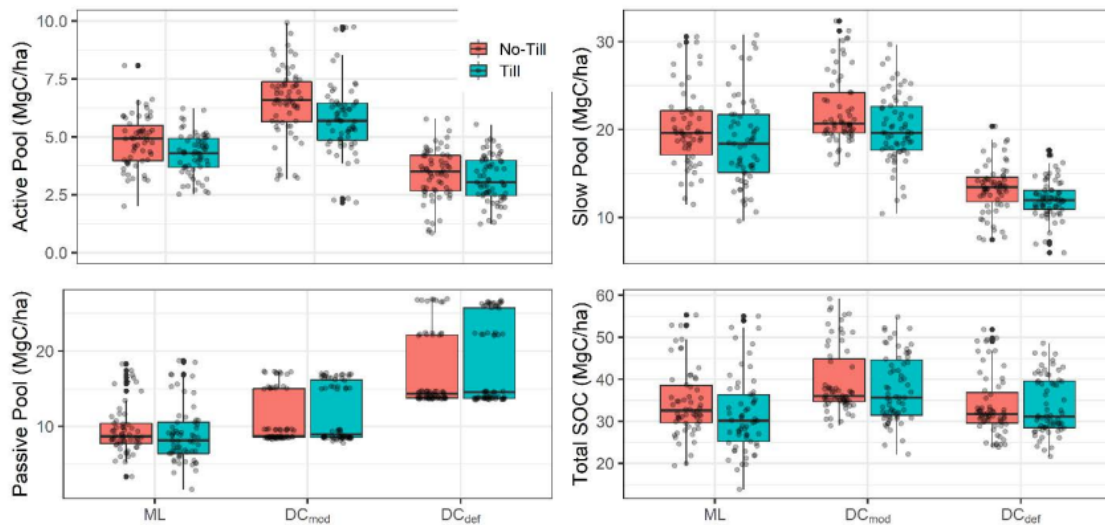
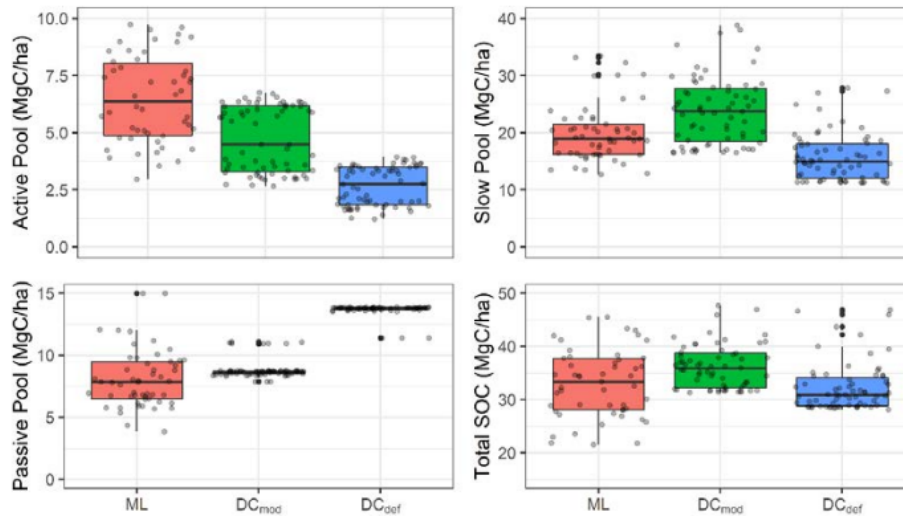


**Figure 2.** Comparison of the machine learning (ML) and DAYCENT simulated SOC using the modified ( $DC_{mod}$ ) and default ( $DC_{def}$ ) models at long-term research sites with a known cropping history. The black dots in the boxplot represent the SOC at the various sites plotted by adding a random value such that they do not overlap with each other.

### 3.1 Model evaluation of total SOC and the distribution of SOC at long-term research sites

The modified model ( $DC_{mod}$ ) linking conceptual soil pools to measurable C fractions showed better representation of the distribution of C stocks across different pools compared to the default model ( $DC_{def}$ ) (Figures 2 & 3). When the mean SOC at these sites were compared to  $DC_{mod}$  and  $DC_{def}$  simulated SOC,  $DC_{mod}$  had better fit ( $R^2 = 0.52$ ) and lower RMSE ( $8.49 \text{ Mg C ha}^{-1}$ ) <sup>43</sup> compared to  $DC_{def}$  ( $R^2 = 0.40$ ; RMSE =  $8.93 \text{ Mg C ha}^{-1}$ ) <sup>43</sup> (Figure S5). The mean SOC based on

12  
516 observation for these sites was  $38.96 \text{ Mg C ha}^{-1}$ , which is comparable to the sum of predicted C  
158  
517 fractions ( $37.07 \text{ Mg C ha}^{-1}$ ) and simulated SOC using  $\text{DC}_{\text{mod}}$  ( $42.30 \text{ Mg C ha}^{-1}$ ) and  $\text{DC}_{\text{def}}$  ( $36.60$   
518  $\text{Mg C ha}^{-1}$ ) models. The  $\text{DC}_{\text{mod}}$  simulated SOC was higher than observation and machine  
519 learning based SOC by 9 and 12%, respectively, while  $\text{DC}_{\text{def}}$  showed under-predicted SOC by  
520 6% compared to observation. Although  $\text{DC}_{\text{mod}}$  showed a tendency toward over-prediction,  
521 assessment of the distribution of SOC demonstrated that  $\text{DC}_{\text{mod}}$  was able to better simulate the  
522 distribution of SOC in soil pools compared to  $\text{DC}_{\text{def}}$ . The  $\text{DC}_{\text{mod}}$  simulated the highest proportion  
11  
523 of C in the slow (56%) pool followed by the passive (30%) and active (14%) pools, which is  
524 comparable to the machine learning model-based estimates of MAOC (57%), PyC (29%) and  
525 POC (14%), respectively. Unlike  $\text{DC}_{\text{mod}}$ ,  $\text{DC}_{\text{def}}$  model simulated the highest proportion of C in  
526 passive (53%), followed by slow (39%) and active (8%) pools (Table S2).



527  
528 **Figure 3.** Comparison of the machine learning (ML) and DAYCENT simulated SOC using the  
529 modified ( $\text{DC}_{\text{mod}}$ ) and default ( $\text{DC}_{\text{def}}$ ) models across different pools at two long-term research  
530 sites dominated by grasslands with a known grazing history. The black dots in the boxplot

531 represent the SOC across different sites plotted by adding a random value such that they do not  
532 overlap with each other.

533 Evaluation of the model performance ( $DC_{mod}$ ) for grasslands and croplands showed that the  
534 modified model ( $DC_{mod}$ ) outperformed the default model ( $DC_{def}$ ) with better model fit ( $R^2 =$   
535 0.60), lower bias ( $-1.94 \text{ Mg C ha}^{-1}$ ) and lower RMSE ( $6.7 \text{ Mg C ha}^{-1}$ ) for grasslands (Figure S6).  
536 The  $DC_{mod}$  also produced better model fit for croplands ( $R^2 = 0.48$ ), but higher bias ( $-5.84 \text{ Mg C}$   
537  $\text{ha}^{-1}$ ) and RMSE ( $8.86 \text{ Mg C ha}^{-1}$ ) compared to the default ( $DC_{def}$ ) model (bias =  $-0.82$  and  
538 RMSE =  $7.45 \text{ Mg C ha}^{-1}$ ). The  $DC_{mod}$  was able to better represent the distribution of C in the  
539 active, slow and passive pools for both grasslands and croplands, while  $DC_{def}$  showed large  
540 discrepancies when representing the distribution of SOC for croplands (Table S2).

541 The results of this exercise demonstrate that optimizing the model parameters to initialize the  
542 conceptual SOC pools by matching with C fraction data can reproduce the distribution of SOC  
543 (Figures 2 & 3), building confidence in the modeling of SOC stocks, and their pool distribution  
544 (Lee and Viscarra Rossel, 2020; Luo et al., 2016). A common approach to initializing soil C  
545 pools is based on the use of soil C steady-state conditions, which is primarily achieved by  
546 running the model over a long period of 100 to 10000 years under native vegetation. However,  
547 this approach has shown large uncertainty in the estimation of contemporary SOC partly due to  
548 differences in parameter values used to determine the initial SOC stocks, which vary many fold  
549 across models (Tian et al., 2015; Todd-Brown et al., 2014). Additionally, the size and  
550 distribution of the soil C pools are constrained by model structure and parameter values  
551 producing large differences in initial conditions, which ultimately propagates into uncertainties  
552 in historical and future projection of SOC change (Ogle et al., 2010; Shi et al., 2018). Relating  
553 these conceptual pools to measurable C fractions by optimizing parameters that control

554 decomposition rates can help to constrain initial pool size and reduce uncertainties related to  
555 initial SOC stocks across different models (Christensen, 1996; Luo et al., 2016; Zimmermann et  
556 al., 2007). Results of this study show that tuning the potential decomposition rates within  
557 reasonable range (Figure 1) can effectively capture the distribution of SOC among different  
558 pools without significantly altering the magnitude of total SOC (Figures 2 & 3).

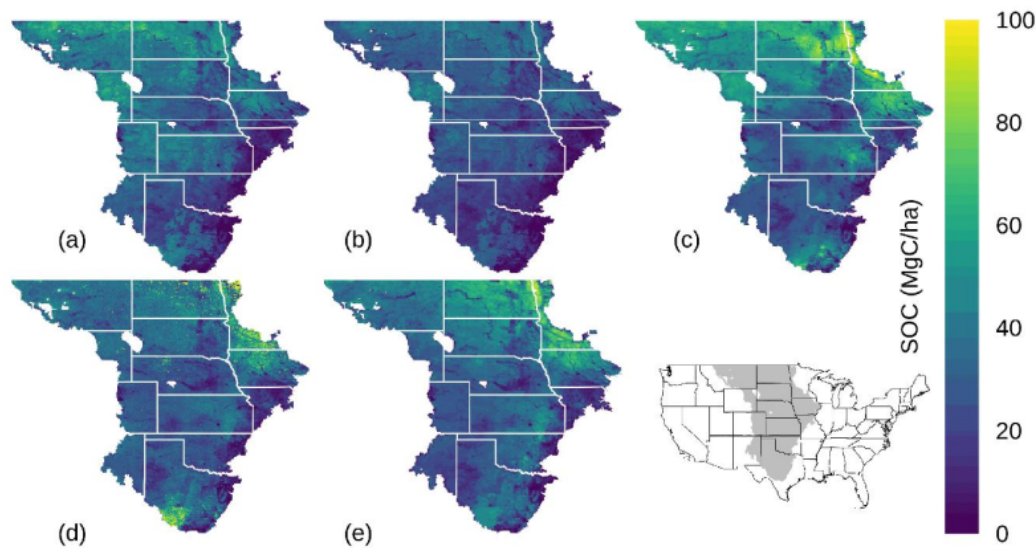
559 While tuning the parameters that control potential decomposition rates, active, and slow pools  
560 were adjusted by  $-3.8 \text{ yr}^{-1}$  (-52% compared to default rate) and  $-0.06 \text{ yr}^{-1}$  (-30%) respectively,  
561 and passive pool was increased by  $0.003 \text{ yr}^{-1}$  (67%) to match with C fractions data at the long-  
562 term research sites. These modifications were done such that the model was able to simulate total  
563 SOC and their distribution under current climatic, and land use conditions while also allowing to  
564 capture the legacy effect of previous land use, crop rotation, and tillage practices. It is important  
565 to note that other soil C models use C fraction data obtained under land use of varying intensities  
566 to run the model to steady state (Zimmermann et al., 2007), although soils under continuous use  
567 are in a transient state (Wieder et al., 2018). The rate and direction of SOC change can be  
568 modified by environmental factors, previous land use, and current management practices (e.g.,  
569 intensity, cropping systems and fertilization/irrigation), which ultimately determine a new  
570 equilibrium or transient state (Chan et al., 2011; Van Groenigen et al., 2014). Here, we run the  
571 model to steady state conditions, and calibrated the SOC stocks to current land use and  
572 management practices by matching with C fractions data at all the sites.

### 573 **3.2 Model evaluation of SOC stocks and their distribution at the regional scale**

574 Evaluation of the model performance at the regional level by comparing model simulations to  
575 three data-driven SOC maps showed that the default ( $\text{DC}_{\text{def}}$ ) model under-predicts SOC stocks  
576 for the contemporary period (2001-2005 average). The modified ( $\text{DC}_{\text{mod}}$ ) model was better able  
577 to reproduce the spatial pattern as observed in the data driven estimates of SOC (Figure 4). The



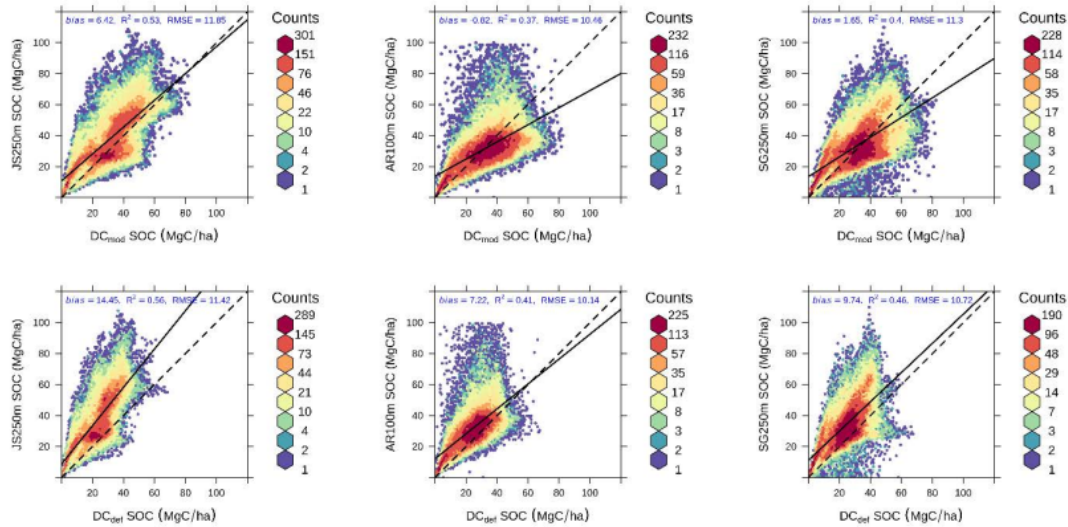
578 <sup>28</sup>DC<sub>mod</sub> simulated contemporary SOC stocks of 34.86 Mg C ha<sup>-1</sup> were closer to the estimates  
 579 based on three data-driven models (32.38 – 39.19 Mg C ha<sup>-1</sup>) (Figure S7). The DC<sub>def</sub> simulated  
 580 <sup>28</sup>SOC stocks of 26.17 Mg C ha<sup>-1</sup>, which is lower than the machine learning based predictions by  
 581 19-33%. Interestingly, both DC<sub>def</sub> and DC<sub>mod</sub> were not able to reproduce the high C stocks in the  
 582 northeastern Great Plains although data driven modeling shows large SOC stocks.



583  
 584 **Figure 4.** Spatial pattern of SOC change during the contemporary period: modified (DC<sub>mod</sub>) (a),  
 585 default (DC<sub>def</sub>) (b), Sanderman <sup>10</sup>et al. (2021) (c), Ramcharan et al. (2018) (d), and Hengl et al.  
 586 (2017) (e). Data-driven SOC maps were scaled by cropland and grassland distribution maps  
 587 before comparing against DAYCENT-simulated SOC.

588 Evaluation of the model performance using a scatterplot shows that calibration of active, slow,  
 589 and passive pools was necessary to produce unbiased estimates of SOC despite having slightly  
 590 higher RMSE values than the default model when compared to the different SOC data sets  
 591 (Figure 5). Among the three data driven models, Sanderman et al. (2021) also provided  
 592 prediction of POC, MAOC, and PyC in the US Great Plains region. Comparison <sup>39</sup>of the

593 distribution of SOC across different pools indicate that the  $DC_{mod}$  was able to reproduce SOC in  
594 the slow/MAOC, and passive/PyC pools but under-predicted the size of the active/POC pool  
595 (Figure S8).



596  
597 **Figure 5.** Scatter plots of the comparison of DAYCENT simulated SOC ( $DC_{mod}$  &  $DC_{def}$ )  
598 against Sanderman et al. (2021) – JS250m, Ramcharan et al. (2018) – AR100m, and Hengl et al.  
599 (2017) – SG250m.

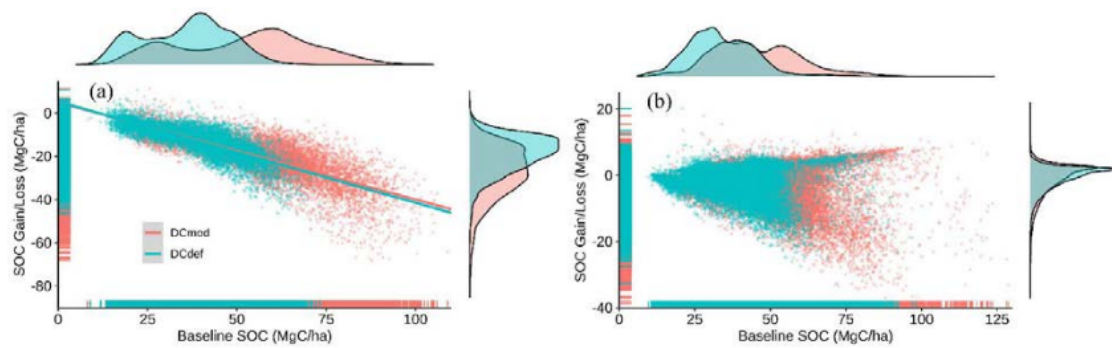
600 While the modified ( $DC_{mod}$ ) model was able to better capture the magnitude and spatial pattern  
601 of SOC when compared against data based on machine learning models, the datasets themselves  
602 present a few challenges when comparing with the results from this study. First, these datasets  
603 were produced using the environmental covariates approach under current climatic and land use  
604 conditions, and thus represent SOC dynamics using aggregated climate, land use, and  
605 environmental conditions over a certain period. However, in the DAYCENT model, we used  
606 annual and daily time series data for climatic and land use conditions to simulate the processes  
607 that control SOM retention and stabilization, which could lead to inconsistencies when  
608 comparing results between this study and data driven products. Second, outputs based on

<sup>3</sup> machine learning models are sensitive to the number of samples used in the training sets. For example, machine learning-based SOC shows higher stocks in the northeastern Great Plains region compared to the DC<sub>mod</sub> or DC<sub>def</sub> models (Figure 4). This may be because the region contains thousands of shallow seasonal wetlands with higher SOC stocks averaging between 78 to 109 <sup>138</sup>Mg C ha<sup>-1</sup> to the depth of 20cm (Tangen and Bansal, 2020). Accounting for the large number of wetlands samples in the training set would likely produce higher SOC stocks in the region. We did not specifically model wetlands SOC and only considered grasslands and croplands, which cover <sup>93</sup>>90% of the land area in the US Great Plains region and as such may have underrepresented these high SOC ecosystems.

### 618 3.3 Historical changes in SOC stocks and their distribution

619 When the baseline SOC (1895-1899 average) values were compared with the current (2001-2005 average) SOC stocks, the modified (DC<sub>mod</sub>) and default (DC<sub>def</sub>) models simulated a loss of 1063 Tg C (12%) and 634 Tg C (10%), respectively. On a per unit area basis, DC<sub>mod</sub> showed higher absolute (17.62 Mg C ha<sup>-1</sup>) and relative (33%) SOC losses compared to the loss of 10.60 Mg C ha<sup>-1</sup> (27%) using DC<sub>def</sub> for croplands. Grasslands showed similar patterns of higher absolute (2.51 Mg C ha<sup>-1</sup>) and relative (4%) SOC losses using DC<sub>mod</sub> compared to the loss of 1.06 Mg C ha<sup>-1</sup> (3%) using DC<sub>def</sub>. Overall, croplands showed a large and significant loss of C when compared against the baseline SOC using both models, while grasslands showed both losses and gains of SOC during 1895-2005 (Figure 6). The SOC loss from conversion of native vegetation to croplands were on average <sup>52</sup>14.70 Mg C ha<sup>-1</sup> and 9.29 Mg C ha<sup>-1</sup> using DC<sub>mod</sub> and DC<sub>def</sub>, respectively. This translates into a relative loss using DC<sub>mod</sub> that is higher than the loss using DC<sub>def</sub> by 58% during 1895-2005. For grid cells under native grasslands, DC<sub>mod</sub> simulated slightly <sup>8</sup>higher average SOC loss (1.96 Mg C ha<sup>-1</sup>) compared to DC<sub>def</sub> (1.39 Mg C ha<sup>-1</sup>).





632

633 **Figure 6.** Changes in contemporary (2001-2005 average) SOC after conversion of native  
634 vegetation to croplands (a) and under native vegetation (b) as a function of baseline (1895-1899  
635 average) SOC stocks. Negative values are losses while positive values are gains of SOC.

636 The simulation of total SOC stocks following historical land use under a changing climate is  
637 constrained by model parameters that determine the time until decomposition, modified by the  
638 interaction of land use intensity with changing climate (Arora and Boer, 2010; Eglin et al.,  
639 2010). Land use change can modify total SOC through its effect on individual soil pools, with  
640 the POC/active pool more vulnerable to loss compared to the MAOC/slow and PyC/passive  
641 pools (Poeplau and Don, 2013). The potential decomposition rates using the modified ( $DC_{mod}$ )  
642 model were adjusted to match C fraction data such that higher SOC was allocated to rapid and  
643 slow cycling pools, which are more vulnerable to loss following land use change and  
644 management intensity at decadal to century time scales (Hobley et al., 2017; Sulman et al.,  
645 2018). We further compared the historical SOC loss following land use change against other  
646 studies to determine the robustness of the new parameterization using  $DC_{mod}$ . The SOC loss rate  
647 using  $DC_{mod}$  are closer to the mean 30 cm loss rate of  $17.7 \text{ Mg C ha}^{-1}$  (Sanderman et al., 2017b),  
648 and relative loss of 42-49% following conversion of forest/pasture to croplands (Guo and  
649 Gifford, 2002). However, it is important to note that these previous studies are not directly

comparable with the results from this study because of differences in sampling depth, the intensity of land use and the time since disturbance.

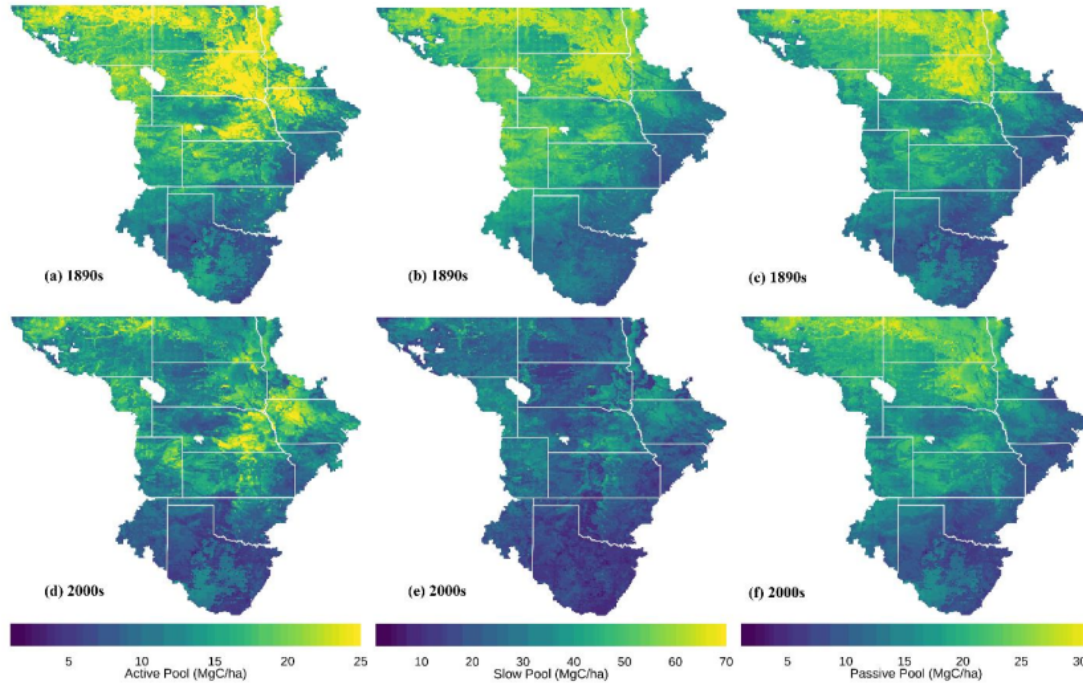


**Figure 7.** The active, slow, and passive soil pools of SOC stocks (20 cm depth) based on the modified ( $DC_{mod}$ ) model under native vegetation (1895-1899 average; top maps) and following land cover land use change (2001-2005 average; bottom maps).

Comparison of the total SOC and its distribution in different pools between the two models provided a more nuanced picture of the effect of new parameterization on SOC stocks and the response of SOC to historical land use. The spatial pattern of the SOC stocks showed that the baseline SOC in the active, slow and passive pools simulated by the modified ( $DC_{mod}$ ) model (Figure 7) were higher than the default ( $DC_{def}$ ) model (Figure S9). As a result, there were higher SOC losses from the active and slow pools using  $DC_{mod}$  compared to  $DC_{def}$  (Figure 7, S9). When averaged over all pixels, the cropland SOC loss in the active, and slow, pools were 0.85, 10.09

663 and gains in the passive pool was 0.34 Mg C ha<sup>-1</sup>, respectively, using DC<sub>def</sub>. The DC<sub>mod</sub>  
664 simulated larger SOC loss for all pools with active, slow, and passive pools losing SOC by 1.48,  
665 16.04 and 0.09 Mg C ha<sup>-1</sup>, respectively. The magnitude of SOC loss from grasslands was lower  
666 compared to croplands for all three pools, with the largest SOC loss from the slow pool of 1.45  
667 and 0.49 Mg C ha<sup>-1</sup> using DC<sub>mod</sub> and DC<sub>def</sub> models, respectively. The distribution of SOC to  
668 different pools indicated that DC<sub>def</sub> had 44%, 43% and 13% SOC in the passive, slow, and active  
669 pools for croplands, while DC<sub>mod</sub> had 57% of the total SOC allocated to the slow pool, followed  
670 by the passive (23%) and active (20%) pools. For grasslands, both models were consistent in  
671 allocating the largest proportion of SOC (59% in default and 70% in modified) to slow pools,  
672 followed by passive and active pools.

673 The differences in the total SOC and their distribution between the models is constrained by the  
674 sensitivity of the SOC pools to environmental, climatic, and management factors (Davidson and  
675 Janssens, 2006; Dungait et al., 2012; Luo et al., 2016). The SOC stocks in the passive pool are  
676 not significantly different between the models at the regional level because the passive pool is  
677 less sensitive to environmental, climatic, and management factors, and it has a smaller  
678 contribution to total SOC (Collins et al., 2000), the SOC stocks in the passive pool were not  
679 significantly different between the models at the regional level. However, the active and slow  
680 pools respond strongly to environmental, climatic, and management constraints, which is largely  
681 driven by rapidly cycling fresh organic matter input in the active pool, and gradually  
682 decomposing detritus in the slow pool (Sherrod et al., 2005). In the DC<sub>mod</sub>, the potential  
683 decomposition rates of the active and slow pools are adjusted, allowing the model to retain more  
684 SOC to match with C fraction data. This modification resulted in higher SOC stocks in these  
685 pools, which translated into higher total losses despite slower turnover rates relative to DC<sub>def</sub>.

Model modification was necessary not only to match total SOC values but also to simulate the distribution of SOC into the active, slow and passive pools.

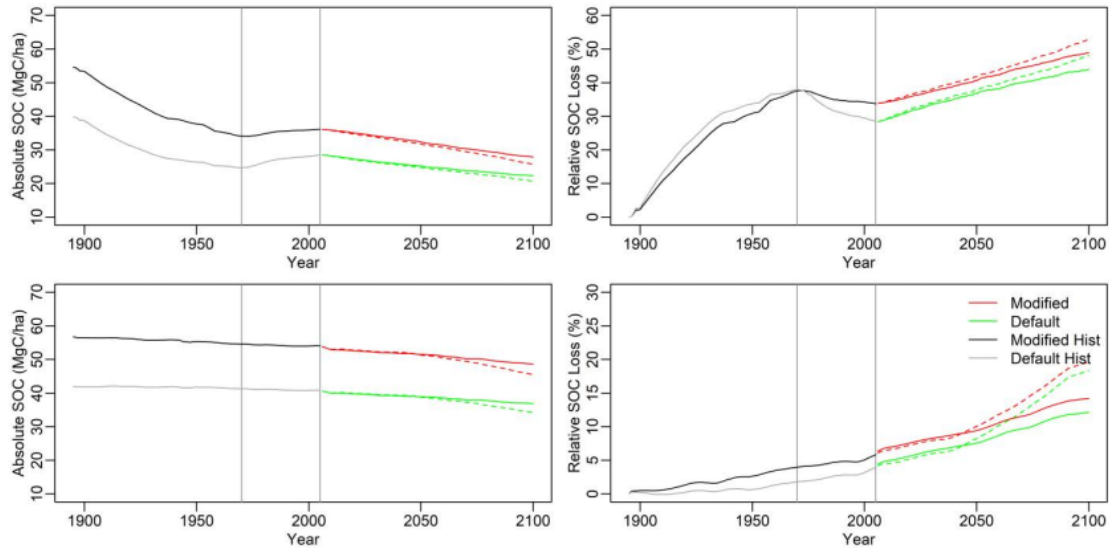


**Figure 8.** Temporal change in the absolute SOC stocks (20 cm depth) for croplands (a) and grasslands (c) and relative SOC loss compared to the 1895 SOC for croplands (b) and grasslands (d) in response to land use under a changing climate through 2100. The solid and dashed lines after 2006 represent RCP4.5 and RCP8.5 climate scenarios, respectively, both under the A2 land cover change scenario.

### 3.4 Future changes in SOC stocks and their distribution

Projection of the SOC dynamics in response to land cover change under a changing climate resulted in greater relative changes for both croplands and grasslands using the modified ( $DC_{mod}$ ) compared to the default ( $DC_{def}$ ) model (Figure 8). Despite greater rates of loss, by the end of the 21<sup>st</sup> century,  $DC_{mod}$  still simulated higher total SOC stocks compared to  $DC_{def}$  model (Table 3). By the end of 21<sup>st</sup> century, the  $DC_{mod}$  simulated total SOC stocks of 2818 and 2563 Tg C for croplands under the RCP4.5 and RCP8.5 scenarios, while the  $DC_{def}$  simulated total SOC stocks



701 of 2266 and 2082 Tg C. Native grasslands had higher SOC stocks of 3310 and 3095 Tg C using  
702 the DC<sub>mod</sub> compared to the SOC stocks of 2505 and 2324 Tg C using the DC<sub>def</sub> under the  
703 RCP4.5 and RCP8.5 scenarios, respectively. On a per unit area basis, absolute loss (difference  
704 between the 2095s and 2000s) were slightly higher for croplands, with a mean loss rate 10.43 Mg  
705 C ha<sup>-1</sup> compared to 8.44 Mg C ha<sup>-1</sup> for grasslands using DC<sub>mod</sub> under the RCP8.5 scenario (Table  
706 3). The DC<sub>def</sub> also simulated similar trend with slightly higher absolute losses for croplands (7.85  
707 Mg C ha<sup>-1</sup>) compared to grasslands (6.55 Mg C ha<sup>-1</sup>) under the RCP8.5 scenario. Relative losses  
708 estimated as a percentage of contemporary SOC stocks were higher in croplands (29% for DC<sub>mod</sub>  
709 vs 28% for DC<sub>def</sub> model) compared to grasslands (16% for both DC<sub>mod</sub> and DC<sub>def</sub> model) under  
710 the RCP8.5 scenario. Using the DC<sub>mod</sub>, the SOC loss rate were 33% and 29% higher for  
711 croplands and grasslands, respectively, compared to the DC<sub>def</sub> by the end of the 21<sup>st</sup> century  
712 under the RCP8.5 scenario. While both models simulated total SOC loss over the 21<sup>st</sup> century,  
713 the difference in SOC between models sums to an additional loss of 1252 Tg SOC under the  
714 RCP8.5 scenario.

715 The turnover rates of SOM are primarily driven by temperature and environmental controls with  
716 significant impact on the dynamics of total SOC changes at decadal to century time scales (Knorr  
717 et al., 2005). The two model versions used the same climate and environmental data and only  
718 differ in the turnover rates of the active, slow, and passive pools. Because the sizes of active, and  
719 slow pools in the modified (DC<sub>mod</sub>) model were larger than the default (DC<sub>def</sub>) model, simulated  
720 absolute and relative losses were higher using the DC<sub>mod</sub> compared to the DC<sub>def</sub> for croplands.  
721 Larger losses using the DC<sub>mod</sub> are primarily associated with the legacy effects of management  
722 intensity and rising temperatures with larger rates of SOC loss from the active, and slow pools  
723 (Crow and Sierra, 2018) of DC<sub>mod</sub> compared to DC<sub>def</sub>. Additionally, the size of the passive pool

724 in  $DC_{def}$  is larger compared to  $DC_{mod}$ , and this pool is less vulnerable to land use intensity and  
725 warming climate compared to active and slow pools. Thus, there was a disproportionately larger  
726 SOC loss driven by the size of the slow pool and the interaction of climate and management  
727 intensity using the  $DC_{mod}$  compared to the  $DC_{def}$ , which translated into larger absolute and  
728 relative losses of SOC. For grasslands, we did not include any management driven changes. Both  
729 absolute and relative losses of SOC stocks in the grasslands are primarily driven by the warming  
730 climate (Jones and Donnelly, 2004), with active and slow pools losing more SOC stocks using  
731  $DC_{mod}$  compared to  $DC_{def}$ . Future work should consider the interactive effects of grazing  
732 management with climate.

733

**Table 3.** DAYCENT (modified and default) simulated absolute changes in total and per unit area soil organic carbon (SOC) during the 2000s, 2045s and 2095s for croplands and grasslands in the US Great Plains region

Time	Total (TgC)						Per Unit Area (MgC/ha)			
	Default (DC <sub>def</sub> )			Modified (DC <sub>mod</sub> )			Default (DC <sub>def</sub> )		Modified (DC <sub>mod</sub> )	
	RCP4.5	RCP8.5		RCP4.5	RCP8.5		RCP4.5	RCP8.5	RCP4.5	RCP8.5
Croplands	2000s	2113		2717			28.51		36.17	
	2045s	1988	1938	2588	2513		25.20	24.80	32.41	31.87
	2095s	2266	2082	2818	2563		22.31	20.66	27.91	25.87
Grasslands	2000s	3891		5160			40.82		54.05	
	2050s	3531	3523	4674	4659		38.90	38.80	51.51	51.34
	2095s	2505	2324	3310	3095		36.88	34.27	48.65	45.61
Total	2000s	6004		7877			NA		NA	
(Croplands +	2045s	5519	5461	7262	7172		NA	NA	NA	NA
Grasslands)	2095s	4771	4406	6128	5658		NA	NA	NA	NA

736 Future land use, management intensity, nitrogen content, and climate interact in different ways to  
737 control C flow from soil pools with different mean residence times, which ultimately determine  
738 total SOC stocks (Deng et al., 2016; Luo et al., 2017; Sulman et al., 2018). Under a warming  
739 climate, SOC formed from fresh organic matter inputs controls the size of the active/POC pool,  
740 which is further constrained by the intensity of land use and is more vulnerable to loss (Crow and  
741 Sierra, 2018; Lavallee et al., 2020). The active/POC pool also acts as a donor to the slow/MAOC  
742 pool with C transfer and rates of SOC accumulation increasingly controlled by temperature  
743 (Crow and Sierra, 2018). In the DAYCENT, regardless of model version, the size of the active  
744 pool is relatively small as fresh organic matter is either decomposed rapidly or quickly enters the  
745 slow pool. Because the slow pool has longer residence times ranging from years to decades, the  
746 slow pool is less vulnerable to loss and can accrue C when transfer rates from the active pool  
747 exceed the rates of decomposition (Collins et al., 2000; Fontaine et al., 2007). In this study, the  
748 rates of decomposition due to rising temperatures had a stronger control on the size of the slow  
749 pool compared to the transfer of SOC from the active pool. As a result, the slow pool continued  
750 to lose SOC under projected climate changes in the future.

#### 751 4 Conclusions

752 In this study, we developed an approach to link conceptual soil pools in biogeochemical models  
753 against C fraction data predicted using a combination of diffuse reflectance spectroscopy and  
754 machine learning. We then quantified the long-term evolution of SOC change and projected the  
755 SOC response to future climate and land cover scenarios using the modified (DC<sub>mod</sub>) model that  
756 has been calibrated to C fraction data. Our results demonstrate that matching the active, slow and  
757 passive pools against POC, MOAC and PyC data lead to better representation of total SOC  
758 stocks and the distribution of SOC into different pools. With the updated model, the long-term



759 legacy effect of past agricultural management results in larger absolute and relative losses of  
 760 SOC compared to the default (DC<sub>def</sub>) model. Projecting the SOC <sup>156</sup>response to climate and land  
 761 cover change into <sup>the</sup> future (2005-2100) indicates that the new model modification (DC<sub>mod</sub>)  
 762 increases SOC losses by 2100 by 32% and 28% for croplands and grasslands, respectively, under  
 763 the RCP8.5 scenario compared to using the DC<sub>def</sub> model.

764 There are several study limitations that need to be addressed in our future work. First, new  
 765 modeling efforts should also consider quantifying how changes in aboveground biomass inputs  
 766 quantity and quality affect SOC dynamics given mixed results in agricultural systems in response  
 767 to litter inputs (Halvorson et al., 2002; Sanderman et al., 2017a). Second, current models rely on  
 768 using <sup>131</sup>clay content to modify rates of SOM stabilization <sup>and</sup> turnover, but recent research has  
 769 shown that other soil physicochemical properties such as <sup>100</sup>exchangeable calcium and extractable  
 770 <sup>iron and aluminum</sup> are <sup>stronger predictors of</sup> SOM content (Rasmussen et al., 2018). Third, new  
 771 modeling efforts should constrain model parameters affecting SOC dynamics by integrating  
 772 them with data-driven modeling and long-term experimental data (Jandl et al., 2014). Finally,  
 773 given the paucity of data related to C fractions, there is increasing need for measurement and  
 774 modeling of C fractions across <sup>142</sup>a wide range of environmental <sup>and</sup> management gradients (Luo et  
 775 <sup>al., 2017</sup>). Despite these limitations, we have shown that models calibrated to pool sizes by  
 776 matching with C fractions can improve long-term SOC predictions by more accurately  
 777 representing <sup>72</sup>soil C transformations <sup>in response to</sup> climate, <sup>land</sup> cover and land <sup>use change</sup>.

#### 778 **Code and Data Availability:**

779 <sup>The</sup> DAYCENT model source code is available in <sup>124</sup>Harvard dataverse repository  
 780 (<https://dataverse.harvard.edu/dataverse/daycent45>). The new parameterization scheme and  
 781 scripts for regional model simulation are available in github

782 (<https://github.com/whrc/DAYCENT-soil-carbon-pools>). Input data for driving the models are  
783 freely available online from different sources and have been cited appropriately in the  
784 manuscript. Long term ecological data are part of 105 United States Department of Agriculture –  
785 Agricultural Research Service and can be requested from the references listed in Table 1.

786 **Author Contributions:** S.D., C.S, and J.S designed the study and model development. S.D.  
787 performed model improvement, calibration, validation and regional historical and future  
788 simulation. All authors contributed to the manuscript.

22  
789 **Competing Interest:** The authors declare that they have no conflict of interest.

## 790 Acknowledgements

791 Funding for this research was provided by USDA NIFA award #2017-67003-26481. We thank  
792 Melannie D Hartman 77 at Colorado State University for providing access to the DAYCENT model  
793 and help with running the model. We also thank staff at 3 the USDA National Soil Survey Center  
794 (NSSC) Kellogg Soil Survey Laboratory (KSSL) for providing access to the soil characterization  
795 database. This research also used data 36 from the Long-Term Agroecosystem Research (LTAR)  
796 network 152 and Columbia Plateau Conservation Research Center (CPCRC), which are both  
797 supported 129 by the United States Department of Agriculture. The NSF 162 Long-term Ecological  
798 Research Program (DEB 1832042) and Michigan State University AgBioResearch provided  
799 funding for the data and soil samples from the Kellogg Biological Station.

## 800 References

- 801 Arora, V.K., Boer, G.J., 2010. Uncertainties in the 20th century carbon budget associated with land use  
802 change. *Global Change Biology* 16, 3327–3348.
- 803 Baker, N.T., 2011. Tillage Practices in the Conterminous United States, 1989–2004—datasets Aggregated  
804 by Watershed. US Department of the Interior, US Geological Survey Reston, Virginia.
- 805 Baldock, J.A., Hawke, B., Sanderman, J., Macdonald, L.M., 2013a. Predicting contents of carbon and its  
806 component fractions in Australian soils from diffuse reflectance mid-infrared spectra. *Soil*  
807 *Research* 51, 577–595.
- 808 Baldock, J.A., Sanderman, J., Macdonald, L.M., Puccini, A., Hawke, B., Szarvas, S., McGowan, J., 2013b.  
809 Quantifying the allocation of soil organic carbon to biologically significant fractions. *Soil*  
810 *Research* 51, 561–576.
- 811 Basso, B., Gargiulo, O., Paustian, K., Robertson, G.P., Porter, C., Grace, P.R., Jones, J.W., 2011.  
812 Procedures for initializing soil organic carbon pools in the DSSAT-CENTURY model for agricultural  
813 systems. *Soil Science Society of America Journal* 75, 69–78.
- 814 Batjes, N.H., 2016. Harmonized soil property values for broad-scale modelling (WISE30sec) with  
815 estimates of global soil carbon stocks. *Geoderma* 269, 61–68.
- 816 Cagnarini, C., Renella, G., Mayer, J., Hirte, J., Schulin, R., Costerousse, B., Della Marta, A., Orlandini, S.,  
817 Menichetti, L., 2019. Multi-objective calibration of RothC using measured carbon stocks and  
818 auxiliary data of a long-term experiment in Switzerland. *European Journal of Soil Science* 70,  
819 819–832.
- 820 Carvalhais, N., Forkel, M., Khomik, M., Bellarby, J., Jung, M., Migliavacca, M., Saatchi, S., Santoro, M.,  
821 Thurner, M., Weber, U., 2014. Global covariation of carbon turnover times with climate in  
822 terrestrial ecosystems. *Nature* 514, 213–217.
- 823 Cavigelli, M.A., Teasdale, J.R., Conklin, A.E., 2008. Long-term agronomic performance of organic and  
824 conventional field crops in the mid-Atlantic region. *Agronomy Journal* 100, 785–794.
- 825 Chan, K.Y., Conyers, M.K., Li, G.D., Helyar, K.R., Poile, G., Oates, A., Barchia, I.M., 2011. Soil carbon  
826 dynamics under different cropping and pasture management in temperate Australia: Results of  
827 three long-term experiments. *Soil Research* 49, 320–328.
- 828 Christensen, B.T., 1996. Matching measurable soil organic matter fractions with conceptual pools in  
829 simulation models of carbon turnover: revision of model structure. *Evaluation of soil organic*  
830 *matter models* 143–159.
- 831 Ciais, P., Sabine, C., Bala, G., Bopp, L., Brovkin, V., Canadell, J., Chhabra, A., DeFries, R., Galloway, J.,  
832 Heimann, M., 2014. Carbon and other biogeochemical cycles, in: *Climate Change 2013: The*  
833 *Physical Science Basis. Contribution of Working Group I to the Fifth Assessment Report of the*  
834 *Intergovernmental Panel on Climate Change. Cambridge University Press*, pp. 465–570.
- 835 Collins, H.P., Elliott, E.T., Paustian, K., Bundy, L.G., Dick, W.A., Huggins, D.R., Smucker, A.J.M., Paul, E.A.,  
836 2000. Soil carbon pools and fluxes in long-term corn belt agroecosystems. *Soil Biology and*  
837 *Biochemistry* 32, 157–168.
- 838 Crow, S.E., Sierra, C.A., 2018. Dynamic, intermediate soil carbon pools may drive future responsiveness  
839 to environmental change. *Journal of environmental quality* 47, 607–616.
- 840 Crowther, T.W., Todd-Brown, K.E., Rowe, C.W., Wieder, W.R., Carey, J.C., Machmuller, M.B., Snoek, B.L.,  
841 Fang, S., Zhou, G., Allison, S.D., 2016. Quantifying global soil carbon losses in response to  
842 warming. *Nature* 540, 104–108.
- 843 Czimczik, C.I., Masiello, C.A., 2007. Controls on black carbon storage in soils. *Global Biogeochemical*  
844 *Cycles* 21.
- 845 Daly, C., Bryant, K., 2013. The PRISM climate and weather system—an introduction. Corvallis, OR: PRISM  
846 climate group.

- 847 Dangal, S.R., Sanderman, J., 2020. Is Standardization Necessary for Sharing of a Large Mid-Infrared Soil  
848 Spectral Library? *Sensors* 20, 6729.
- 849 Dangal, S.R., Sanderman, J., Wills, S., Ramirez-Lopez, L., 2019. Accurate and precise prediction of soil  
850 properties from a large mid-infrared spectral library. *Soil Systems* 3, 11.
- 851 Davidson, E.A., Janssens, I.A., 2006. Temperature sensitivity of soil carbon decomposition and feedbacks  
852 to climate change. *Nature* 440, 165–173.
- 853 Del Grosso, S., Ojima, D., Parton, W., Mosier, A., Peterson, G., Schimel, D., 2002. Simulated effects of  
854 dryland cropping intensification on soil organic matter and greenhouse gas exchanges using the  
855 DAYCENT ecosystem model. *Environmental pollution* 116, S75–S83.
- 856 Del Grosso, S.J., Parton, W.J., Mosier, A.R., Hartman, M.D., Brenner, J., Ojima, D.S., Schimel, D.S., 2001.  
857 Simulated interaction of carbon dynamics and nitrogen trace gas fluxes using the DAYCENT  
858 model. *Modeling carbon and nitrogen dynamics for soil management* 303–332.
- 859 Deng, L., Zhu, G., Tang, Z., Shanguan, Z., 2016. Global patterns of the effects of land-use changes on soil  
860 carbon stocks. *Global Ecology and Conservation* 5, 127–138.
- 861 Doetterl, S., Stevens, A., Six, J., Merckx, R., Van Oost, K., Pinto, M.C., Casanova-Katny, A., Muñoz, C.,  
862 Boudin, M., Venegas, E.Z., 2015. Soil carbon storage controlled by interactions between  
863 geochemistry and climate. *Nature Geoscience* 8, 780–783.
- 864 Dungait, J.A., Hopkins, D.W., Gregory, A.S., Whitmore, A.P., 2012. Soil organic matter turnover is  
865 governed by accessibility not recalcitrance. *Global Change Biology* 18, 1781–1796.
- 866 Eglin, T., Ciais, P., Piao, S.L., Barré, P., Bellassen, V., Cadule, P., Chenu, C., Gasser, T., Koven, C.,  
867 Reichstein, M., 2010. Historical and future perspectives of global soil carbon response to climate  
868 and land-use changes. *Tellus B: Chemical and Physical Meteorology* 62, 700–718.
- 869 Falcone, J.A., LaMotte, A.E., 2016. National 1-kilometer rasters of selected census of agriculture statistics  
870 allocated to land use for the time period 1950 to 2012. US Geological Survey Data Release.
- 871 Fontaine, S., Barot, S., Barré, P., Bdioui, N., Mary, B., Rumpel, C., 2007. Stability of organic carbon in  
872 deep soil layers controlled by fresh carbon supply. *Nature* 450, 277–280.
- 873 Gollany, H., 2016. CQESTR simulation of dryland agroecosystem soil organic carbon changes under  
874 climate change scenarios. *Synthesis and Modeling of Greenhouse Gas Emissions and Carbon*  
875 *Storage in Agricultural and Forest Systems to Guide Mitigation and Adaptation* 6, 59–87.
- 876 Grandy, A.S., Sinsabaugh, R.L., Neff, J.C., Stursova, M., Zak, D.R., 2008. Nitrogen deposition effects on  
877 soil organic matter chemistry are linked to variation in enzymes, ecosystems and size fractions.  
878 *Biogeochemistry* 91, 37–49.
- 879 Guo, L.B., Gifford, R.M., 2002. Soil carbon stocks and land use change: a meta analysis. *Global change*  
880 *biology* 8, 345–360.
- 881 Halvorson, A.D., Wienhold, B.J., Black, A.L., 2002. Tillage, nitrogen, and cropping system effects on soil  
882 carbon sequestration. *Soil science society of America journal* 66, 906–912.
- 883 Hartman, M.D., Merchant, E.R., Parton, W.J., Gutmann, M.P., Lutz, S.M., Williams, S.A., 2011. Impact of  
884 historical land-use changes on greenhouse gas exchange in the US Great Plains, 1883–2003.  
885 *Ecological Applications* 21, 1105–1119.
- 886 Hengl, T., Mendes de Jesus, J., Heuvelink, G.B., Ruiperez Gonzalez, M., Kilibarda, M., Blagotić, A.,  
887 Shanguan, W., Wright, M.N., Geng, X., Bauer-Marschallinger, B., 2017. SoilGrids250m: Global  
888 gridded soil information based on machine learning. *PLoS one* 12, e0169748.
- 889 Hicks, W., Rossel, R.V., Tuomi, S., 2015. Developing the Australian mid-infrared spectroscopic database  
890 using data from the Australian Soil Resource Information System. *Soil Research* 53, 922–931.
- 891 Hobley, E., Baldock, J., Hua, Q., Wilson, B., 2017. Land-use contrasts reveal instability of subsoil organic  
892 carbon. *Global Change Biology* 23, 955–965.
- 893 Hsieh, Y.-P., 1993. Radiocarbon signatures of turnover rates in active soil organic carbon pools. *Soil*  
894 *Science Society of America Journal* 57, 1020–1022.

- 895 Ingram, L.J., Stahl, P.D., Schuman, G.E., Buyer, J.S., Vance, G.F., Ganjegunte, G.K., Welker, J.M., Derner,  
896 J.D., 2008. Grazing impacts on soil carbon and microbial communities in a mixed-grass  
897 ecosystem. *Soil Science Society of America Journal* 72, 939–948.
- 898 Jandl, R., Rodeghiero, M., Martinez, C., Cotrufo, M.F., Bampa, F., van Wesemael, B., Harrison, R.B.,  
899 Guerrini, I.A., Richter Jr, D. deB, Rustad, L., 2014. Current status, uncertainty and future needs in  
900 soil organic carbon monitoring. *Science of the total environment* 468, 376–383.
- 901 Janssens, I.A., Dieleman, W., Luyssaert, S., Subke, J.-A., Reichstein, M., Ceulemans, R., Ciais, P., Dolman,  
902 A.J., Grace, J., Matteucci, G., 2010. Reduction of forest soil respiration in response to nitrogen  
903 deposition. *Nature geoscience* 3, 315–322.
- 904 Jarvis, A., Reuter, H.I., Nelson, A., Guevara, E., 2008. Hole-filled SRTM for the globe Version 4, available  
905 from the CGIAR-CSI SRTM 90m Database.
- 906 Jobbágy, E.G., Jackson, R.B., 2000. The vertical distribution of soil organic carbon and its relation to  
907 climate and vegetation. *Ecological applications* 10, 423–436.
- 908 Jones, M.B., Donnelly, A., 2004. Carbon sequestration in temperate grassland ecosystems and the  
909 influence of management, climate and elevated CO<sub>2</sub>. *New Phytologist* 164, 423–439.
- 910 Kelly, R.H., Parton, W.J., Hartman, M.D., Stretch, L.K., Ojima, D.S., Schimel, D.S., 2000. Intra-annual and  
911 interannual variability of ecosystem processes in shortgrass steppe. *Journal of Geophysical*  
912 *Research: Atmospheres* 105, 20093–20100.
- 913 Kittel, T.G., Rosenbloom, N.A., Royle, J.A., Daly, C., Gibson, W.P., Fisher, H.H., Thornton, P., Yates, D.N.,  
914 Aulenbach, S., Kaufman, C., 2004. VEMAP phase 2 bioclimatic database. I. Gridded historical  
915 (20th century) climate for modeling ecosystem dynamics across the conterminous USA. *Climate*  
916 *Research* 27, 151–170.
- 917 Klein Goldewijk, K., Beusen, A., Doelman, J., Stehfest, E., 2017. Anthropogenic land use estimates for the  
918 Holocene–HYDE 3.2. *Earth System Science Data* 9, 927–953.
- 919 Knorr, W., Prentice, I.C., House, J.I., Holland, E.A., 2005. Long-term sensitivity of soil carbon turnover to  
920 warming. *Nature* 433, 298–301.
- 921 Lal, R., 2018. Digging deeper: A holistic perspective of factors affecting soil organic carbon sequestration  
922 in agroecosystems. *Global Change Biology* 24, 3285–3301.
- 923 Lal, R., 2004. Carbon sequestration in dryland ecosystems. *Environmental management* 33, 528–544.
- 924 Lavalée, J.M., Soong, J.L., Cotrufo, M.F., 2020. Conceptualizing soil organic matter into particulate and  
925 mineral-associated forms to address global change in the 21st century. *Global Change Biology*  
926 26, 261–273.
- 927 Lee, J., Viscarra Rossel, R.A., 2020. Soil carbon simulation confounded by different pool initialisation.  
928 *Nutrient Cycling in Agroecosystems* 116, 245–255.
- 929 Liebig, M.A., Gross, J.R., Kronberg, S.L., Phillips, R.L., 2010. Grazing management contributions to net  
930 global warming potential: A long-term evaluation in the Northern Great Plains. *Journal of*  
931 *Environmental Quality* 39, 799–809.
- 932 Luo, Y., Ahlström, A., Allison, S.D., Batjes, N.H., Brovkin, V., Carvalhais, N., Chappell, A., Ciais, P.,  
933 Davidson, E.A., Finzi, A., 2016. Toward more realistic projections of soil carbon dynamics by  
934 Earth system models. *Global Biogeochemical Cycles* 30, 40–56.
- 935 Luo, Z., Feng, W., Luo, Y., Baldock, J., Wang, E., 2017. Soil organic carbon dynamics jointly controlled by  
936 climate, carbon inputs, soil properties and soil carbon fractions. *Global Change Biology* 23,  
937 4430–4439.
- 938 Metherell, A., Harding, L., Cole, C., Parton, W., 1994. CENTURY soil organic matter model environment,  
939 technical documentation, agroecosystem version 4.0 GPSR Technical Report No. 4. Great Plains  
940 System Research Unit, USDA-ARS, Fort Collins, CO.
- 941 Nachtergaele, F., van Velthuisen, H., Verelst, L., 2012. Harmonized World Soil Database Version 1.2.  
942 Food and Agriculture Organization of the United Nations (FAO). International Institute for



- Applied Systems Analysis (IIASA), ISRIC-World Soil Information, Institute of Soil Science–Chinese Academy of Sciences (ISSCAS), Joint Research Centre of the European Commission (JRC).
- Ogle, S.M., Breidt, F.J., Easter, M., Williams, S., Killian, K., Paustian, K., 2010. Scale and uncertainty in modeled soil organic carbon stock changes for US croplands using a process-based model. *Global Change Biology* 16, 810–822.
- Omerik, J.M., Griffith, G.E., 2014. Ecoregions of the conterminous United States: evolution of a hierarchical spatial framework. *Environmental management* 54, 1249–1266.
- Page, K.L., Dalal, R.C., Dang, Y.P., 2014. How useful are MIR predictions of total, particulate, humus, and resistant organic carbon for examining changes in soil carbon stocks in response to different crop management? A case study. *Soil Research* 51, 719–725.
- Parton, W.J., Hartman, M., Ojima, D., Schimel, D., 1998. DAYCENT and its land surface submodel: description and testing. *Global and planetary Change* 19, 35–48.
- Parton, W.J., Schimel, D.S., Cole, C.V., Ojima, D.S., 1987. Analysis of factors controlling soil organic matter levels in Great Plains grasslands. *Soil Science Society of America Journal* 51, 1173–1179.
- Parton, W.J., Stewart, J.W., Cole, C.V., 1988. Dynamics of C, N, P and S in grassland soils: a model. *Biogeochemistry* 5, 109–131.
- Paul, E.A., Morris, S.J., Bohm, S., 2001. The determination of soil C pool sizes and turnover rates: biophysical fractionation and tracers. *Assessment methods for soil carbon* 14, 193–206.
- Poeplau, C., Don, A., 2013. Sensitivity of soil organic carbon stocks and fractions to different land-use changes across Europe. *Geoderma* 192, 189–201.
- Ramcharan, A., Hengl, T., Nauman, T., Brungard, C., Waltman, S., Wills, S., Thompson, J., 2018. Soil property and class maps of the conterminous United States at 100-meter spatial resolution. *Soil Science Society of America Journal* 82, 186–201.
- Ramirez-Lopez, L., Behrens, T., Schmidt, K., Stevens, A., Demattê, J.A.M., Scholten, T., 2013. The spectrum-based learner: A new local approach for modeling soil vis-NIR spectra of complex datasets. *Geoderma* 195, 268–279.
- Rasmussen, C., Heckman, K., Wieder, W.R., Keiluweit, M., Lawrence, C.R., Berhe, A.A., Blankinship, J.C., Crow, S.E., Druhan, J.L., Pries, C.E.H., 2018. Beyond clay: towards an improved set of variables for predicting soil organic matter content. *Biogeochemistry* 137, 297–306.
- Riahi, K., Rao, S., Krey, V., Cho, C., Chirkov, V., Fischer, G., Kindermann, G., Nakicenovic, N., Rafaj, P., 2011. RCP 8.5—A scenario of comparatively high greenhouse gas emissions. *Climatic change* 109, 33–57.
- Sanderman, J., Baldock, J.A., Dangal, S.R., Ludwig, S., Potter, S., Rivard, C., Savage, K., 2021. Soil organic carbon fractions in the Great Plains of the United States: an application of mid-infrared spectroscopy. *Biogeochemistry* 1–18.
- Sanderman, J., Creamer, C., Baisden, W.T., Farrell, M., Fallon, S., 2017a. Greater soil carbon stocks and faster turnover rates with increasing agricultural productivity. *Soil* 3, 1–16.
- Sanderman, J., Hengl, T., Fiske, G.J., 2017b. Soil carbon debt of 12,000 years of human land use. *Proceedings of the National Academy of Sciences* 114, 9575–9580.
- Sanford Jr, R.L., Parton, W.J., Ojima, D.S., Lodge, D.J., 1991. Hurricane effects on soil organic matter dynamics and forest production in the Luquillo Experimental Forest, Puerto Rico: results of simulation modeling. *Biotropica* 364–372.
- Schmer, M.R., Jin, V.L., Wienhold, B.J., Varvel, G.E., Follett, R.F., 2014. Tillage and residue management effects on soil carbon and nitrogen under irrigated continuous corn. *Soil Science Society of America Journal* 78, 1987–1996.
- Schmidt, M.W., Torn, M.S., Abiven, S., Dittmar, T., Guggenberger, G., Janssens, I.A., Kleber, M., Kögel-Knabner, I., Lehmann, J., Manning, D.A., 2011. Persistence of soil organic matter as an ecosystem property. *Nature* 478, 49–56.

- 991 Schwalm, C.R., Glendon, S., Duffy, P.B., 2020. RCP8. 5 tracks cumulative CO<sub>2</sub> emissions. *Proceedings of*  
992 *the National Academy of Sciences* 117, 19656–19657.
- 993 Sherrod, L.A., Peterson, G.A., Westfall, D.G., Ahuja, L.R., 2005. Soil organic carbon pools after 12 years in  
994 no-till dryland agroecosystems. *Soil Science Society of America Journal* 69, 1600–1608.
- 995 Shi, Z., Crowell, S., Luo, Y., Moore, B., 2018. Model structures amplify uncertainty in predicted soil  
996 carbon responses to climate change. *Nature communications* 9, 1–11.
- 997 Sindelar, A.J., Schmer, M.R., Jin, V.L., Wienhold, B.J., Varvel, G.E., 2015. Long-term corn and soybean  
998 response to crop rotation and tillage. *Agronomy Journal* 107, 2241–2252.
- 999 Sinsabaugh, R.L., Gallo, M.E., Lauber, C., Waldrop, M.P., Zak, D.R., 2005. Extracellular enzyme activities  
1000 and soil organic matter dynamics for northern hardwood forests receiving simulated nitrogen  
1001 deposition. *Biogeochemistry* 75, 201–215.
- 1002 Six, J., Conant, R.T., Paul, E.A., Paustian, K., 2002. Stabilization mechanisms of soil organic matter:  
1003 implications for C-saturation of soils. *Plant and soil* 241, 155–176.
- 1004 Skjemstad, J.O., Spouncer, L.R., Cowie, B., Swift, R.S., 2004. Calibration of the Rothamsted organic  
1005 carbon turnover model (RothC ver. 26.3), using measurable soil organic carbon pools. *Soil*  
1006 *Research* 42, 79–88.
- 1007 Sohl, T.L., Sleeter, B.M., Saylor, K.L., Bouchard, M.A., Reker, R.R., Bennett, S.L., Sleeter, R.R., Kanengieter,  
1008 R.L., Zhu, Z., 2012. Spatially explicit land-use and land-cover scenarios for the Great Plains of the  
1009 United States. *Agriculture, Ecosystems & Environment* 153, 1–15.
- 1010 Stockmann, U., Adams, M.A., Crawford, J.W., Field, D.J., Henakaarchchi, N., Jenkins, M., Minasny, B.,  
1011 McBratney, A.B., De Courcelles, V. de R., Singh, K., 2013. The knowns, known unknowns and  
1012 unknowns of sequestration of soil organic carbon. *Agriculture, Ecosystems & Environment* 164,  
1013 80–99.
- 1014 Sulman, B.N., Moore, J.A., Abramoff, R., Averill, C., Kivlin, S., Georgiou, K., Sridhar, B., Hartman, M.D.,  
1015 Wang, G., Wieder, W.R., 2018. Multiple models and experiments underscore large uncertainty in  
1016 soil carbon dynamics. *Biogeochemistry* 141, 109–123.
- 1017 Syswerda, S.P., Corbin, A.T., Mokma, D.L., Kravchenko, A.N., Robertson, G.P., 2011. Agricultural  
1018 management and soil carbon storage in surface vs. deep layers. *Soil Science Society of America*  
1019 *Journal* 75, 92–101.
- 1020 Tangen, B.A., Bansal, S., 2020. Soil organic carbon stocks and sequestration rates of inland, freshwater  
1021 wetlands: Sources of variability and uncertainty. *Science of The Total Environment* 749, 141444.
- 1022 Thomson, A.M., Calvin, K.V., Smith, S.J., Kyle, G.P., Volke, A., Patel, P., Delgado-Arias, S., Bond-Lamberty,  
1023 B., Wise, M.A., Clarke, L.E., 2011. RCP4. 5: a pathway for stabilization of radiative forcing by  
1024 2100. *Climatic change* 109, 77–94.
- 1025 Thornton, P.E., Thornton, M.M., Mayer, B.W., Wilhelmi, N., Wei, Y., Devarakonda, R., Cook, R., 2012.  
1026 Daymet: Daily surface weather on a 1 km grid for North America, 1980–2008. Oak Ridge National  
1027 Laboratory (ORNL) Distributed Active Archive Center for Biogeochemical Dynamics (DAAC).
- 1028 Tian, H., Lu, C., Yang, J., Banger, K., Huntzinger, D.N., Schwalm, C.R., Michalak, A.M., Cook, R., Ciais, P.,  
1029 Hayes, D., 2015. Global patterns and controls of soil organic carbon dynamics as simulated by  
1030 multiple terrestrial biosphere models: Current status and future directions. *Global*  
1031 *Biogeochemical Cycles* 29, 775–792.
- 1032 Todd-Brown, K.E.O., Randerson, J.T., Hopkins, F., Arora, V., Hajima, T., Jones, C., Shevliakova, E., Tjiputra,  
1033 J., Volodin, E., Wu, T., 2014. Changes in soil organic carbon storage predicted by Earth system  
1034 models during the 21st century. *Biogeosciences* 11, 2341–2356.
- 1035 Torn, M.S., Kleber, M., Zavaleta, E.S., Zhu, B., Field, C.B., Trumbore, S.E., 2013. A dual isotope approach  
1036 to isolate soil carbon pools of different turnover times. *Biogeosciences* 10, 8067–8081.
- 1037 Torn, M.S., Trumbore, S.E., Chadwick, O.A., Vitousek, P.M., Hendricks, D.M., 1997. Mineral control of soil  
1038 organic carbon storage and turnover. *Nature* 389, 170–173.

- 1039 Trumbore, S.E., 1997. Potential responses of soil organic carbon to global environmental change.  
1040 Proceedings of the National Academy of Sciences 94, 8284–8291.
- 1041 Van Groenigen, K.J., Qi, X., Osenberg, C.W., Luo, Y., Hungate, B.A., 2014. Faster decomposition under  
1042 increased atmospheric CO<sub>2</sub> limits soil carbon storage. *Science* 344, 508–509.
- 1043 Wieder, W.R., Hartman, M.D., Sulman, B.N., Wang, Y.-P., Koven, C.D., Bonan, G.B., 2018. Carbon cycle  
1044 confidence and uncertainty: Exploring variation among soil biogeochemical models. *Global*  
1045 *change biology* 24, 1563–1579.
- 1046 Wiesmeier, M., Urbanski, L., Hobbey, E., Lang, B., von Lützow, M., Marin-Spiotta, E., van Wesemael, B.,  
1047 Rabot, E., Ließ, M., Garcia-Franco, N., 2019. Soil organic carbon storage as a key function of soils-  
1048 A review of drivers and indicators at various scales. *Geoderma* 333, 149–162.
- 1049 Zimmermann, M., Leifeld, J., Schmidt, M.W.I., Smith, P., Fuhrer, J., 2007. Measured soil organic matter  
1050 fractions can be related to pools in the RothC model. *European Journal of Soil Science* 58, 658–  
1051 667.
- 1052
- 1053



# Improving soil carbon estimates by linking conceptual pools against measurable carbon fractions in the DAYCENT Model Version 4.5

ORIGINALITY REPORT

20%

SIMILARITY INDEX

## PRIMARY SOURCES

1	Pan Chen, Yongping Yuan, Wenhong Li, Stephen LeDuc, Tyler Lark, Xuesong Zhang, Christopher Clark. "Assessing Recent Crop Expansion on Water Quality in the Missouri River Basin Using the SWAT Model", Journal of Advances in Modeling Earth Systems, 2021 <small>Crossref</small>	231 words — 2%
2	<a href="#">arxiv.org</a> <small>Internet</small>	140 words — 1%
3	<a href="#">www.mdpi.com</a> <small>Internet</small>	58 words — < 1%
4	<a href="#">worldwidescience.org</a> <small>Internet</small>	57 words — < 1%
5	Sylvia S. Nyawira, Melannie D. Hartman, Trung H. Nguyen, Andrew J. Margenot et al. "Simulating soil organic carbon in maize-based systems under improved agronomic management in Western Kenya", Soil and Tillage Research, 2021 <small>Crossref</small>	53 words — < 1%
6	<a href="#">www.tandfonline.com</a> <small>Internet</small>	51 words — < 1%

- 
- 7 Melannie D. Hartman, Emily R. Merchant, William J. Parton, Myron P. Gutmann, Susan M. Lutz, Stephen A. Williams. "Impact of historical land-use changes on greenhouse gas exchange in the U.S. Great Plains, 1883–2003", Ecological Applications, 2011  
Crossref 48 words — < 1%
- 
- 8 eprints.lib.hokudai.ac.jp  
Internet 41 words — < 1%
- 
- 9 MARC CORBEELS. "Soil carbon storage potential of direct seeding mulch-based cropping systems in the Cerrados of Brazil", Global Change Biology, 9/2006  
Crossref 33 words — < 1%
- 
- 10 bg.copernicus.org  
Internet 30 words — < 1%
- 
- 11 "Sustainable agroecosystems in climate change mitigation", Wageningen Academic Publishers, 2014  
Crossref 29 words — < 1%
- 
- 12 openresearch-repository.anu.edu.au  
Internet 28 words — < 1%
- 
- 13 www.sgcp.ncsu.edu  
Internet 27 words — < 1%
- 
- 14 Wieder, William R., Jennifer Boehnert, and Gordon B. Bonan. "Evaluating soil biogeochemistry parameterizations in Earth system models with observations : Soil Biogeochemistry in ESMs", Global Biogeochemical Cycles, 2014.  
Crossref 25 words — < 1%
- 
- 15 escholarship.org

25 words — &lt; 1%

[16 www.frontiersin.org](http://www.frontiersin.org)

Internet

25 words — &lt; 1%

17 Kuo-Hsien Chang, Jon Warland, Paul Voroney, Paul Bartlett, Claudia Wagner-Riddle. "Using DayCENT to Simulate Carbon Dynamics in Conventional and No-Till Agriculture", Soil Science Society of America Journal, 2013

Crossref

23 words — &lt; 1%

[18 www.nrel.colostate.edu](http://www.nrel.colostate.edu)

Internet

23 words — &lt; 1%

19 Bruno Basso, Osvaldo Gargiulo, Keith Paustian, G. Philip Robertson, Cheryl Porter, Peter R. Grace, James W. Jones. "Procedures for Initializing Soil Organic Carbon Pools in the DSSAT-CENTURY Model for Agricultural Systems", Soil Science Society of America Journal, 2011

Crossref

21 words — &lt; 1%

[20 eprints.qut.edu.au](http://eprints.qut.edu.au)

Internet

21 words — &lt; 1%

[21 Recarbonization of the Biosphere, 2012.](#)

Crossref

20 words — &lt; 1%

[22 coek.info](http://coek.info)

Internet

20 words — &lt; 1%

[23 hdl.handle.net](http://hdl.handle.net)

Internet

20 words — &lt; 1%

[24 edepot.wur.nl](http://edepot.wur.nl)

Internet

19 words — &lt; 1%

25	<a href="http://orbi.uliege.be">orbi.uliege.be</a> Internet	19 words — < 1 %
26	<a href="http://www.biogeosciences.net">www.biogeosciences.net</a> Internet	19 words — < 1 %
27	Abdalla, M.. "Testing DayCent and DNDC model simulations of N <sup>2</sup> O fluxes and assessing the impacts of climate change on the gas flux and biomass production from a humid pasture", Atmospheric Environment, 201008 Crossref	18 words — < 1 %
28	<a href="http://ediss.uni-goettingen.de">ediss.uni-goettingen.de</a> Internet	18 words — < 1 %
29	<a href="http://www.fao.org">www.fao.org</a> Internet	18 words — < 1 %
30	<a href="http://www.iiss.nic.in">www.iiss.nic.in</a> Internet	18 words — < 1 %
31	<a href="http://epdf.pub">epdf.pub</a> Internet	17 words — < 1 %
32	<a href="http://lib.dr.iastate.edu">lib.dr.iastate.edu</a> Internet	17 words — < 1 %
33	<a href="http://link.springer.com">link.springer.com</a> Internet	17 words — < 1 %
34	<a href="http://vuir.vu.edu.au">vuir.vu.edu.au</a> Internet	17 words — < 1 %
35	P.K. Dash, Pratap Bhattacharyya, K.S. Roy, S. Neogi, A.K. Nayak. "Environmental constraints' sensitivity of soil organic carbon decomposition to	16 words — < 1 %

temperature, management practices and climate change",  
Ecological Indicators, 2019

Crossref

- 
- 36 [digitalcommons.unl.edu](https://digitalcommons.unl.edu) 16 words — < 1%  
Internet
- 
- 37 [epdf.tips](https://epdf.tips) 16 words — < 1%  
Internet
- 
- 38 [eprints.nottingham.ac.uk](https://eprints.nottingham.ac.uk) 16 words — < 1%  
Internet
- 
- 39 [www.tdx.cat](http://www.tdx.cat) 16 words — < 1%  
Internet
- 
- 40 Eyles, Alieta, Garth Coghlan, Marcus Hardie, Mark Hovenden, and Kerry Bridle. "Soil carbon sequestration in cool-temperate dryland pastures: mechanisms and management options", Soil Research, 2015. 15 words — < 1%  
Crossref
- 
- 41 Shuai Wang, Kabindra Adhikari, Qianlai Zhuang, Hanlong Gu, Xinxin Jin. "Impacts of urbanization on soil organic carbon stocks in the northeast coastal agricultural areas of China", Science of The Total Environment, 2020 15 words — < 1%  
Crossref
- 
- 42 [eprints.lse.ac.uk](https://eprints.lse.ac.uk) 15 words — < 1%  
Internet
- 
- 43 Carlo Camarotto, Ilaria Piccoli, Nicola Dal Ferro, Riccardo Polese, Francesca Chiarini, Lorenzo Furlan, Francesco Morari. "Have we reached the turning point? Looking for evidence of SOC increase under conservation 14 words — < 1%

- 
- 44 [slidelegend.com](#) 14 words — < 1 %  
Internet
- 
- 45 Deli Chen. "N<sub>2</sub>O emissions from agricultural lands: a synthesis of simulation approaches", Plant and Soil, 08/2008 13 words — < 1 %  
Crossref
- 
- 46 Global Change – The IGBP Series, 2007. 13 words — < 1 %  
Crossref
- 
- 47 Peng, C.. "Modelling the response of net primary productivity (NPP) of boreal forest ecosystems to changes in climate and fire disturbance regimes", Ecological Modelling, 19991020 13 words — < 1 %  
Crossref
- 
- 48 [ecommons.usask.ca](#) 13 words — < 1 %  
Internet
- 
- 49 [webdoc.sub.gwdg.de](#) 13 words — < 1 %  
Internet
- 
- 50 Jielin Ge, Wenting Xu, Qing Liu, Zhiyao Tang, Zongqiang Xie. "Patterns and environmental controls of soil organic carbon density in Chinese shrublands", Geoderma, 2020 12 words — < 1 %  
Crossref
- 
- 51 Jonathan Sanderman, Jeffrey A. Baldock, Shree R. S. Dangal, Sarah Ludwig, Stefano Potter, Charlotte Rivard, Kathleen Savage. "Soil organic carbon 12 words — < 1 %

fractions in the Great Plains of the United States: an application of mid-infrared spectroscopy", Biogeochemistry, 2021

Crossref

---

52 Zhenghong Tan. "Carbon balance of a primary tropical seasonal rain forest", Journal of Geophysical Research, 07/03/2010 12 words — < 1%

Crossref

---

53 eprints.whiterose.ac.uk 12 words — < 1%

Internet

---

54 A Vergunst. "Recombination in the Plant Genome and its Application in Biotechnology", Critical Reviews in Plant Sciences, 1/1999 11 words — < 1%

Crossref

---

55 J. J. Jiménez, R. Lal. "Mechanisms of C Sequestration in Soils of Latin America", Critical Reviews in Plant Sciences, 2006 11 words — < 1%

Crossref

---

56 Jean-François Lamarque, G. Page Kyle, Malte Meinshausen, Keywan Riahi et al. "Global and regional evolution of short-lived radiatively-active gases and aerosols in the Representative Concentration Pathways", Climatic Change, 2011 11 words — < 1%

Crossref

---

57 Nimai Senapati, Abad Chabbi, André Faé Giostri, Jagadeesh B. Yeluripati, Pete Smith. "Modelling nitrous oxide emissions from mown-grass and grain-cropping systems: Testing and sensitivity analysis of DailyDayCent using high frequency measurements", Science of The Total Environment, 2016 11 words — < 1%

Crossref

---

58 Oelbermann, M.. "Carbon sequestration in tropical and temperate agroforestry systems: a review with examples from Costa Rica and southern Canada", Agriculture, Ecosystems and Environment, 200412 11 words — < 1%  
Crossref

---

59 Viscarra Rossel, R. A., and W. S. Hicks. "Soil organic carbon and its fractions estimated by visible-near infrared transfer functions : Vis-NIR estimates of organic carbon and its fractions", European Journal of Soil Science, 2015. 11 words — < 1%  
Crossref

---

60 hot-world-info.blogspot.com 11 words — < 1%  
Internet

---

61 pure.uva.nl 11 words — < 1%  
Internet

---

62 push-zb.helmholtz-muenchen.de 11 words — < 1%  
Internet

---

63 ses.library.usyd.edu.au 11 words — < 1%  
Internet

---

64 Abdalla, Mohamed, Matthew Saunders, Astley Hastings, Mike Williams, Pete Smith, Bruce Osborne, Gary Lanigan, and Mike B. Jones. "Simulating the impacts of land use in Northwest Europe on Net Ecosystem Exchange (NEE): The role of arable ecosystems, grasslands and forest plantations in climate change mitigation", The Science of The Total Environment, 2013. 10 words — < 1%  
Crossref

---

65 Cheng, Kun, Stephen M. Ogle, William J. Parton, and Genxing Pan. "Predicting methanogenesis 10 words — < 1%



from rice paddies using the DAYCENT ecosystem model",  
Ecological Modelling, 2013.

Crossref

- 66 Cowie, Annette L., Vanessa E. Lonergan, S. M. Fazle Rabbi, Flavio Fornasier, Catriona Macdonald, Steven Harden, Akitomo Kawasaki, and Brajesh K. Singh. "Impact of carbon farming practices on soil carbon in northern New South Wales", Soil Research, 2013.

10 words — < 1%

Crossref

- 67 Grace L. Miner, Neil C. Hansen, Daniel Inman, Lucretia A. Sherrod, G. A. Peterson. "Constraints of No-Till Dryland Agroecosystems as Bioenergy Production Systems", Agronomy Journal, 2013

10 words — < 1%

Crossref

- 68 Zhongkui Luo, Enli Wang, Brett A. Bryan, Darran King, Gang Zhao, Xubin Pan, Ulrike Bende-Michl. "Meta-modeling soil organic carbon sequestration potential and its application at regional scale", Ecological Applications, 2013

10 words — < 1%

Crossref

- 69 [conservancy.umn.edu](http://conservancy.umn.edu)

Internet

10 words — < 1%

- 70 [digital.lib.washington.edu](http://digital.lib.washington.edu)

Internet

10 words — < 1%

- 71 [dokumen.pub](http://dokumen.pub)

Internet

10 words — < 1%

- 72 [greenhouse.gov.au](http://greenhouse.gov.au)

Internet

10 words — < 1%

- 73 [mafiadoc.com](http://mafiadoc.com)

Internet

10 words — < 1%

74 [paduaresearch.cab.unipd.it](http://paduaresearch.cab.unipd.it)  
Internet

10 words — < 1%

75 [skemman.is](http://skemman.is)  
Internet

10 words — < 1%

76 [studyres.com](http://studyres.com)  
Internet

10 words — < 1%

77 [ueaeprints.uea.ac.uk](http://ueaeprints.uea.ac.uk)  
Internet

10 words — < 1%

78 [vtechworks.lib.vt.edu](http://vtechworks.lib.vt.edu)  
Internet

10 words — < 1%

79 [www.biogeosciences-discuss.net](http://www.biogeosciences-discuss.net)  
Internet

10 words — < 1%

80 [www.epa.gov](http://www.epa.gov)  
Internet

10 words — < 1%

81 [www.ipcc-nggip.iges.or.jp](http://www.ipcc-nggip.iges.or.jp)  
Internet

10 words — < 1%

82 [www.ipcc.ch](http://www.ipcc.ch)  
Internet

10 words — < 1%

83 [www.nrcs.usda.gov](http://www.nrcs.usda.gov)  
Internet

10 words — < 1%

84 [www.openagrar.de](http://www.openagrar.de)  
Internet

10 words — < 1%

85 [www.umaine.edu](http://www.umaine.edu)

---

86 Aoesta K. Mohammed, Daniel R. Hirmas, Attila Nemes, Daniel Giménez. "Exogenous and endogenous controls on the development of soil structure", *Geoderma*, 2020 9 words — < 1%  
Crossref

---

87 Cerri, C.E.P.. "Simulating SOC changes in 11 land use change chronosequences from the Brazilian Amazon with RothC and Century models", *Agriculture, Ecosystems and Environment*, 200709 9 words — < 1%  
Crossref

---

88 Craig Rasmussen, Heather Throckmorton, Garrett Liles, Katherine Heckman, Stephen Meding, William Horwath. "Controls on Soil Organic Carbon Partitioning and Stabilization in the California Sierra Nevada", *Soil Systems*, 2018 9 words — < 1%  
Crossref

---

89 Emily F. Solly, Valentino Weber, Stephan Zimmermann, Lorenz Walthert, Frank Hagedorn, Michael W. I. Schmidt. "Is the content and potential preservation of soil organic carbon reflected by cation exchange capacity? A case study in Swiss forest soils", *Biogeosciences Discussions*, 2019 9 words — < 1%  
Crossref

---

90 Kefeng Wang, Changhui Peng, Qiuhan Zhu, Xiaolu Zhou, Meng Wang, Kerou Zhang, Gangsheng Wang. "Modeling Global Soil Carbon and Soil Microbial Carbon by Integrating Microbial Processes into the Ecosystem Process Model TRIPLEX-GHG", *Journal of Advances in Modeling Earth Systems*, 2017 9 words — < 1%  
Crossref

91 Mohamad I. Hejazi. "Regression-based approach to low flow prediction in the Maryland Piedmont region under joint climate and land use change", Hydrological Processes, 07/01/2007

Crossref

92 Ota, Masakazu, Haruyasu Nagai, and Jun Koarashi. "Root and dissolved organic carbon controls on subsurface soil carbon dynamics: A model approach : CONTROLS ON SUBSURFACE CARBON DYNAMICS", Journal of Geophysical Research Biogeosciences, 2013.

Crossref

93 Rachel K. Owen, Elisabeth B. Webb, David A. Haukos, Keith W. Goyne. "Projected climate and land use changes drive plant community composition in agricultural wetlands", Environmental and Experimental Botany, 2020

Crossref

94 Rees, R.M.. "The role of plants and land management in sequestering soil carbon in temperate arable and grassland ecosystems", Geoderma, 200509

Crossref

95 Smith, W.N., B.B. Grant, C.A. Campbell, B.G. McConkey, R.L. Desjardins, R. Kröbel, and S.S. Malhi. "Crop residue removal effects on soil carbon: Measured and inter-model comparisons", Agriculture Ecosystems & Environment, 2012.

Crossref

96 WEIMIN JU. "Hydrological effects on carbon cycles of Canada's forests and wetlands", Tellus B, 2/2006

Crossref

97	<a href="#">Zhao, Gang, Brett A. Bryan, Darran King, Zhongkui Luo, Enli Wang, Xiaodong Song, and Qiang Yu.</a> <a href="#">"Impact of agricultural management practices on soil organic carbon: simulation of Australian wheat systems", Global Change Biology, 2013.</a> Crossref	9 words — < 1%
98	<a href="#">erepository.uonbi.ac.ke:8080</a> Internet	9 words — < 1%
99	<a href="#">github.com</a> Internet	9 words — < 1%
100	<a href="#">iopscience.iop.org</a> Internet	9 words — < 1%
101	<a href="#">prodinra.inra.fr</a> Internet	9 words — < 1%
102	<a href="#">www.agriculturejournals.cz</a> Internet	9 words — < 1%
103	<a href="#">www.calrecycle.ca.gov</a> Internet	9 words — < 1%
104	<a href="#">www.kiran.nic.in</a> Internet	9 words — < 1%
105	<a href="#">www.labome.org</a> Internet	9 words — < 1%
106	<a href="#">www.nature.com</a> Internet	9 words — < 1%
107	<a href="#">Brandani, Carolina B., Thalita F. Abbruzzini, Stephen Williams, Mark Easter, Carlos E. Pellegrino</a>	8 words — < 1%

Cerri, and Keith Paustian. "Simulation of management and soil interactions impacting SOC dynamics in sugarcane using the Century Model", GCB Bioenergy, 2014.

Crossref

---

108 Fatih Evrendilek, Mohan K Wali. "Modelling long-term C dynamics in croplands in the context of climate change: a case study from Ohio", Environmental Modelling & Software, 2001

8 words — < 1%

Crossref

---

109 Gomez-Casanovas, Nuria, Tara W. Hudiburg, Carl J. Bernacchi, William Parton, and Evan H. DeLucia. "Nitrogen deposition and greenhouse gas emissions from grasslands: uncertainties and future directions", Global Change Biology, 2015.

8 words — < 1%

Crossref

---

110 Guoping Tang. "Simulating the climatic effects on vegetation: approaches, issues and challenges", Progress in Physical Geography, 10/01/2008

8 words — < 1%

Crossref

---

111 Hongqing Wang, Joseph D. Cornell, Charles A.S. Hall, David P. Marley. "Spatial and seasonal dynamics of surface soil carbon in the Luquillo Experimental Forest, Puerto Rico", Ecological Modelling, 2002

8 words — < 1%

Crossref

---

112 Humberto Blanco-Canqui. "Mechanisms of Carbon Sequestration in Soil Aggregates", Critical Reviews in Plant Sciences, 11/1/2004

8 words — < 1%

Crossref

---

113 Jonathan Gray, Senani Karunaratne, Thomas Bishop, Brian Wilson, Manoharan Veeragathipillai. "Driving factors of soil organic carbon fractions over New South Wales, Australia", Geoderma, 2019

8 words — < 1%

114 Jonathan R. Straube, Maosi Chen, William J. Parton, Shinichi Asso, Yan-An Liu, Dennis S. Ojima, Wei Gao. "Development of the DayCent-Photo model and integration of variable photosynthetic capacity", *Frontiers of Earth Science*, 2018

Crossref

115 Juhwan Lee, Raphael A. Viscarra Rossel. "Soil carbon simulation confounded by different pool initialisation", *Nutrient Cycling in Agroecosystems*, 2019

Crossref

116 Luitgard Schwendenmann, Elise Pendall. "Response of soil organic matter dynamics to conversion from tropical forest to grassland as determined by long-term incubation", *Biology and Fertility of Soils*, 2008

Crossref

117 Mathieu Chassé, Suzanne Lutfalla, Lauric Cécillon, François Baudin, Samuel Abiven, Claire Chenu, Pierre Barré. "Long-term bare-fallow soil fractions reveal thermo-chemical properties controlling soil organic carbon dynamics", *Biogeosciences*, 2021

Crossref

118 Roberta Farina, Renata Sándor, Mohamed Abdalla, Jorge Álvaro - Fuentes et al. "Ensemble modelling, uncertainty and robust predictions of organic carbon in long - term bare - fallow soils", *Global Change Biology*, 2020

Crossref

119 Stephen J. Del Grosso, Hero T. Gollany, Melissa Reyes-Fox. "Simulating Soil Organic Carbon Stock Changes in Agroecosystems using CQESTR, DayCent, and IPCC Tier 1 Methods", *American Society of Agronomy*, 2015

Crossref

120 Tian, Hanqin, Chaoqun Lu, Jia Yang, Kamaljit Banger, Deborah N. Huntinzger, Christopher R. Schwalm, Anna M. Michalak, Robert Cook, Philippe Ciais, Daniel Hayes, Maoyi Huang, Akihiko Ito, Atul Jain, Huimin Lei, Jiafu Mao, Shufen Pan, Wilfred M. Post, Shushi Peng, Benjamin Poulter, Wei Ren, Daniel Ricciuto, Kevin Schaefer, Xiaoying Shi, Bo Tao, Weile Wang, Yaxing Wei, Qichun Yang, Bowen Zhang, and Ning Zeng. "Global Patterns and controls of soil organic carbon dynamics as simulated by multiple terrestrial biosphere models: current status and future directions : Modeling global soil carbon dynamics", Global Biogeochemical Cycles, 2015.

Crossref

121 Xiaoyu Liu, Yongcun Zhao, Xuezheng Shi, Yang Liu, Shihang Wang, Dongsheng Yu. "Sensitivity and uncertainty analysis of CENTURY-modeled SOC dynamics in upland soils under different climate-soil-management conditions: a case study in China", Journal of Soils and Sediments, 2016

Crossref

122 Zhen Yu, Chaoqun Lu, Peiyu Cao, Hanqin Tian. "Long-term terrestrial carbon dynamics in the Midwestern United States during 1850-2015: Roles of land use and cover change and agricultural management", Global Change Biology, 2018

Crossref

123 Zhongkui Luo, Yiqi Luo, Guocheng Wang, Jianyang Xia, Changhui Peng. "Warming - induced global soil carbon loss attenuated by downward carbon movement", Global Change Biology, 2020

Crossref

124 [acp.copernicus.org](http://acp.copernicus.org)

Internet



125	<a href="http://agupubs.onlinelibrary.wiley.com">agupubs.onlinelibrary.wiley.com</a> Internet	8 words — < 1%
126	<a href="http://blogs.cornell.edu">blogs.cornell.edu</a> Internet	8 words — < 1%
127	<a href="http://d-nb.info">d-nb.info</a> Internet	8 words — < 1%
128	<a href="http://digitalcommons.usu.edu">digitalcommons.usu.edu</a> Internet	8 words — < 1%
129	<a href="http://docs.wixstatic.com">docs.wixstatic.com</a> Internet	8 words — < 1%
130	<a href="http://documents.mx">documents.mx</a> Internet	8 words — < 1%
131	<a href="http://ecoss.nau.edu">ecoss.nau.edu</a> Internet	8 words — < 1%
132	<a href="http://erepository.uonbi.ac.ke">erepository.uonbi.ac.ke</a> Internet	8 words — < 1%
133	<a href="http://espace.library.uq.edu.au">espace.library.uq.edu.au</a> Internet	8 words — < 1%
134	<a href="http://essd.copernicus.org">essd.copernicus.org</a> Internet	8 words — < 1%
135	<a href="http://etheses.whiterose.ac.uk">etheses.whiterose.ac.uk</a> Internet	8 words — < 1%
136	<a href="http://landcover.usgs.gov">landcover.usgs.gov</a> Internet	8 words — < 1%

137	<a href="http://mro.massey.ac.nz">mro.massey.ac.nz</a> Internet	8 words — < 1%
138	<a href="http://notulaebotanicae.ro">notulaebotanicae.ro</a> Internet	8 words — < 1%
139	<a href="http://nrel.colostate.edu">nrel.colostate.edu</a> Internet	8 words — < 1%
140	<a href="http://tel.archives-ouvertes.fr">tel.archives-ouvertes.fr</a> Internet	8 words — < 1%
141	<a href="http://w3.ufsm.br">w3.ufsm.br</a> Internet	8 words — < 1%
142	<a href="http://www.agronomyaustraliaproceedings.org">www.agronomyaustraliaproceedings.org</a> Internet	8 words — < 1%
143	<a href="http://www.science.gov">www.science.gov</a> Internet	8 words — < 1%
144	<a href="http://www.uniassignment.com">www.uniassignment.com</a> Internet	8 words — < 1%
145	Cole D. Gross, Robert B. Harrison. "The Case for Digging Deeper: Soil Organic Carbon Storage, Dynamics, and Controls in Our Changing World", <i>Soil Systems</i> , 2019 Crossref	7 words — < 1%
146	Mikhailova, E.. "Modeling soil organic matter dynamics after conversion of native grassland to long-term continuous fallow using the CENTURY model", <i>Ecological Modelling</i> , 20000805 Crossref	7 words — < 1%

147 Milne, E.. "National and sub-national assessments of soil organic carbon stocks and changes: The GEFSOC modelling system", Agriculture, Ecosystems and Environment, 200709

Crossref

7 words — < 1%

148 Stephen M. Ogle. "Uncertainty in estimating land use and management impacts on soil organic carbon storage for US agricultural lands between 1982 and 1997", Global Change Biology, 11/2003

Crossref

7 words — < 1%

149 Wenfang Xu, Jinfeng Chang, Philippe Ciais, Bertrand Guenet et al. "Reducing Uncertainties of Future Global Soil Carbon Responses to Climate and Land Use Change With Emergent Constraints", Global Biogeochemical Cycles, 2020

Crossref

7 words — < 1%

150 D. S. Chianese, , C. A. Rotz, and T. L. Richard. "Simulation of Carbon Dioxide Emissions from Dairy Farms to Assess Greenhouse Gas Reduction Strategies", Transactions of the ASABE, 2009.

Crossref

6 words — < 1%

151 Ecosystem Services and Carbon Sequestration in the Biosphere, 2013.

Crossref

6 words — < 1%

152 Hero T. Gollany, Steve J. DelGrosso, Curtis J. Dell, Paul. R. Adler, Robert W. Polumsky. "Assessing the effectiveness of agricultural conservation practices in maintaining soil organic carbon under contrasting agroecosystems and changing climate", Soil Science Society of America Journal, 2021

Crossref

6 words — < 1%

---

153 Jean Steiner, Shannon McNeeley, Karen Cozzetto, Amber N. Childress. "Great Plains Regional Technical Input Report", Springer Science and Business Media LLC, 2015

6 words — < 1%

Crossref

---

154 Qian, H. Y., J. J. Pan, and B. Sun. "The relative impact of land use and soil properties on sizes and turnover rates of soil organic carbon pools in Subtropical China", Soil Use and Management, 2013.

6 words — < 1%

Crossref

---

155 R. Nieder, D. K. Benbi. "Carbon and Nitrogen in the Terrestrial Environment", Springer Science and Business Media LLC, 2008

6 words — < 1%

Crossref

---

156 Robert J. Hijmans, Susan E. Cameron, Juan L. Parra, Peter G. Jones, Andy Jarvis. "Very high resolution interpolated climate surfaces for global land areas", International Journal of Climatology, 2005

6 words — < 1%

Crossref

---

157 Rodrigo S. Nicoloso, Telmo J. C. Amado, Charles W. Rice. "Assessing strategies to enhance soil carbon sequestration with the DSSAT-CENTURY model", European Journal of Soil Science, 2020

6 words — < 1%

Crossref

---

158 Rémi Cardinael, Thomas Eglin, Bertrand Guenet, Cathy Neill, Sabine Houot, Claire Chenu. "Is priming effect a significant process for long-term SOC dynamics? Analysis of a 52-years old experiment", Biogeochemistry, 2015

6 words — < 1%

Crossref

---

159 Soil Carbon, 2014.

160 T. Eglin, P. Ciais, S.L. Piao, P. Barre, V. Bellassen, P. Cadule, C. Chenu, T. Gasser, C. Koven, M. Reichstein, P. Smith. "Historical and future perspectives of global soil carbon response to climate and land-use changes", *Tellus B: Chemical and Physical Meteorology*, 2017

Crossref

161 Todd-Brown, K. E. O., J. T. Randerson, F. Hopkins, V. Arora, T. Hajima, C. Jones, E. Shevliakova, J. Tjiputra, E. Volodin, T. Wu, Q. Zhang, and S. D. Allison. "Changes in soil organic carbon storage predicted by Earth system models during the 21st century", *Biogeosciences*, 2014.

Crossref

162 W. R. Wieder, A. S. Grandy, C. M. Kallenbach, G. B. Bonan. "Integrating microbial physiology and physiochemical principles in soils with the Microbial-Mineral Carbon Stabilization (MIMICS) model", *Biogeosciences Discussions*, 2014

Crossref

163 edoc.ub.uni-muenchen.de

Internet

6 words — &lt; 1%

EXCLUDE QUOTES ON

EXCLUDE MATCHES OFF

EXCLUDE BIBLIOGRAPHY ON